ISSN 2686-7575 (Online)

ТОНКИЕ ХИМИЧЕСКИЕ ТЕХНОЛОГИИ

Fine Chemical Technologies

- Theoretical Bases of Chemical Technology
- Chemistry and Technology of Organic Substances
- Chemistry and Technology of Medicinal Compounds and Biologically Active Substances
- Biochemistry and Biotechnology
- Synthesis and Processing of Polymers and Polymeric Composites
- Chemistry and Technology of Inorganic Materials
- Analytical Methods in Chemistry and Chemical Technology
- Mathematical Methods and Information Systems in Chemical Technology

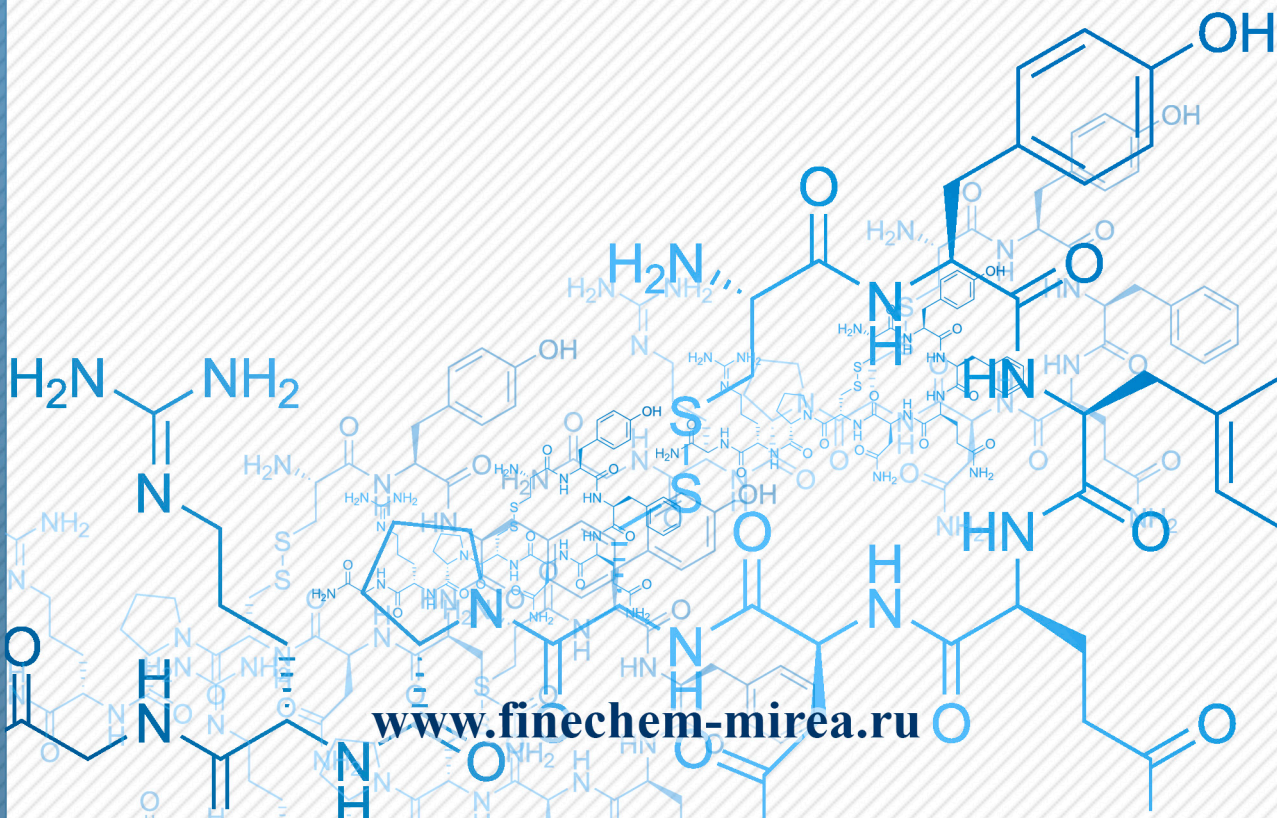

17(3)

2022

www.finechem-mirea.ru

ISSN 2686-7575 (Online)

ТОНКИЕ ХИМИЧЕСКИЕ ТЕХНОЛОГИИ

Fine Chemical Technologies

- Theoretical Bases of Chemical Technology
- Chemistry and Technology of Organic Substances
- Chemistry and Technology of Medicinal Compounds and Biologically Active Substances
- Biochemistry and Biotechnology
- Synthesis and Processing of Polymers and Polymeric Composites
- Chemistry and Technology of Inorganic Materials
- Analytical Methods in Chemistry and Chemical Technology
- Mathematical Methods and Information Systems in Chemical Technology

Tonkie Khimicheskie Tekhnologii = Fine Chemical Technologies
Vol. 17, No. 3, 2022

Тонкие химические технологии = Fine Chemical Technologies
Том 17, № 3, 2022

https://doi.org/10.32362/2410-6593-2022-17-3
www.finechem-mirea.ru

https://doi.org/10.32362/2410-6593 ***www.finechem-mirea.ru***

Tonkie Khimicheskie Tekhnologii =
Fine Chemical Technologies
2022, vol. 17, no. 3

The peer-reviewed scientific and technical journal Fine Chemical Technologies highlights the modern achievements of fundamental and applied research in the field of fine chemical technologies, including theoretical bases of chemical technology, chemistry and technology of medicinal compounds and biologically active substances, organic substances and inorganic materials, biochemistry and biotechnology, synthesis and processing of polymers and polymeric composites, analytical and mathematical methods and information systems in chemistry and chemical technology.

Founder and Publisher

Federal State Budget
Educational Institution of Higher Education
"MIREA – Russian Technological University"
78, Vernadskogo pr., Moscow, 119454, Russian Federation.
Publication frequency: bimonthly.
The journal was founded in 2006. The name was Vestnik MITHT until 2015 (ISSN 1819-1487).

The journal is included into the List of peer-reviewed science press of the State Commission for Academic Degrees and Titles of the Russian Federation.
The journal is indexed:
SCOPUS, DOAJ, Chemical Abstracts, Science Index, RSCI, Ulrich's International Periodicals Directory

86, Vernadskogo pr., Moscow, 119571, Russian Federation.
Phone: +7(495) 246-05-55 (#2-88)
E-mail: *seredina@mirea.ru*

The registration number ПИ № ФС 77–74580 was issued in December 14, 2018 by the Federal Service for Supervision of Communications, Information Technology, and Mass Media of Russia

The subscription index of *Pressa Rossii*: **36924**

Тонкие химические технологии =
Fine Chemical Technologies
2022, том 17, № 3

Научно-технический рецензируемый журнал «Тонкие химические технологии» освещает современные достижения фундаментальных и прикладных исследований в области тонких химических технологий, включая теоретические основы химической технологии, химию и технологию лекарственных препаратов и биологически активных соединений, органических веществ и неорганических материалов, биохимию и биотехнологию, синтез и переработку полимеров и композитов на их основе, аналитические и математические методы и информационные системы в химии и химической технологии.

Учредитель и издатель

федеральное государственное бюджетное
образовательное учреждение высшего образования
«МИРЭА – Российский технологический университет»
119454, РФ, Москва, пр-кт Вернадского, д. 78.
Периодичность: один раз в два месяца.
Журнал основан в 2006 году. До 2015 года издавался под названием «Вестник МИТХТ» (ISSN 1819-1487).

Журнал входит в Перечень ведущих рецензируемых научных журналов ВАК РФ.
Индексируется:
SCOPUS, DOAJ, Chemical Abstracts, РИНЦ (Science Index), RSCI, Ulrich's International Periodicals Directory

119571, Москва, пр. Вернадского, 86, оф. Л-119.
Тел.: +7(495) 246-05-55 (#2-88)
E-mail: *seredina@mirea.ru*

Регистрационный номер и дата принятия решения о регистрации СМИ: ПИ № ФС 77-74580 от 14.12.2018 г. СМИ зарегистрировано Федеральной службой по надзору в сфере связи, информационных технологий и массовых коммуникаций (Роскомнадзор)

Индекс по Объединенному каталогу «Пресса России»: **36924**

ТОНКИЕ ХИМИЧЕСКИЕ ТЕХНОЛОГИИ
Fine Chemical Technologies
17(3)
2022

CONTENTS

СОДЕРЖАНИЕ

THEORETICAL BASES OF CHEMICAL TECHNOLOGY

ТЕОРЕТИЧЕСКИЕ ОСНОВЫ ХИМИЧЕСКОЙ ТЕХНОЛОГИИ

ISSN 2686-7575 (Online)

https://doi.org/10.32362/2410-6593-2022-17-3-189-200

UDC 544.342

RESEARCH ARTICLE

Analysis of the rectifying separation of H_2O–D_2O mixture into light and heavy water by means of mathematical modeling

Tatyana G. Korotkova✉, Gennady I. Kasyanov

Kuban State Technological University, Krasnodar, 350072 Russia
✉*Corresponding author, e-mail: korotkova1964@mail.ru*

Abstract

Objectives. *To apply an analytical method for the calculation of a distillation column for the production of D_2O at a two-column Kuhn installation operating under vacuum: to simulate the Kuhn installation in the Hysys software; and to compare experimental and calculated data.*

Methods. *Analytical method for the calculation of distillation columns "from stage to stage," from the lower theoretical separation stage (TSS) to the upper stage. This method is based on phase equilibrium at the TSS with known data of input flows and component concentrations in the column bottoms. Hysys was used as modeling software.*

Results. *Comparison of the calculation results with Kuhn's experimental data testified to the high calculation accuracy of the vapor–liquid phase equilibrium for the H_2O–D_2O mixture at the TSS. The convergence of the D_2O material balance for the entire installation was 0.005%. The identification parameter was the number of the column feed plate. Simulation of the Kuhn installation in the Hysys software showed a qualitative agreement of D_2O concentrations in material flows. The UNIQUAC (UNIversal QUAsiChemical) model was used to calculate activity coefficients. The found values of the number of theoretical separation stages (NTSS) in both columns, were 88 and 153 taking into account the reboiler and condenser. This is less than the experimental 295 and 400, respectively. The discrepancy can be explained by the increased phase equilibrium H_2O constant in the UNIQUAC model. However, the convergence of the material balance in terms of D_2O was high and amounted to $1.38 \cdot 10^{-6}$%. The absolute error of the found concentrations in material flows did not exceed 0.12 mol %.*

Conclusions. *The results obtained indicated the possible use of the Hysys modeling software when searching for and optimizing the operating mode of the block diagram of a cascade of distillation columns with direct and recycle flows to separate a mixture of water into light and*

heavy water. The final results obtained with regard to the operating mode, inlet and outlet material flows (flow rate, composition, temperature, and pressure drop across the column) are recommended for use in the analytical program for the calculation of the distillation column to refine the NTSS and distribution profile of the concentrations of the H_2O and D_2O components along the height of the column.

Keywords: *light water, heavy water, Hysys, continuous distillation, separation factor, activity coefficients of H_2O and D_2O*

For citation: Korotkova T.G., Kasyanov G.I. Analysis of the rectifying separation of H_2O–D_2O mixture into light and heavy water by means of mathematical modeling. *Tonk. Khim. Tekhnol. = Fine Chem. Technol.* 2022;17(3):189–200 (Russ., Eng.). https://doi.org/10.32362/2410-6593-2022-17-3-189-200

НАУЧНАЯ СТАТЬЯ

Анализ ректификационного разделения смеси H_2O–D_2O на легкую и тяжелую воду методом математического моделирования

Т.Г. Короткова✉, Г.И. Касьянов

Кубанский государственный технологический университет, Краснодар, 350072 Россия
✉Автор для переписки, e-mail: korotkova1964@mail.ru

Аннотация

Цели. *Применение аналитического метода расчета ректификационной колонны для получения D_2O в двухколонной установке Куна, работающей под вакуумом. Моделирование установки Куна в программной среде Hysys. Сравнение экспериментальных и расчетных данных.*
Методы. *Аналитический метод расчета ректификационной колонны «от ступени к ступени» от нижней теоретической ступени разделения (ТСР) к верхней, основанный на фазовом равновесии на ТСР при известных исходных данных входных потоков и концентраций компонентов в кубе колонны. Среда моделирования Hysys.*
Результаты. *Сравнение результатов расчета с экспериментальными данными Куна свидетельствовало о высокой точности расчета равновесия фаз пар – жидкость для смеси H_2O–D_2O на ТСР. Сходимость материального баланса по D_2O по установке в целом составила 0.005%. Параметром идентификации являлся номер тарелки питания колонны. Моделирование установки Куна в среде Hysys показало качественное согласование концентраций D_2O в материальных потоках. Для расчета коэффициентов активности использована модель UNIversal QUAsiChemical (UNIQUAC). Найденные значения числа теоретических ступеней разделения (ЧТСР) в обеих колоннах с учетом ребойлера и конденсатора составляют 88 и 153, что меньше экспериментальных 295 и 400 соответственно. Расхождение объясняется повышенным значением константы фазового равновесия H_2O модели UNIQUAC, однако сходимость материального баланса по D_2O высокая и составляет $1.38 \cdot 10^{-6}$%. Абсолютная погрешность найденных значений концентраций в материальных потоках не превышает 0.12 мол. %.*
Выводы. *Полученные результаты свидетельствуют о возможном применении среды моделирования Hysys для поиска и оптимизации режима работы структурной схемы каскада ректификационных колонн с прямыми и рецикловыми потоками для разделения смеси воды*

на легкую и тяжелую воду. Полученные конечные результаты по режиму работы, входным и выходным материальным потокам (расход, состав, температура, перепад давлений по колонне) рекомендовано использовать в аналитической программе расчета ректификационной колонны для уточнения ЧТСР и профиля распределения концентраций компонентов H_2O и D_2O по высоте колонны.

Ключевые слова: *легкая вода, тяжелая вода, Hysys, непрерывная ректификация, коэффициент разделения, коэффициенты активности H_2O и D_2O*

Для цитирования: Короткова Т.Г., Касьянов Г.И. Анализ ректификационного разделения смеси H_2O–D_2O на легкую и тяжелую воду методом математического моделирования. *Тонкие химические технологии*. 2022;17(3):189–200. https://doi.org/10.32362/2410-6593-2022-17-3-189-200

INTRODUCTION

It is impossible to improve and optimize technological schemes for the separation of homogeneous mixtures by the method of rectification without the use of modern software for modeling complex chemical-technological systems (CCTS). For this purpose, modern software is equipped with a library of component properties, modules for calculating apparatuses, mathematical modules for ensuring the convergence of calculations, equations for calculating the properties of a multicomponent mixture, etc. The availability of programming tools and the level of development of visualization allows such software as Matlab (Matrix Laboratory) to be created. This tool is a package of applied programs for technical calculations, engineering, and scientific problems in any industry. SPSS Statistics (Statistical Package for the Social Sciences) is a computer program for applied research and statistical data processing. ChemCad (Chemical Computer-Aided Design) is used mainly in modeling processes and flowsheets of chemical and petrochemical industries. Ansys Fluent is a software and computational complex for modeling the flows of liquids and gasses in the aerospace industry, automotive, turbomachinery, oil and gas, and chemical industries. Hysys (Aspen Hysys) is a programming software for technological schemes of an arbitrary structure of chemical and technological industries and other software packages for computer simulation.

Simulation of CCTS allows the results obtained to be analyzed not on an operational plant, but in computer systems with a range of different devices and technological modes of their operation. This optimizes the technological scheme allowing the desired product quality to be achieved or energy costs minimized with subsequent implementation in industrial production.

The widespread use of Hysys in CCTS modeling is due to the multi-circuit architecture in Hysys which allows an arbitrary number of circuits to be created within one calculation. If necessary, you can use your own thermodynamic package of properties in each subcircuit. A large scheme can be divided into separate sections and the mode of operation of a particular section of the technological scheme can be found. Therefore, the structure of the technological scheme, consisting of a set of apparatuses and devices, changing the parameters of their operation mode, such as process temperature, pressure, and component composition can be optimized.

In [1], the designs of heat pumps of closed and open “pipe in pipe” types were considered, while the adequacy of the computer model of the “rectification unit–heat pump of closed type” system was checked using the Hysys simulation software. In [2], the Hysys software was used to perform a simulation of a crude oil distillation unit. This included four main stages: preliminary evaporation, atmospheric, stabilizing, and vacuum.

When water is separated by distillation into light (H_2O) and heavy (D_2O) water, the number of theoretical separation stages (NTSS) is very large. Therefore, a cascade of several columns of tray or packed type is used rather than one distillation column [3]. The Hysys data library contains the physicochemical properties of the H_2O and D_2O components. In this case, the use of modern modeling software for the analysis and improvement of such

CCTS is reasonable and necessary. However, there are no publications on the study of the use of the Hysys simulation software for the separation of a mixture of H_2O–D_2O into light and heavy water.

In this paper, we propose the use of Hysys simulation software for the development of technological schemes consisting of a cascade of distillation columns with direct and recycle flows to separate the H_2O–D_2O mixture into light and heavy water. This is followed by refinement of the NTSS and the profile of the distribution of component concentrations along the height of the column based on the analytical column calculation method [4].

METHODS

The modeling of distillation is based on the calculation of the vapor–liquid phase equilibrium at the theoretical separation stage (TSS), the reliability of the description of which affects the quality of the separated products. The main difficulty is the choice of an equation for calculating the activity coefficients of the components.

The group composition models the following: UNIversal Functional Activity Coefficient (UNIFAC), UNIversal QUAsiChemical (UNIQUAC), Non Random Two Liquid (NRTL) models, etc. It also models their modifications [5], which have proven themselves well in the calculation of column distillation apparatuses in the chemical industry. Such have been widely developed in chemical [6], oil refining, petrochemical [7], and alcohol industries [8, 9] in the separation of multicomponent mixtures with a slight deviation from the Raoult law and azeotropic mixtures in the production of bioethanol [10, 11], characterized by strong nonideality.

In the analytical methods proposed for calculating column apparatus when separating a mixture of H_2O–D_2O into light and heavy water, the activity coefficients γ_{H_2O} and γ_{D_2O} were not considered [3], or the mixture was classified as ideal both in the liquid and vapor phases [12]. It is equivalent to equating the activity coefficients to units.

We have shown [4] that the H_2O–D_2O mixture is not ideal, i.e., it does not obey the Raoult law. Based on the material balance equations, the equilibrium equation, and the equation for calculating the separation coefficient (H.C. Urey), Eqs. (1) and (2) for calculating the activity coefficients of the H_2O and D_2O components were obtained based on the assumption that the mixture being separated consists of two components H_2O and D_2O. A method for the calculation of the column "from stage to stage," including the calculation of phase equilibrium on the TSS, was proposed.

$$\gamma_{H_2O} = \frac{1}{\frac{P^{\circ}_{H_2O}}{P} x_{H_2O} + \alpha_{H-D} \frac{P^{\circ}_{D_2O}}{P} x_{D_2O}}, \quad (1)$$

$$\gamma_{D_2O} = \frac{1}{\frac{1}{\alpha_{H-D}} \frac{P^{\circ}_{H_2O}}{P} x_{H_2O} + \frac{P^{\circ}_{D_2O}}{P} x_{D_2O}}, \quad (2)$$

The activity coefficients of the H_2O and D_2O components are interconnected by the separation factor α_{H-D}.

$$\gamma_{D_2O} = \alpha_{H-D} \cdot \gamma_{H_2O} \quad (3)$$

Based on a comparison of experimental and calculated data, the applicability of this method to the separation of an isotopic mixture of H_2O–D_2O into light and heavy water is shown.

RESULTS AND DISCUSSION

Let us apply the method of calculating a distillation column for separating a mixture of H_2O–D_2O, as described in [4], to the well-known experimental two-column Kuhn installation for obtaining D_2O. The material balance of this installation is shown in Fig. 1 [13]. The height of the separating part of the first stage is 530 cm; the height of the equivalent theoretical stage (HETS) is 1.8 cm; the height of the separating part of the second stage is 680 cm; while HETS is 1.7 cm. The pressure in the upper part of the first stage is 120 mm Hg, and the pressure in the upper part of the second stage is 60 mm Hg. The calculation will be carried out for each stage separately. In relation to the hardly volatile component D_2O, the input flow (feed) divides the column into two parts: the upper (exhaustive) and the lower (strengthening). By analyzing the initial data of the Kuhn installation (Fig. 1), we can determine the values of the quantities necessary for modeling each stage (Tables 1 and 2). In Fig. 1 and in Tables 1 and 2, the concentration of D_2O is given in mol %.

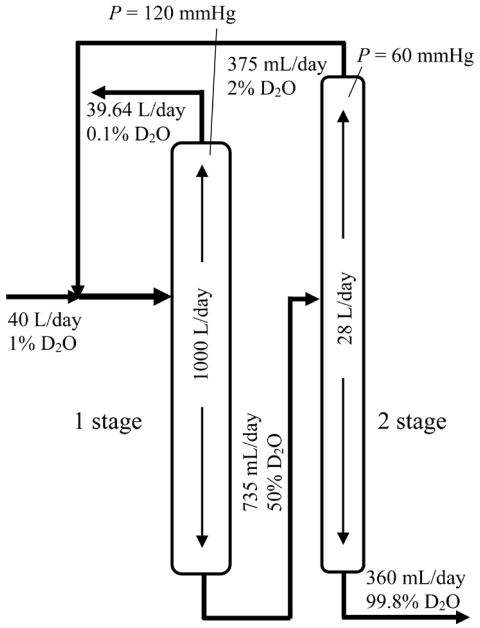

Fig. 1. Scheme of material balance of two-stage Kuhn plant to obtain D_2O.

In Tables 1 and 2, the reflux ratio R is defined as the ratio of the amount of liquid stream flowing down the column, to the amount of distillate withdrawn from the top of the column. The molar flow rates of material flows are determined by known expressions. These expressions take into account the average value of the density and the average value of the molar mass of the flow, depending on the concentrations of the H_2O and D_2O components in the flow. When recalculating, the following is assumed: the molar mass of H_2O is 18.02 kg/kmol, D_2O is 20.03 kg/kmol; while the density, taking into account the separation process under vacuum H_2O, is 998 kg/m^3, D_2O 1108 kg/m^3 [14, 15]. NTSS in columns is determined by the ratio of the height of the separating part of the stage to HETS. In the first approximation, it is assumed when modeling that the pressure at the bottom of the first stage is 18 kPa, the pressure of the second stage is 9 kPa.

The feed plate number was taken as the identification parameter. The calculation of the column was carried out by the method "from stage to stage" from the bottom up. The plates are numbered from bottom to top. The results of the calculation are shown in Fig. 2. The convergence of the material

Table 1. Initial data of the Kuhn installation

Stage number	Material flows							
	L/day				kmol/day			
	F	*D*	*W*	Rec	*F*	*D*	*W*	Rec
1 stage	40	39.64	0.735	0.375	2.20202	2.18216	0.0405	0.02064
2 stage	0.735	0.375	0.36	–	0.0405	0.02064	0.01986	–

Note: *F* is feed; *D* is distillate; *W* is bottom residue; Rec is recycling.

Table 2. Initial data of the Kuhn installation (continued)

Stage number	D_2O concentration, mol %				*P*, kPa	*R*	*f*	NTSS
	x_F	x_D	x_W	x_{rec}				
1 stage	1.0	0.1	50	2.0	16	25.227	1.0091	295
2 stage	50	2.0	99.8	–	8	74.667	1.9622	400

Note: x_F, x_D, x_W, x_{rec} are D_2O concentrations in feed, distillate, bottoms, and recycle, respectively; *P* is the pressure of the top of the column; *R* is the reflux ratio; $f = F/D$.

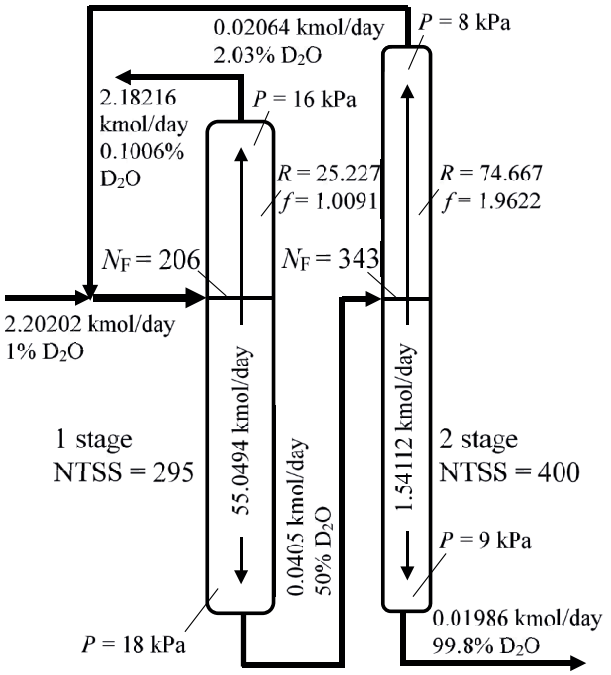

Fig. 2. Calculated data for the two-column Kuhn installation based on the analytical calculation method.

balance for D_2O for the entire plant was 0.0005%. The profile of the change in D_2O concentration along the height of the columns at the first and second stages is shown in Fig. 3.

Point *a* characterizes the transition from the strengthening part of the column to the exhaustive part. The observed break in the curves of the concentration profile corresponds to the general ideas regarding the change in concentrations in the liquid phase in the feed zone of the distillation column.

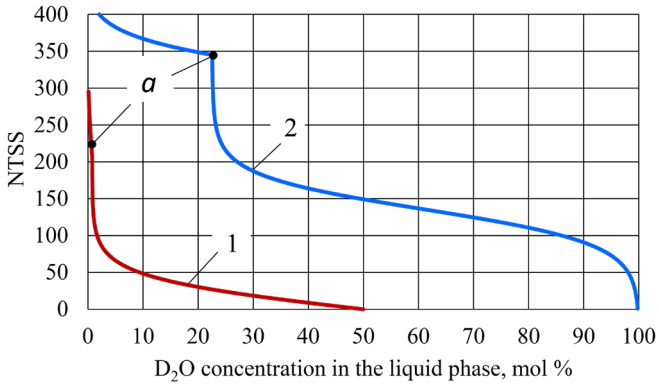

Fig. 3. Profile of change in the D_2O concentration along the height of the columns based on the analytical method of calculation: (1) first stage; (2) second stage.

Analysis of the dependence of the activity coefficient of the H_2O and D_2O components on the mixture composition at $P = const$

Based on the algorithm for calculating the boiling point of a mixture of H_2O–D_2O, as described in [4], incorporating a block for calculating phase equilibrium on TSS, a program was developed in the Borland Pascal language. As an example, in Fig. 4 shows the results of calculating the activity coefficients of the H_2O and D_2O components for atmospheric pressure P = 101.325 kPa and for reduced pressure P = 60 kPa, with a change in the D_2O concentration in the liquid phase from 0 to 100 mol %. The accuracy of calculating the boiling point of the mixture on the plate is $\varepsilon = 10^{-10}$°C.

Based on the appearance of the dependences of the activity coefficients γ_{H_2O} and γ_{D_2O} (Fig. 4), it can be concluded that they are practically straight lines at P = const. This is because the separation coefficient α_{H-D} depends on the pressure and boiling point of the H_2O–D_2O mixture, which changes slightly with a change in the composition of the mixture at P = const. However, with a pressure drop along the height of the column, as shown in [4], the change in the activity coefficients of these components is nonlinear. The values of the activity coefficients of both components are within unity, while the value of the activity coefficient of deuterium oxide γ_{D_2O} is greater than that of hydrogen oxide γ_{H_2O} in the entire range of concentrations. This result is embedded in Eq. (3), in which the separation factor $\alpha_{H-D} > 1$. Also, $\gamma_{D_2O} > 1$, but $\gamma_{H_2O} < 1$, and at concentrations equal to 1, the activity coefficients are also equal to 1.

Activity coefficients γ_{H_2O} and γ_{D_2O}, calculated by the UNIQUAC group composition method.

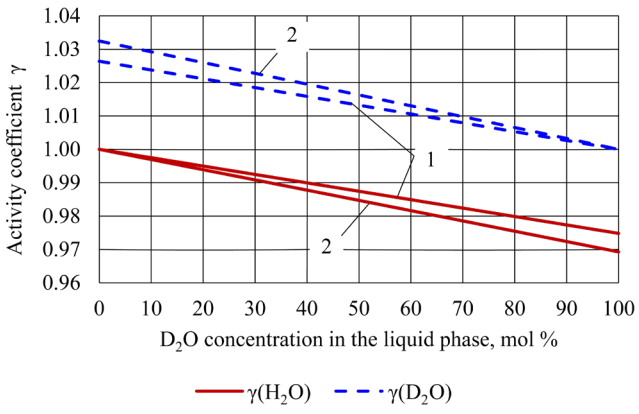

Fig. 4. Dependence of the activity coefficients of the H_2O and D_2O components calculated by Eqs. (1) and (2) on the D_2O concentration in the liquid phase at: (1) P = 101.325 kPa and (2) P = 60 kPa.

The mathematical form is given in [5]: it changes from 0.997 to 1.000 when D_2O changes from 0 to 100 mol % in a mixture of H_2O–D_2O. The calculation was carried out at P = 101.325 kPa and P = 60 kPa. Therefore, their values are almost equal to 1, which is typical for ideal mixtures.

The predicted parameters of the binary energy interaction Δu_{12} and Δu_{21} of the UNIQUAC model between the molecules of the H_2O and D_2O components were taken from the database of the Hysys software (Table 3).

Optimizing the parameters of the energy binary interaction Δu_{12} and Δu_{21} of the UNIQUAC model in the range of change from $-\infty$ to $+\infty$ did not lead to an increase in the accuracy of calculating α_{H-D} the H_2O–D_2O mixture. It should be noted that for large values of the binary interaction parameters Δu_{12} and Δu_{21} regardless of their sign, the equilibrium curve in the x–y diagram intersects the diagonal of the square, meaning the presence of an azeotrope point. This is not supported by experimental data and the industrial method for separating a mixture of H_2O and D_2O, i.e., the H_2O–D_2O mixture is not azeotropic. A similar picture was obtained when optimizing the parameters of the NRTL equation (Δg_{12}, Δg_{21}, and α_{12}). Therefore, further calculations give the parameters presented in Table 3.

The calculated value of the separation factor α_{H-D} using the UNIQUAC model at atmospheric pressure was 1.053 (at $x_{H_2O} = x_{D_2O}$ = 0.5 mol %), while the experimental value was 1.026 [16]. The values of the separation factors in the analytical calculation of the activity coefficients γ_{H_2O} and γ_{D_2O} are consistent with the experimental values.

Figure 5 shows the curves of the separation factors, constructed according to Eq. (4) and according to the UNIQUAC method. The vapor pressure of the pure component was calculated using the Antoine equation, the mathematical form of which and the equation constants are given in [4].

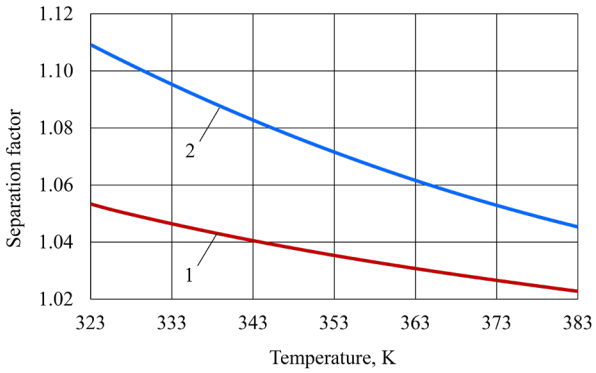

Fig. 5. Dependence of the separation factor on temperature: (1) calculation according to Eq. (4); (2) calculation according to UNIQUAC.

$$\alpha_{H-D} = \sqrt{\frac{P^{\circ}_{H_2O}}{P^{\circ}_{D_2O}}} \quad (4)$$

Thus, when considering the H_2O–D_2O isotopic mixture as ideal, the separation factor α_{H-D} (curve 2, Fig. 5) exceeds the known experimental data considered by us in [17]. This data is consistent with that constructed using Eq. (4) (curve 1, Fig. 5), and coincides with the curve based on the analytical calculation method.

Let us consider the effect of the difference in the separation factor thus defined on the phase equilibrium in the vapor–liquid system of the H_2O–D_2O binary mixture. Let us take the phase equilibrium constant K_{H_2O} as the ratio of the equilibrium molar concentrations of H_2O in the vapor y_{H_2O} and liquid x_{H_2O} phases. We will carry out the calculation based on the UNIQUAC method and Eq. (5).

$$K_{H_2O} = \frac{y_{H_2O}}{x_{H_2O}} = \frac{P^{\circ}_{H_2O}}{P}\gamma_{H_2O}, \quad (5)$$

where γ_{H_2O} will be calculated with Eq. (1) and the separation factor in Eq. (1) is determined by Eq. (4).

Table 3. Parameters of the UNIQUAC model (according to Hysys)

Component	*r*	*q*	Δu_{12}, cal/mol, H_2O (1)	Δu_{21}, cal/mol, D_2O (2)
H_2O (1)	0.92	1.3997	–	−48.413
D_2O (2)	0.92	1.3998	48.724	–

Note: *r* and *q* are volume and area parameters of the components. The energy parameters of the binary interaction Δu_{12} and Δu_{21} are given at the universal gas constant R = 1.98721 cal/(mol·K).

The results of the calculation are shown in Fig. 6 for two pressures P = 101.325 kPa and P = 60 kPa. Data analysis in Fig. 6 shows that with decreasing pressure, the phase equilibrium constant of the highly volatile component H_2O increases, while with an increase in the concentration of H_2O in the liquid phase, it also decreases at x_{H_2O} = 1. The constant is equal to one, which is already known. A change in pressure does not lead to a change in the qualitative picture of the phase equilibrium constant. The shape of the curves is close to linear at P = const. However, when calculating distillation columns, the pressure drop across the column has a significant effect on the nonlinearity of this dependence [4]. The value of the phase equilibrium constant in the calculation by the UNIQUAC method is greater than in the analytical calculation method, which includes the calculation of the separation factor α_{H-D} according to the Urey's Eq. (4). Despite a slight difference in hundredths, this discrepancy, as will be shown below, leads to a significant decrease in the NTSS as determined in Hysys software when calculating the activity coefficients using the UNIQUAC method.

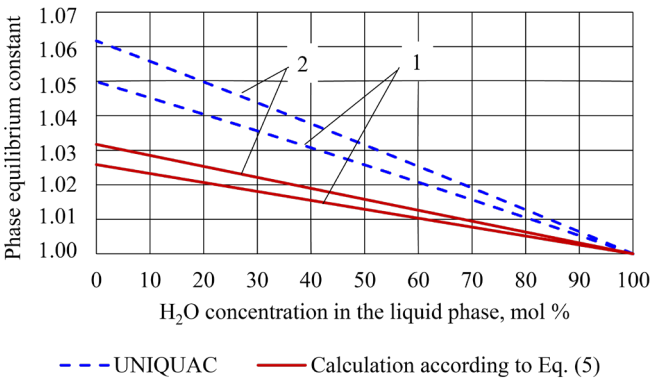

Fig. 6. Dependence of the H_2O phase equilibrium constant on its composition in the liquid phase for the H_2O–D_2O mixture: (1) P = 101.325 kPa; (2) P = 60 kPa.

Thus, the main influence on the phase equilibrium constant is exerted by the vapor pressure of the pure component, which can be determined with a high level of accuracy. We do not recommend taking the activity coefficients of the H_2O and D_2O components equal to 1 into the analytical calculation method, since the H_2O–D_2O mixture is not ideal.

Let us simulate a two-column Kuhn installation in the Hysys software. The block diagram with the calculation results in tabular form in the Hysys graphical software is shown in Fig. 7. The pressure in the upper part of the columns was determined according to Kuhn's experimental data, and is 0.016 MPa (120 mm Hg) for the first stage, 0.008 MPa (60 mm Hg) for the second stage. The pressure in the lower part of the column of the first stage was 0.018 MPa, while the pressure of the second stage was 0.009 MPa. In the column of the first stage, the reflux ratio and the amount of withdrawal of distillate were taken as active specifications; while in the column of the second stage—the reflux ratio and the amount of with drawal of the distillate residue. The calculation of the activity coefficients of the H_2O and D_2O components was performed using the UNIQUAC method. We took the NTSS and the number of the feed plate for each column as identification parameters. The simulation results are given in Table 4 and in the flow tables in Fig. 7.

For the first stage, the NTSS was 86, excluding the reboiler and condenser, the feed plate was numbered 67th. For the second stage, the NTSS was 151; the feed plate was 136th. The TSS values discovered in both columns were 88 and 153, including the reboiler and condenser. These were less than the experimental values (295 and 400) in the Kuhn installation. The D_2O concentration profile was smoother (Fig. 8) compared to the profile shown in Fig. 3. This can be explained by the error in calculating the phase equilibrium constants

Table 4. Material balance of the two-column Kuhn plant in the Hysys environment

Stage number	Material flows, kmol/day				D_2O concentration, mol %				*R*	NTSS	N_F
	F	*D*	*W*	Rec	x_F	x_D	x_W	x_{rec}			
1 stage	2.2159	2.1959	0.04069	0.02077	1	0.10242	49.997	2.0851	25.23	86	67
2 stage	0.04069	0.02077	0.01991	–	49.997	2.0851	99.977	–	74.67	151	136

Note: N_F is the feed plate number; number of theoretical separation stages (NTSS) does not include a reboiler and a dephlegmator condenser.

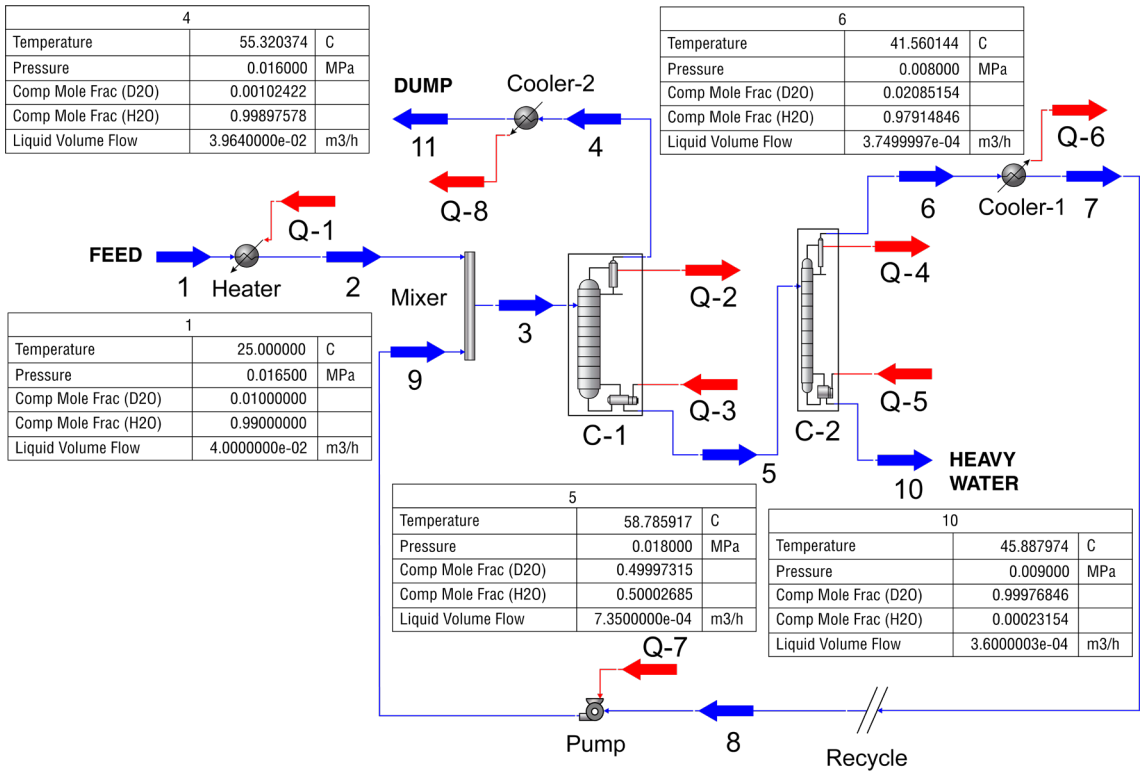

Fig. 7. Graphical interface of the Kuhn installation in the Hysys software: C-1, C-2 are distillation columns; 1–11 are material flows; Q-1–Q-8 are energy (heat) flows.

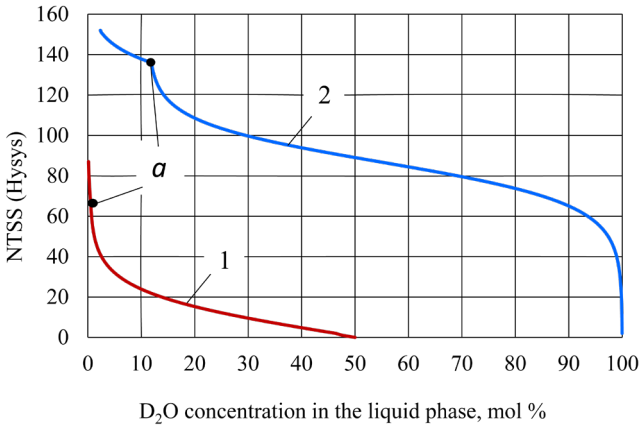

Fig. 8. Profile of change in D_2O concentration along the height of the columns (according to the calculation data in the Hysys simulation software): (1) first stage; (2) second stage.

using the UNIQUAC method. However, the convergence of the material balance for D_2O was $1.38 \cdot 10^{-6}$% and the absolute error of the found values of concentrations in material flows did not exceed 0.12 mol %.

The results obtained indicate that the Hysys software can be recommended when searching for and optimizing the block diagram of a cascade of distillation columns with direct and recycle flows, designed to separate a mixture of H_2O–D_2O. The calculated data obtained in Hysys on the inlet and outlet flows of each column (flow rate, composition, temperature, and pressure) can be used in the analytical program for the calculation of the distillation column to refine the NTSS and the distribution profile of the concentrations of the H_2O and D_2O components along the height of the column.

CONCLUSIONS

The simulation of an experimental two-column Kuhn installation for D_2O production was carried out based on the analytical method for calculating the column, as well as using Hysys simulation software. The calculation of the activity coefficients of the H_2O and D_2O components in the analytical method of calculation was performed according to Eqs. (1) and (2), and in the Hysys software, according to the UNIQUAC equation. Both calculations showed sufficient convergence of calculated and experimental data in material flows. The NTSS found in the Hysys software in both columns, taking into account the reboiler and condenser, are 88 and 153. This is less than the experimental 295 and 400, respectively.

Analysis of the graphical dependences of the activity coefficients γ_{H_2O} and γ_{D_2O} of the H_2O and D_2O components on the D_2O concentration in the liquid phase at P = 101.325 kPa and P = 60 kPa, calculated by Eqs. (1) and (2), showed that $\gamma_{D_2O} > 1$ and $\gamma_{H_2O} < 1$, and at concentrations equal to 1, the activity coefficients are equal to 1. The main influence on the phase equilibrium constant is exerted by the vapor pressure of the pure component, which is determined with a high level of accuracy.

The activity coefficients of the H_2O and D_2O components calculated by the UNIQUAC method at P = 101.325 kPa and P = 60 kPa vary in the range from 0.997 to 1.000. However, both are less than 1, affecting the value of the separation coefficient $\alpha_{H–D}$, which at atmospheric pressure was 1.053 (at $x_{H_2O} = x_{D_2O}$ = 0.5 mole fractions), while the experimental value was 1.026.

An overestimated value of the separation factor $\alpha_{H–D}$ led to an increase in the phase equilibrium constant of H_2O, which affected the NTSS in the column. However, the convergence of the material balance for D_2O is high and amounted to $1.38 \cdot 10^{-6}$%. The absolute error of the values of concentrations in material flows did not exceed 0.12 mol %.

As a result of the studies, it can be concluded that the Hysys software can be further used to search, analyze, and optimize the operating mode of technological schemes which consist of a cascade (from 2 or more) distillation columns equipped with direct and recycle flows to separate a mixture of H_2O–D_2O, in order to obtain heavy or light water with a given content of deuterium oxide under industrial conditions. After developing the circuit in the Hysys software and determining the operating mode and parameters of the inlet and outlet flows (flow rate, composition, temperature, pressure drop across the column, etc.), the NTSS in the columns must be refined based on an analytical calculation using Eqs. (1) and (2) for the calculation of activity coefficients γ_{H_2O} and γ_{D_2O} of the H_2O and D_2O components, while the profile of changes in the concentrations of the components along the height of the column must also be determined.

Authors' contribution

All authors equally contributed to the research work.

The authors declare no conflicts of interest.

REFERENCES

1. Plotnikova L.V., Chilikova I.I., Sitnikov S.Y., Ukhlin V.E., Efremov G.I., Kislov A.P. Computer model of the power system with inclusion of a heat pump in the process of separation. *E3S Web of Conf*. 2019;124:01032. https://doi.org/10.1051/e3sconf/201912401032

2. Sotelo D., Favela-Contreras A., Lozoya C., Beltran-Carbajal F., Dieck-Assad G., Sotelo C. Dynamic simulation of a crude oil distillation plant using Aspen-Hysys. *Int. J. Simul. Model.* 2019;18(2):229–241. https://doi.org/10.2507/IJSIMM18(2)465

3. Magomedbekov E.P., Belkin D.Yu., Rastunova I.L., Sazonov A.B., Selivanenko I.L., Kulov N.N. Simulation and Optimization of the Deprotiation Cascade of a Heavy-Water Moderator. *Theor. Found. Chem. Eng*. 2017;51(2):133–141. https://doi.org/10.1134/S004057951702004X

[Original Russian Text: Magomedbekov E.P., Belkin D.Yu., Rastunova I.L., Sazonov A.B., Selivanenko I.L., Kulov N.N. Simulation and Optimization of the Deprotiation Cascade of a Heavy-Water Moderator. *Teoreticheskie osnovy khimicheskoi tekhnologii*. 2017;51(2):131–139 (in Russ.). https://doi.org/10.7868/S0040357117020051]

4. Korotkova T.G., Kas'yanov G.I. Calculating a Rectification Column for Separating Mixtures of Light and Heavy Water. *Russ. J. Phys. Chem.* 2021;95(5):1051–1060. https://doi.org/10.1134/S0036024421050186

СПИСОК ЛИТЕРАТУРЫ

1. Plotnikova L.V., Chilikova I.I., Sitnikov S.Y., Ukhlin V.E., Efremov G.I., Kislov A.P. Computer model of the power system with inclusion of a heat pump in the process of separation. *E3S Web of Conf*. 2019;124:01032. https://doi.org/10.1051/e3sconf/201912401032

2. Sotelo D., Favela-Contreras A., Lozoya C., Beltran-Carbajal F., Dieck-Assad G., Sotelo C. Dynamic simulation of a crude oil distillation plant using Aspen-Hysys. *Int. J. Simul. Model.* 2019;18(2):229–241. https://doi.org/10.2507/IJSIMM18(2)465

3. Магометбеков Э.П., Белкин Д.Ю., Растунова И.Л., Сазонов А.Б., Селиваненко И.Л., Кулов Н.Н. Математическое моделирование и оптимизация каскада депротизации тяжеловодного замедлителя. *Теор. основы хим. технологии.* 2017;51(2):131–139. https://doi.org/10.7868/S0040357117020051

4. Короткова Т.Г., Касьянов Г.И. Метод расчета ректификационной колонны для разделения смеси легкой и тяжелой воды. *Журн. физ. химии*. 2021;95(5):800–809. https://doi.org/10.31857/S0044453721050186

5. Уэйлес С. *Фазовые равновесия в химической технологии*: в 2 ч.; пер. с англ. А.В. Беспалова, А.П. Жукова, В.В. Паукова. М.: Мир; 1989. Ч. 1. 301 с. Ч. 2. 360 с.

6. Alshbuki E.H., Bey M.M., Mohamed A.A. Simulation Production of Dimethylether (DME) from Dehydration of Methanol Using Aspen Hysys. *Sch. Int. J. Chem. Mater. Sci.* 2020;3(2):13–18. https://doi.org/10.36348/sijcms.2020.v03i02.002

[Original Russian Text: Korotkova T.G., Kas'yanov G.I. Calculating a Rectification Column for Separating Mixtures of Light and Heavy Water. *Zhurnal fizicheskoi khimii*. 2021;95(5):800–809 (in Russ.). https://doi.org/10.31857/S0044453721050186]

5. Walas S. *Fazovye ravnovesiya v khimicheskoi tekhnologii* (*Phase equilibria in chemical technology*). In 2 v.; transl. from Engl. Moscow: Mir; 1989. V. 1. 301 p. V. 2. 360 p. (in Russ.).

6. Alshbuki E.H., Bey M.M., Mohamed A.A. Simulation Production of Dimethylether (DME) from Dehydration of Methanol Using Aspen Hysys. *Sch. Int. J. Chem. Mater. Sci*. 2020;3(2):13–18. https://doi.org/10.36348/sijcms.2020.v03i02.002

7. Ivanov I.V., Lotkhov V.A., Kulov N.N. Modeling of batch extractive distillation. *Theor. Found. Chem. Eng.* 2017;51(3):253–261. https://doi.org/10.1134/S004057951703006X

[Original Russian Text: Ivanov I.V., Lotkhov V.A., Kulov N.N. Modeling of batch extractive distillation. *Teoreticheskie osnovy khimicheskoi tekhnologii*. 2017;51(3):239–247 (in Russ.). https://doi.org/10.7868/S004035711703006X]

8. Gil I.D., Uyazán A.M., Aguilar J.L., Rodríguez G., Caicedo L.A. Separation of ethanol and water by extractive distillation with salt and solvent as entrainer: process simulation. *Braz. J. Chem. Eng*. 2008;25(01):207–215. https://doi.org/10.1590/S0104-66322008000100021

9. Korotkova T.G., Konstantinov E.N. Modeling technology for food alcohol on distillation plant. *Izvestiya vuzov. Pishchevaya tekhnologiya = Food Technology.* 2012;1(325):108–111 (in Russ.).

10. Jorge L.M.M, Polli P.A., Nicolin D.J., Jorge R.M.M., Paraíso P.R., Filho R.M. Simulation and analysis of an industrial column system of bioethanol distillation heated by vapor direct injection. *ENGEVISTA*. 2015;17(2):254–265. https://doi.org/10.22409/engevista.v17i2.657

11. Korotkova T.G., Konstantinov E.N. Production technology of anhydrous ethyl alcohol azeotropic method. *Izvestiya vuzov. Pishchevaya tekhnologiya = Food Technology.* 2013;1(331):72–76 (in Russ.).

12. Bhattacharyya R, Bhanja K. Studies on the Dynamic Behaviour and Hydraulic Characteristics of a Water Distillation Column. *Chem. Technol. Ind. J.* 2018;13(2):125. URL: https://www.tsijournals.com/articles/studies-on-the-dynamic-behaviour-and-hydraulic-characteristics-of-a-water-distillation-column-13803.html

13. Krell E. *Handbuch der Labaratoriumsdestillation*. Berlin; 1976.

[Krel' E. *Rukovodstvo po laboratornoi peregonke*. (*Handbook on laboratory distillation*) transl. from German. Moscow: Khimiya; 1980. 520 p. (in Russ.).]

14. Vargaftik N.B. *Spravochnik po teplofizicheskim svoistvam gazov i zhidkostei* (*Reference book on thermophysical properties of gases and liquids*). Moscow: Nauka; 1972. 720 p. (in Russ.).

15. Volkov A.I., Zharskii I.M. *Bol'shoi khimicheskii spravochnik* (*Big chemical reference book*). Minsk: Sovremennaya shkola; 2005. 608 p. (in Russ.).

16. Rozenkevich M.B., Rastunova I.L. Theoretical foundations of isotope separation processes. In: *Interaction of Hydrogen Isotopes with Structural Materials*: *Abstracts of presentations at the V International Conference and IX International School for Young Scientists and Specialists*. Sarov; 2015. P. 57–76 (in Russ.). URL: http://book.sarov.ru/wp-content/uploads/2017/12/IHISM-14-5.pdf

7. Иванов И.В., Лотхов В.А., Кулов Н.Н. Моделирование процесса периодической экстрактивной ректификации. *Теор. основы хим. технологии.* 2017;51(3):239–247. https://doi.org/10.7868/S004035711703006X

8. Gil I.D., Uyazán A.M., Aguilar J.L., Rodríguez G., Caicedo L.A. Separation of ethanol and water by extractive distillation with salt and solvent as entrainer: process simulation. *Braz. J. Chem. Eng*. 2008;25(01):207–215. https://doi.org/10.1590/S0104-66322008000100021

9. Короткова Т.Г., Константинов Е.Н. Моделирование технологии получения пищевого спирта на брагоректификационной установке. *Изв. вузов. Пищевая технология*. 2012;1(325):108–111.

10. Jorge L.M.M, Polli P.A., Nicolin D.J., Jorge R.M.M., Paraíso P.R., Filho R.M. Simulation and analysis of an industrial column system of bioethanol distillation heated by vapor direct injection. *ENGEVISTA*. 2015;17(2):254–265. https://doi.org/10.22409/engevista.v17i2.657

11. Короткова Т.Г., Константинов Е.Н. Технология получения безводного этилового спирта азеотропным методом. *Изв. вузов. Пищевая технология.* 2013;1(331):72–76.

12. Bhattacharyya R, Bhanja K. Studies on the Dynamic Behaviour and Hydraulic Characteristics of a Water Distillation Column. *Chem. Technol. Ind. J.* 2018;13(2):125. URL: https://www.tsijournals.com/articles/studies-on-the-dynamic-behaviour-and-hydraulic-characteristics-of-a-water-distillation-column-13803.html

13. Крель Э. *Руководство по лабораторной перегонке*: пер. с нем. М.: Химия; 1980. 520 с.

14. Варгафтик Н.Б. *Справочник по теплофизическим свойствам газов и жидкостей*. М.: Наука; 1972. 720 с.

15. Волков А.И., Жарский И.М. *Большой химический справочник*. Минск: Современная школа; 2005. 608 с.

16. Розенкевич М.Б., Растунова И.Л. *Теоретические основы процессов разделения изотопов. Взаимодействие изотопов водорода с конструкционными материалами. IHISM'14: Сборник докладов Пятой Международной конференции и Девятой Международной школы молодых ученых и специалистов им. А.А. Курдюмова*. Саров: ФГУП «РФЯЦ-ВНИИЭФ»; 2015. С. 57–76. URL: http://book.sarov.ru/wp-content/uploads/2017/12/IHISM-14-5.pdf

17. Korotkova T.G., Kasyanov G.I., Baryshev M.G. Validation for adequacy description of the vapor-liquid phase equilibrium at the theoretical step when separating a mixture of light and heavy water by rectification. *Egyptian J. Chem*. 2022;65(2):591–595**.** https://doi.org/10.21608/ejchem.2021.94114.4433

17. Korotkova T.G., Kasyanov G.I., Baryshev M.G. Validation for adequacy description of the vapor-liquid phase equilibrium at the theoretical step when separating a mixture of light and heavy water by rectification. *Egyptian J. Chem*. 2022;65(2):591–595.

About the authors:

Tatyana G. Korotkova, Dr. Sci. (Eng.), Professor, Department of Life Safety, Kuban State Technological University (2, Moskovskaya ul., Krasnodar, 350072, Russia). E-mail: korotkova1964@mail.ru. Scopus Author ID 56195415000, ResearcherID AAQ-3126-2021, RSCI SPIN-code 3212-7120, https://orcid.org/0000-0001-9278-871X

Gennady I. Kasyanov, Dr. Sci. (Eng.), Professor, Department of Food Technology of Animal Origin, Kuban State Technological University (2, Moskovskaya ul., Krasnodar, 350072, Russia). E-mail: g_kasjanov@mail.ru. Scopus Author ID 57063475000, RSCI SPIN-code 1518-7974, https://orcid.org/0000-0001-9848-7715

Об авторах:

Короткова Татьяна Германовна, д.т.н., доцент, профессор кафедры безопасности жизнедеятельности ФГБОУ ВО «Кубанский государственный технологический университет (350072, Россия, г. Краснодар, ул. Московская, д. 2). E-mail: korotkova1964@mail.ru. Scopus Author ID 56195415000, ResearcherID AAQ-3126-2021, SPIN-код РИНЦ 3212-7120, https://orcid.org/0000-0001-9278-871X

Касьянов Геннадий Иванович, д.т.н., профессор, профессор кафедры технологии продуктов питания животного происхождения ФГБОУ ВО «Кубанский государственный технологический университет (350072, Россия, г. Краснодар, ул. Московская, д. 2). E-mail: g_kasjanov@mail.ru. Scopus Author ID 57063475000, SPIN-код РИНЦ 1518-7974, https://orcid.org/0000-0001-9848-7715

The article was submitted: March 31, 2022; approved after reviewing: April 12, 2022; accepted for publication: June 13, 2022.

Translated from Russian into English by H. Moshkov
Edited for English language and spelling by Dr. David Mossop

CHEMISTRY AND TECHNOLOGY OF ORGANIC SUBSTANCES

ХИМИЯ И ТЕХНОЛОГИЯ ОРГАНИЧЕСКИХ ВЕЩЕСТВ

ISSN 2686-7575 (Online)

https://doi.org/10.32362/2410-6593-2022-17-3-201-209

UDC 547.464.7

RESEARCH ARTICLE

Heterogeneous catalytic reduction of substituted 5-acyl-1,3-dioxanes

Airat I. Musin[1], Yulianna G. Borisova[2,✉], Gul'nara Z. Raskil'dina[2], Rustem R. Daminev[2], Artur R. Davletshin[2], Simon S. Zlotskii[2]

[1]Institute of Chemical Technology and Engineering, Ufa State Petroleum Technological University, Sterlitamak, 453118 Russia
[2]Ufa State Petroleum Technological University, Ufa, 450064 Russia
[✉]Corresponding author, e-mail: yulianna_borisova@mail.ru

Abstract

Objectives. *To study the hydrogenation of substituted 5-acyl-1,3-dioxanes in the presence of metal-containing catalysts (Pt/Re, Pd/C, Ni/kieselguhr, and Ni/Mo).*
Methods. *In order to determine the qualitative and quantitative composition of the reaction masses, the following analysis methods were used: gas-liquid chromatography (using the Kristall 2000 hardware complex); mass-spectroscopy (using Chromatec-Kristall 5000M device with NIST 2012); nuclear magnetic resonance (NMR) spectrometry (using Bruker AM-500 device with operating frequencies of 500 and 125 MHz).*
Results. *Hydrogenation of substituted 5-acyl-1,3-dioxanes obtained by condensation of carbonyl compounds with paraformaldehyde and sulfuric acid was used to synthesize heterocyclic alcohols in the presence of metal-containing catalysts with a conversion of the initial ketones of 60–90% and a formation selectivity of target products of 70–90%. Substances were analyzed and confirmed by gas-liquid chromatography, mass spectrometry and NMR spectroscopy.*
Conclusions. *The best catalyst for the reduction of substituted 5-acyl-1,3-dioxanes is Pd/C. By using this catalyst, it is possible to achieve a high selectivity for the formation of the corresponding heterocyclic alcohols at a conversion rate of the initial ketones of 60–90%.*

Keywords: *hydrogenation, 5-acyl-1,3-dioxanes, heterocyclic alcohols, catalysts Pt/Re, Pd/C, Ni/kieselguhr, Ni/Mo*

For citation: Musin A.I., Borisova Yu.G., Raskil'dina G.Z., Daminev R.R., Davletshin A.R., Zlotskii S.S. Heterogeneous catalytic reduction of substituted 5-acyl-1,3-dioxanes. *Tonk. Khim. Tekhnol. = Fine Chem. Technol*. 2022;17(3):201–209 (Russ., Eng.). https://doi.org/10.32362/2410-6593-2022-17-3-201-209

НАУЧНАЯ СТАТЬЯ

Гетерогенно-каталитическое восстановление замещенных 5-ацил-1,3-диоксанов

А.И. Мусин[1], Ю.Г. Борисова[2,✉], Г.З. Раскильдина[2], Р.Р. Даминев[2], А.Р. Давлетшин[2], С.С. Злотский[2]

[1]Институт химических технологий и инжиниринга Уфимского государственного нефтяного технического университета, Стерлитамак, 453118 Россия
[2]Уфимский государственный нефтяной технический университет, Уфа, 450064 Россия
[✉]Автор для переписки, e-mail: yulianna_borisova@mail.ru

Аннотация

Цели. *Изучить гидрирование замещенных 5-ацил-1,3-диоксанов в присутствии металлосодержащих катализаторов (Pt/Re, Pd/C, «Ni на кизельгуре», Ni/Mo).*
Методы. *Для определения качественного и количественного состава реакционных масс были использованы следующие методы анализа: газожидкостная хроматография (на аппаратно-программном комплексе «Кристалл 2000»), масс-спектроскопия (на приборе «Хроматэк-Кристалл 5000М» с базой NIST 2012), и спектроскопия ядерного магнитного резонанса (ЯМР-спектроскопия) (на приборе «BrukerAM-500» с рабочими частотами 500 и 125 МГц).*
Результаты. *Гидрированием замещенных 5-ацил-1,3-диоксанов, полученных конденсацией карбонильных соединений с параформом с использованием серной кислоты, синтезированы гетероциклические спирты в присутствии металлосодержащих катализаторов с конверсией исходных кетонов 60–90% и селективностью образования целевых продуктов 70–90%. Вещества проанализированы и доказаны методами газожидкостной хроматографии, масс-спектрометрии и ЯМР-спектроскопии.*
Выводы. *Установлено, что лучшим катализатором восстановления замещенных 5-ацил-1,3-диоксанов является Pd/C, позволяющий достичь высокой селективности образования соответствующих гетероциклических спиртов при конверсии исходных кетонов 60–90%.*

Ключевые слова: *гидрирование, 5-ацил-1,3-диоксаны, гетероциклические спирты катализаторы Pt/Re, Pd/C, «Ni на кизельгуре», Ni/Mo*

Для цитирования: Мусин А.И., Борисова Ю.Г., Раскильдина Г.З., Даминев Р.Р., Давлетшин А.Р., Злотский С.С. Гетерогенно-каталитическое восстановление замещенных 5-ацил-1,3-диоксанов. *Тонкие химические технологии*. 2022;17(3):201–209. https://doi.org/10.32362/2410-6593-2022-17-3-201-209

INTRODUCTION

Oxymethyl-1,3-dioxacycloalkanes and their derivatives, ethers, esters, thioethers, etc., which exhibit various biologically active properties, are used as corrosion inhibitors, plant protection chemicals [1–3].

The primary method for obtaining alcohols containing a cycloacetal fragment involves the condensation of 1,1,1-trioxymethylalkanes with carbonyl compounds [4, 5]. However, in a number of cases, the use of secondary 1,3-dioxacycloalkane alcohols becomes necessary. Although it has been proposed that these can be obtained by reduction of the keto group in 5-acyl-1,3-dioxanes with metal hydrides [6], such a hydrogenation method is of little use for preparative synthesis under industrial conditions.

In this connection, the present work is aimed at studying the heterogeneous catalytic reduction of substituted 5-acyl-1,3-dioxanes in the presence of various metal-containing catalysts (Pd/C, Ni/kieselguhr, Pt/Re, Ni/Mo).

MATERIALS AND METHODS

After analyzing the reaction masses, the mass spectra of the compounds were recorded using the Chromatec-Kristall 5000M hardware-software complex (*Chromatec*, Russia) with the NIST 2012 database (*National Institute of Standards and Technology*, USA). Analysis conditions were as follows: length of capillary quartz column was 30 m, analysis duration was 20 min, ion source temperature was 260°C, transition line temperature was 300°C, scanning range was 30–300 Da, pressure 37–43 was mTorr, carrier gas was helium, and heating rate was 20 deg/min. Mass spectra of the compounds were obtained using the electron impact ionization method. ^{1}H and ^{13}C nuclear magnetic resonance (NMR) spectra were recorded on a Bruker AM-500 spectrometer (*Bruker*, USA) with operating frequencies of 500 and 125 MHz, respectively; the solvent was $CDCl_3$. Chemical shifts are given on a scale of δ (ppm) relative to tetramethylsilane as an internal standard. Spin-spin coupling constants (*J*) are given in Hz.

Starting ketones **1**–**5** were obtained according to the previously presented procedure [7].

1-(5-Methyl-1,3-dioxan-5-yl)ethanone **1**. $T_{b.p.}$ = 99–101°C (3 mm Hg). Colorless liquid. ^{1}H NMR spectrum ($CDCl_3$, δ, ppm): 0.92 s (3H, $\underline{CH_3}C$), 2.22 s (3H, $\underline{CH_3}CO$), 3.45 d (2H, 2 $C\underline{CH_2}$, *J* = 11.6), 4.24 d (2H, 2 $C\underline{CH_2}$, *J* = 11.6), 4.70 d (1H, $\underline{CH_a}O$, *J* = 6.1), 4.74 d (1H, $\underline{CH_b}O$, *J* = 6.0). ^{13}C NMR spectrum ($CDCl_3$, δ, ppm): 18.28 ($\underline{CH_3}C$), 26.96 ($\underline{CH_3}CO$), 51.15 (C), 71.22 (2 CH_2), 94.55 (CH_2O), 208.92 (C=O).

Mass spectrum, *m/z* (I_{rel}, %): 144 (2) [M^+], 114 (30), 84 (10), 72 (40), 69 (50), 57 (30), 43 (100).

1-(5-Ethyl-1,3-dioxan-5-yl)ethanone **2**. $T_{b.p.}$ = 110–112°C (3 mm Hg). Colorless liquid. ^{1}H NMR spectrum ($CDCl_3$, δ, ppm): 0.75 t (3H, $\underline{CH_3}CH_2$, *J* = 7.6), 1.48 q (2H, $CH_3\underline{CH_2}$, *J* = 7.6, 15.3), 2.25 s (3H, $\underline{CH_3}CO$), 3.57 d (2H, 2 $C\underline{CH_2}$, *J* = 11.5), 4.32 d (2H, 2 $C\underline{CH_2}$, *J* = 11.5), 4.68 d (1H, $\underline{CH_a}O$, *J* = 6.0), 4.88 d (1H, $\underline{CH_b}O$, *J* = 5.9). ^{13}C NMR spectrum ($CDCl_3$, δ, ppm): 7.78 ($\underline{CH_3}CH_2$,), 25.08 ($CH_3\underline{CH_2}$), 26.98 ($\underline{CH_3}CO$), 51.10 (C), 71.95 (2 CH_2), 94.17 (CH_2O), 208.91 (C=O).

Mass spectrum, *m/z* (I_{rel}, %): 158 (1) [M^+], 128 (10), 99 (5), 83 (30), 71 (7), 67 (10), 57 (20), 43 (100).

1-(5-Isopropyl-1,3-dioxan-5-yl)ethanone **3**. $T_{b.p.}$ = 129–131°C (3 mm Hg). Colorless liquid. ^{1}H NMR spectrum ($CDCl_3$, δ, ppm): 0.9 d (3H, $\underline{CH_3}CH$, *J* = 7.0), 1.00 d (3H, $\underline{CH_3}CH$, *J* = 7.0), 1.63 m (2H, $CH_3\underline{CH}$), 2.27 s (3H, $\underline{CH_3}CO$), 3.48 d (2H, 2 $C\underline{CH_2}$, *J* = 11.5), 4.34 d (2H, 2 $C\underline{CH_2}$, *J* = 11.4), 4.62 d (1H, $\underline{CH_a}O$, *J* = 6.0), 4.98 d (1H, $\underline{CH_b}O$, *J* = 6). ^{13}C NMR spectrum ($CDCl_3$, δ, ppm): 16.02 ($\underline{CH_3}CH$), 26.94 ($\underline{CH_3}CO$), 29.29 ($CH_3\underline{CH}$), 51.18 (C), 71.76 (2 CH_2), 94.12 (CH_2O), 209.93 (C=O).

Mass spectrum, *m/z* (I_{rel}, %): 158 (2) [M^+], 12 (50), 110 (20), 99 (30), 86 (70), 83 (80), 71 (20), 57 (40), 43 (100).

1-(5-Methyl-1,3-dioxan-5-yl)propan-1-one **4**. $T_{b.p.}$ = 129–131°C (3 mm Hg). Colorless liquid. ^{1}H NMR spectrum ($CDCl_3$, δ, ppm): 1.05 t (3H, $\underline{CH_3}CH_2$, *J* = 7.2), 1.33 s (3H, $\underline{CH_3}C$,), 2.25 q (3H, $\underline{CH_2}CH_3$ *J* = 7.5, 12.0), 3.46 d (2H, 2 $C\underline{CH_2}$, *J* = 11.2), 4.32 d (2H, 2 $C\underline{CH_2}$, *J* = 11.0), 4.62 d (1H, $\underline{CH_a}O$, *J* = 6.0), 4.98 d (1H, $\underline{CH_b}O$, *J* = 6.1). ^{13}C NMR spectrum ($CDCl_3$, δ, ppm): 9.77 ($\underline{CH_3}CH_2$), 16.33 ($\underline{CH_3}C$), 29.94 ($\underline{CH_2}CO$), 51.13 (C), 73.76 (2 CH_2), 94.12 (CH_2O), 209.92 (C=O).

Mass spectrum, *m/z* (I_{rel}, %): 158 (1) [M^+], 110 (25), 99 (60), 86 (30), 83 (40), 71 (20), 57 (40), 43 (100).

(5-Methyl-1,3-dioxan-5-yl)(phenyl)methanone **5**. $T_{b.p.}$ = 156–157°C (1 mm Hg). Colorless liquid. ^{1}H NMR spectrum ($CDCl_3$, δ, ppm): 1.34 s (3H, $\underline{CH_3}$), 3.78 d (2H, 2 $\underline{CH_2}$, *J* = 11.2), 4.44 d (2H, 2 $\underline{CH_2}$, *J* = 11.3), 4.84 d (1H, $\underline{CH_a}O$, *J* = 5.0), 4.98 d (1H, $\underline{CH_b}O$, *J* = 5.2), 7.4–7.8 m (5H, Ph-). ^{13}C NMR spectrum ($CDCl_3$, δ, ppm): 18.93 ($\underline{CH_3}$), 47.56 (C), 73.34 (2 CH_2), 91.91 (CH_2O), 205.43 (C=O).

Mass spectrum, *m/z* (I_{rel}, %): 206 (1) [M^+], 188 (20), 176 (40), 108 (100), 87 (20), 81 (90), 55 (60).

General method for hydrogenation of ketones 1–5

In order to study the process of hydrogenation of ketones to obtain alcohols, catalytic hydroprocessing systems, which are widely available in the petrochemical industry, are used [8, 9].

The following commercially available catalysts were used: Pd supported on activated carbon, PK-400 catalyst grade with a Pd content of 2 wt % (*Redkinsky catalyst plant*, Russia); Ni/kieselguhr catalyst—basic nickel carbonate on kieselguhr with the addition of graphite (*Sintez-Kaustik*, Russia) with a Ni content of 45 wt %; Pt/Re catalyst supported on alumina, catalyst grade RB-44 U (*Olkat*, Russia) with a Pt content of 0.25 wt % and Re of 0.4 wt %; bifunctional Ni/Mo catalyst supported on alumina, catalyst grade TK-743 (*Haldor Topsoe*, Denmark) with a Ni content of 5 wt % and Mo of 25 wt %).

The used catalytic systems have proven themselves well in the hydrogenation of acetylene and carbonyl compounds impurities, as well as in the process of hydrocracking, etc. [8–14] (Table 1).

For hydrogenation, a Katakon flow catalytic unit (*Katakon*, Russia) was used, comprising a metal reactor with a heating jacket, a burette for feeding raw materials, an automatic pump, and a control unit. Operating parameters of the installation were as follows: volume of the reaction zone was 15 cm^3, temperature range was 50–600°C, pressure was up to 100 atm.

The required catalyst (Pd/C, Ni/kieselguhr, Pt/Re, or Ni/Mo) was loaded into a flow reactor with a volume of 15 cm^3. The catalyst was activated in a stream of nitrogen or hydrogen at 350–450°C. Additionally, while cooling the reactor to 200°C at a rate of 0.27 mL/min, 15 mL of ketone and hydrogen were supplied at a rate of 0.230 mL/min. The pressure was set at 8 atm. The resulting catalyzate was filtered off and evaporated.

Using this hydrogenation method, the following alcohols were obtained:

1-(5-Methyl-1,3-dioxan-5-yl)ethanol **6**. $T_{b.p.}$ = 105–106°C (3 mm Hg). Colorless liquid. ^{1}H NMR spectrum ($CDCl_3$, δ, ppm): 0.83 s (3H, $\underline{CH_3}C$), 1.14 d (3H, $\underline{CH_3}CH_2$, J = 6.5), 2.22 s (3H, $\underline{CH_3}CO$), 3.45 dd (2H, 2 $C\underline{CH_2}$, J = 11.4, 11.5), 3.75 d (1H, $\underline{CH}OH$, J = 11.4), 4.24 dd (2H, 2 $C\underline{CH_2}$, J = 11.6, 11.2), 4.70 d (1H, $\underline{CH_a}O$, J = 6.1), 4.74 d (1H, $\underline{CH_b}O$, J = 6.0). ^{13}C NMR spectrum ($CDCl_3$, δ, ppm): 14.28 ($\underline{CH_3}C$), 18.47 ($\underline{CH_3}C$), 26.96 ($\underline{CH_3}CO$), 39.66 (C), 69.44 (CH), 71.43 (CCH_2), 71.92 ($C\underline{CH_2}$), 94.55 (CH_2O).

Mass spectrum, m/z (I_{rel}, %): 146 (2) [M^+], 98 (10), 86 (20), 72 (100), 57 (95), 43 (90).

1-(5-Ethyl-1,3-dioxan-5-yl)ethanol **7**. $T_{b.p.}$ = 122–123°C (3 mm Hg). Colorless liquid. ^{1}H NMR spectrum ($CDCl_3$, δ, ppm): 0.8 t (3H, $\underline{CH_3}CH_2$, J = 11.9), 1.15 d (1H, $\underline{CH_3}CH$, J = 6.5), 1.42–1.55 m (2H, $CH_3\underline{CH_2}$), 3.75 dd (2H, 2 $C\underline{CH_2}$, J = 11.7, 11.4), 3.88 d (1H, $\underline{CH}OH$, J = 11.6), 4.08 dd (2H, $C\underline{CH_2}$, J = 6.8, 10.5), 4.75 d (1H, $\underline{CH_a}O$, J = 6), 4.85 d (1H, $\underline{CH_b}O$, J = 6.0). ^{13}C NMR spectrum ($CDCl_3$, δ, ppm): 8.49 ($\underline{CH_3}CH_2$), 17.49 ($\underline{CH_3}CH$), 26.81 ($CH_3\underline{CH_2}$), 37.74 (C), 68.38 (CHOH), 73.46 ($C\underline{CH_2}$), 74.13 ($C\underline{CH_2}$), 94.05 (CH_2O).

Mass spectrum, m/z (I_{rel}, %): 160 (≤1) [M^+], 98 (10), 86 (60), 72 (100), 57 (95), 43 (90).

1-(5-Isopropyl-1,3-dioxan-5-yl)ethanol **8**. $T_{b.p.}$ = 131–132°C (2 mm Hg). Colorless liquid. ^{1}H NMR spectrum ($CDCl_3$, δ, ppm): 0.9 d (3H, $\underline{CH_3}CH$, J = 9.1), 1.00 d (3H, $\underline{CH_3}CH$, J = 7), 1.27 d (1H, $CH_3\underline{CH}$, J = 6.5), 1.73–1.81 m (2H, $CH_3\underline{CH}$), 3.72 dd

Table 1. Physicochemical and textural characteristics of the catalytic systems used

No.	Indicator	Catalyst			
		Pd/C	Ni/kieselguhr	Pt/Re	Ni/Mo
1	Metal content, wt %	2	45	0.25–0.4	5–25
2	Granule size, mm	2.8–5.5	4.0–5.0	1.6	1.5–3.0
3	Bulk density, g/cm^3	0.52–0.6	1.0–1.3	0.69–0.72	0.58–0.65
4	Specific surface area, m^2/g	230	280	170–210	180
5	Metal particle size, nm	1.5–2	6–8	4–6	4–6
6	Pore volume, cm^3/g	0.5	0.6	0.5	0.85–0.96

(2H, C$\underline{CH_2}$, J = 6.0, 11.0), 4.00 d (1H, CHOH, J = 11.6), 4.12 dd (2H, C$\underline{CH_2}$, J = 6.6, 11.5), 4.67 d (1H, $\underline{CH_a}$O, J = 5.8), 4.88 d (1H, $\underline{CH_b}$O, J = 5.8). ^{13}C NMR spectrum ($CDCl_3$, δ, ppm): 16.02 ($\underline{CH_3}$CH), 19.27 ($CH_3\underline{CH}$), 26.91 ($\underline{CH_3}$CO), 39.17 (C), 68.44 ($\underline{CH}$OH), 72.41 (C$\underline{CH_2}$), 72.66 (C$\underline{CH_2}$), 94.14 (CH_2O).

Mass spectrum, m/z (I_{rel}, %): 160 (2) [M^+], 72 (60), 57 (50), 45 (30), 43 (70), 39 (20), 32 (100).

1-(5-Methyl-1,3-dioxan-5-yl)propan-1-ol **9**. $T_{b.p.}$ = 114–116°C (2 mm Hg). Colorless liquid. ^{1}H NMR spectrum ($CDCl_3$, δ, ppm): 1.02 t (3H, $\underline{CH_3}CH_2$, J = 7.5), 1.33 s (3H, $\underline{CH_3}$C,), 2.12 d (1H, $\underline{CH_a}$, J = 8.0), 2.23 d (1H, $\underline{CH_b}$, J = 8.1). 3.98 d (1H, $\underline{CH}$OH, J = 11.4), 4.32 dd (4H, 2 C$\underline{CH_2}$, J = 11.0, 7.0), 4.77 d (1H, $\underline{CH_a}$O, J = 6.0), 4.94 d (1H, $\underline{CH_b}$O, J = 6.1). ^{13}C NMR spectrum ($CDCl_3$, δ, ppm): 11.77 ($\underline{CH_3}CH_2$), 16.35 ($\underline{CH_3}$C), 27.93 ($\underline{CH_2}$CO), 39.17 (C), 68.42 ($\underline{CH}$OH), 72.47 (C$\underline{CH_2}$), 74.61 (C$\underline{CH_2}$), 94.12 (CH_2O).

Mass spectrum, m/z (I_{rel}, %): 160 (1) [M^+], 99 (60), 86 (80), 71 (40), 57 (70), 43 (100).

5-Methyl-1,3-dioxan-5-yl-(phenyl)methanone **10**. $T_{b.p.}$ = 163–165°C (1 mm Hg). Colorless liquid. ^{1}H NMR spectrum ($CDCl_3$, δ, ppm): 1.06 s (3H, $\underline{CH_3}$), 3.79 dd (2H, C$\underline{CH_2}$, J = 11.7, 11.4), 3.94 d (1H, $\underline{CH}$OH, J = 11.0), 4.08 dd (2H, C$\underline{CH_2}$, J = 6.8, 10.5), 4.88 d (1H, $\underline{CH_a}$O, J = 5.2), 4.92 d (1H, $\underline{CH_b}$O, J = 5.2), 7.2–7.8 m (5H, Ph-). ^{13}C NMR spectrum ($CDCl_3$, δ, ppm): 18.81 ($\underline{CH_3}$), 39.51 (C), 73.32 (2 CH_2), 75.31 (CH), 91.94 (CH_2O), 129.44–139.22 (Ph-).

Mass spectrum, m/z (I_{rel}, %): 208 (1) [M^+], 108 (100), 104 (60), 87 (20), 55 (60).

RESULTS AND DISCUSSION

Previously [7], we showed that in a hydrogen flow in the presence of a Pd/C catalyst, 5-acyl--1,3-dioxanes are reduced to the corresponding heterocyclic alcohols. Continuing this work, we studied the hydrogenation of heterocyclic ketones **1**–**5** in the presence of a number of industrial metal-containing catalysts: Pd/C, Ni/kieselguhr, Pt/Re, or Ni/Mo.

Among the catalysts studied (Table 2), the best performance was demonstrated by Pd/C, which is used in the reduction of unsaturated and carbonyl compounds [15–19]. The conversion on Pt- and Ni-catalysts was 1.5–2.5 times lower; in all cases, the selectivity was more than 70%.

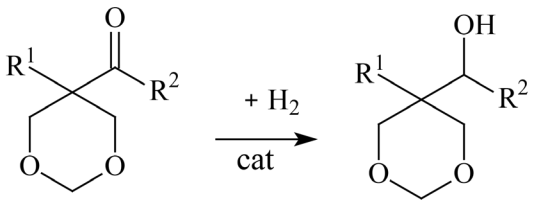

1–5 **6–10**

$R^1 = CH_3$, $R^2 = CH_3$ (**1**, **6**), $R^1 = C_2H_5$, $R^2 = CH_3$ (**2**, **7**)
$R^1 = i\text{-}C_3H_7$, $R^2 = CH_3$ (**3**, **8**), $R^1 = CH_3$, $R^2 = C_2H_5$ (**4**, **9**)
$R^1 = CH_3$, R^2 = Ph (**5**, **10**)

Scheme 1. Hydrogenation of 5-acyl-1,3-dioxanes.

Table 2. Hydrogenation of substituted 5-acyl-1,3-dioxanes **1**–**5** in the presence of various catalysts. Synthesis conditions: 200°C, reaction time = 1 h, molar ratio of ketone/H_2 = 1 : 6.

Starting compounds	Reaction products	Catalyst							
		Pd/C		Pt/Re		Ni/kieselguhr		Ni/Mo	
		*C**, %	*S**, %	*C*, %	*S*, %	*C*, %	*S*, %	*C*, %	*S*, %
1	**6**	80	98	70	95	50	85	40	95
2	**7**	90	95	50	95	40	80	40	90
3	**8**	80	95	40	95	30	80	20	95
4	**9**	60	95	50	80	30	60	30	80
5	**10**	65	95	40	70	25	75	20	70

Note: *C* is a conversion, %; *S* is a selectivity, %.

The conversion of ketones **1**–**5** is also affected by substituents having different structures at the carbonyl group and the 5th position of the 1,3-dioxane ring. The ethyl and phenyl radicals at the C=O group reduce the conversion of compounds **4** and **5**. The activity of ketones **2** and **3**, containing ethyl or isopropyl groups in the 5th position, slightly decreases as compared to methyl ethyl ketone derivative **1**.

It is noted that the hydrogenation of ketone **5** did not reveal products of complete or partial reduction of the aromatic nucleus.

CONCLUSIONS

The heterogeneous Pd/C catalyst allows 5-acyl-1,3-dioxanes to be reduced to the corresponding alcohols with a selectivity of more than 95%. Ni-containing catalysts are significantly less active when used in this process.

Acknowledgments

The study was supported by Ufa State Petroleum Technological University Leadership Project Competition for 2022, No. 15-2-22.

Authors' contributions

A.I. Musin – conducting research, literature review on the topic of the article;

Yu.G. Borisova – collection and processing of the material, writing the text of the article;

G.Z. Raskil'dina – statistical processing;

A.R. Davletshin – processing of the material;

R.R. Daminev – consultation on planning, methodology, and research implementation;

S.S. Zlotskii – development of the concept of scientific work, critical revision with the introduction of valuable intellectual content.

The authors declare no conflicts of interest.

REFERENCES

1. Gafarov N.A., Kushnarenko V.M., Bugai D.E. *Ingibitory korrozii*: v 2 t. T. 2. *Diagnostika i zashchita ot korrozii pod napryazheniem neftegazopromyslovogo oborudovaniya* (*Corrosion Inhibitors*: in 2 v. V. 2. *Diagnostics and Protection against Corrosion under Stress of Oil and Gas Equipment*). Moscow: Khimiya; 2002. 367 p. (in Russ.).

2. Yakovenko E.A., Baimurzina Yu.L., Raskil'dina G.Z., Zlotskii S.S. Synthesis and herbicidal and antioxidant activity of a series of hetero- and carbocyclic derivatives of monochloroacetic acid. *Russ. J. Appl. Chem*. 2020;93(5):712–720. https://doi.org/10.1134/S1070427220050122

3. Kuz'mina, U.S., Raskil'dina, G.Z., Ishmetova, D.V., *et al*. Cytotoxic activity against SH-SY5Y neuroblastoma cells of heterocyclic compounds containing *gem*-dichlorocyclopropane and/or 1,3-dioxacycloalkane fragments. *Pharm. Chem. J.* 2022;55(12):1293–1298. https://doi.org/10.1007/s11094-022-02574-6

[Original Russian Text: Kuz'mina, U.S., Raskil'dina, G.Z., Ishmetova, D.V., *et al*. Cytotoxic activity against SH-SY5Y neuroblastoma cells of heterocyclic compounds containing gem-dichlorocyclopropane and/or 1,3-dioxacycloalkane fragments. *Khimiko-Farmatsevticheskii Zhurnal*. 2022;55(12):27–32 (in Russ.). https://doi.org/10.30906/0023-1134-2021-55-12-27-32]

4. Maximov A.L., Nekhaev A.I., Ramazanov D.N. Ethers and acetals, promising petrochemicals from renewable sources. *Pet. Chem*. 2015;55(1):1–21. https://doi.org/10.1134/S0965544115010107

СПИСОК ЛИТЕРАТУРЫ

1. *Ингибиторы коррозии*: в 2 т. Т. 2. Гафаров Н.А., Кушнаренко В.М., Бугай Д.Е. *Диагностика и защита от коррозии под напряжением нефтегазопромыслового оборудования*. М.: Химия; 2002. 367 с.

2. Yakovenko E.A., Baimurzina Yu.L., Raskil'dina G.Z., Zlotskii S.S. Synthesis and herbicidal and antioxidant activity of a series of hetero- and carbocyclic derivatives of monochloroacetic acid. *Russ. J. Appl. Chem*. 2020;93(5):712–720. https://doi.org/10.1134/S1070427220050122

3. Кузьмина У.Ш., Раскильдина Г.З., Ишметова Д.В. Сахабутдинова Г.Н., Джумаев Ш.Ш., Борисова Ю.Г., Вахитова Ю.В., Злотский С.С. Цитотоксическая активность гетероциклических соединений, содержащих *гем*-дихлорциклопропановый и/или 1,3-диоксациклоалкановый фрагменты, в отношении клеток линии SH-SY5Y. *Химико-фармацевтический журнал.* 2021;55(12):27–32. https://doi.org/10.30906/0023-1134-2021-55-12-27-32

4. Максимов А.Л., Нехаев А.И., Рамазанов Д.Н. Простые эфиры и ацетали – перспективные продукты нефтехимии из возобновляемого сырья. *Нефтехимия*. 2015;55(1):3–24. https://doi.org/10.7868/S0028242115010104

5. Samoilov V., Goncharova A., Zarezin D., Kniazeva M., Ladesov A., Maximov A. Bio-based solvents and gasoline components from renewable 2,3-butanediol and 1,2-propanediol: synthesis and characterization. *Molecules*. 2020; 25(7):1723. https://doi.org/10.3390/molecules25071723

[Original Russian Text: Maximov A.L., Nekhaev A.I., Ramazanov D.N. Ethers and acetals, promising petrochemicals from renewable sources. *Neftekhimiya*. 2015;55(1):3–24 (in Russ.). https://doi.org/10.7868/S0028242115010104]

5. Samoilov V., Goncharova A., Zarezin D., Kniazeva M., Ladesov A., Maximov A. Bio-based solvents and gasoline components from renewable 2,3-butanediol and 1,2-propanediol: synthesis and characterization. *Molecules.* 2020; 25(7):1723. https://doi.org/10.3390/molecules25071723

6. Zlotskij S.S., Lesnikova E.T., Rachmankulov D.L., Timpe H.-J. Synthese von 5-Hydroxyalkyl- und 5-Alkenyl-1,3-dioxanen. *Z. Chem*. 1990;30(8):281–282. https://doi.org/10.1002/zfch.19900300804

7. Borisova Y.G., Musin A.I., Yakupov N.V., Daminev R.R., Zlotskii S.S. Pd/C-catalyzed hydrogenation of substituted 5-acyl-1,3-dioxanes. *Russ. J. Gen. Chem*. 2021;91(9):1619–1622. https://doi.org/10.1134/S1070363221090036

8. Golosman E.Z., Efremov V.N. Industrial catalysts for the carbon oxides hydrogenation. *Kataliz v promyshlennosti = Catalysis in Industry*. 2012;(5):36–55 (in Russ.).

9. Oosthuizen R.S., Nyamori V.O. Carbon nanotubes as supports for palladium and bimetallic catalysts for use in hydrogenation reactions. *Platinum Metals Rev*. 2011;55(3):154–169. https://doi.org/10.1595/147106711X577274

10. Khazipova A.N., Grigor'eva N.G., Korzhova L.F., Kutepov B.I. Hydrogenation of α-methylstyrene linear dimers in the presence of Pd- and Ni-containing catalysts. *Russ. J. Appl. Chem*. 2009;82(6):1065–1069. https://doi.org/10.1134/S1070427209060251

11. Mironenko R.M., Lavrenov A.V. An essay on the history of catalytic hydrogenation of organic compounds. From P. Sabatier and V.N. Ipatieff to the present days. *Kataliz v promyshlennosti = Catalysis in Industry*. 2021;21(4):259–273 (in Russ.). https://doi.org/10.18412/1816-0387-2021-4-259-273

12. Karimov O.Kh. Purification of isoprene from acetylene impurities on the nickel catalyst. *Promyshlennoe proizvodstvo i ispol'zovanie elastomerov = Industrial Production and Use Elastomers*. 2019;(1):3–5 (in Russ.). https://doi.org/10.24411/2071-8268-2019-10101

13. Belyi A.S., Smolikov M.D., Kir'yanov D.I., Udras I.E. Modern views on the state of platinum in supported catalysts for production of motor fuels. *Russ. J. Gen. Chem.* 2007;77(12):2243–2254. https://doi.org/10.1134/S1070363207120298

[Original Russian Text: Belyi A.S., Smolikov M.D., Kir'yanov D.I., Udras I.E. Modern views on the state of platinum in supported catalysts for production of motor fuels. *Rossiiskii Khimicheskii Zhurnal*. 2007;51(4):38–47 (in Russ).]

14. Millan-Agorio M., Ramires T., Bermudes J.M., Puron G., Pinilla J.L. Crude oil refining catalyst and method of producing same: Pat. Application number PCT/RU20 15/000546. Publ. 02.02.2017.

15. Kaluža L. Activity of transition metal sulfides supported on Al_2O_3, TiO_2 and ZrO_2 in the parallel hydrodesulfurization of 1-benzothiophene and hydrogenation of 1-methyl-cyclohex--1-ene. *React. Kinet. Mech. Cat*. 2015;114(2):781–794. https://doi.org/10.1007/s11144-014-0809-9

16. Touchy A.S., Hakim Siddiki S.M., Kon K., Shimizu K. Heterogeneous Pt catalysts for reductive amination of levulinic acid to pyrrolidones. *ACS Catalysis*. 2014;4(9):3045–3050. https://doi.org/10.1021/CS500757K

6. Zlotskij S.S., Lesnikova E.T., Rachmankulov D.L., Timpe H.-J. Synthese von 5-Hydroxyalkyl- und 5-Alkenyl-1,3-dioxanen. *Z. Chem.* 1990;30(8):281–282. https://doi.org/10.1002/zfch.19900300804

7. Борисова Ю.Г., Мусин А.И., Якупов Н.В., Раскильдина Г.З., Даминев Р.Р., Злотский С.С. Гидрирование замещенных 5-ацил-1,3-диоксанов в присутствии катализатора Pd/C. *Журн. общей химии*. 2021;91(9):1328–1332.

8. Голосман Е.З., Ефремов В.Н. Промышленные катализаторы гидрирования оксидов углерода. *Катализ в промышленности.* 2012;(5):36–55.

9. Oosthuizen R.S., Nyamori V.O. Carbon nanotubes as supports for palladium and bimetallic catalysts for use in hydrogenation reactions. *Platinum Metals Rev*. 2011;55(3):154–169. https://doi.org/10.1595/147106711X577274

10. Khazipova A.N., Grigor'eva N.G., Korzhova L.F., Kutepov B.I. Hydrogenation of α-methylstyrene linear dimers in the presence of Pd- and Ni-containing catalysts. *Russ. J. Appl. Chem.* 2009;82(6):1065–1069. https://doi.org/10.1134/S1070427209060251

11. Мироненко Р.М., Лавренов А.В. Очерк по истории каталитического гидрирования органических соединений. От П. Сабатье до В.Н. Ипатьева. *Катализ в промышленности*. 2021;21(4):259–273. https://doi.org/10.18412/1816-0387-2021-4-259-273

12. Каримов О.Х. Очистка изопрена от ацетиленовых примесей на никелевом катализаторе. *Промышленное производство и использование эластомеров*. 2019;(1):3–5. https://doi.org/10.24411/2071-8268-2019-10101

13. Белый А.С., Смоликов М.Д., Кирьянов Д.И., Удрас И.Е. Современные представления о состоянии платины в нанесенных катализаторах для производства моторных топлив. *Российский Химический Журнал*. 2007;51(4):38–47.

14. Миллан-Агорио М., Рамирес Т., Бермудес Ж.М., Пурон Г., Пинилла Ж.Л. *Катализатор переработки тяжелых нефтей и способ его приготовления*: Пат. WO2017018905. Application number PCT/RU20 15/000546. Publ. 02.02.2017.

15. Kaluža L. Activity of transition metal sulfides supported on Al_2O_3, TiO_2 and ZrO_2 in the parallel hydrodesulfurization of 1-benzothiophene and hydrogenation of 1-methyl-cyclohex-1-ene. *React. Kinet. Mech. Cat*. 2015;114(2):781–794. https://doi.org/10.1007/s11144-014-0809-9

16. Touchy A.S., Hakim Siddiki S.M., Kon K., Shimizu K. Heterogeneous Pt catalysts for reductive amination of levulinic acid to pyrrolidones. *ACS Catalysis*. 2014;4(9):3045–3050. https://doi.org/10.1021/CS500757K

17. Шарова Е.С., Фалеев С.А., Иванчина Э.Д., Гынгазова М.С., Полубоярцев Д.С., Кравцов А.В. Динамика свойств Pt-катализаторов риформинга в процессе промышленной эксплуатации. *Катализ в промышленности*. 2013;(3):48–53.

18. Mao Z., Gu H., Lin X. Recent advances of Pd/C-catalyzed reactions. *Catalysts*.2021;11(9):1078. https://doi.org/10.3390/catal11091078

19. Du R., Zhu C., Zhang P., Fan R. Selective hydrogenation of aromatic aminoketones by Pd/C catalysis. *Synthetic Communications*. 2008;38(17):2889–2897. https://doi.org/10.1080/00397910801993719

17. Sharova E.S., Faleev S.A., Ivanchina E.D., Gingazova M.S., Poluboyartsev D.S., Kravtsov A.V. Dynamics of properties of Pt-reforming catalysts in industrial operation. *Kataliz v promyshlennosti = Catalysis in Industry*. 2013;(3):48–53 (in Russ).

18. Mao Z., Gu H., Lin X. Recent advances of Pd/C-catalyzed reactions. *Catalysts.* 2021;11(9):1078. https://doi.org/10.3390/catal11091078

19. Du R., Zhu C., Zhang P., Fan R. Selective hydrogenation of aromatic aminoketones by Pd/C catalysis. *Synthetic Communications.* 2008;38(17):2889–2897. https://doi.org/10.1080/00397910801993719

About the authors:

Airat I. Musin, Postgraduate Student, Department of General, Analytical and Applied Chemistry, Ufa State Petroleum Technological University, Branch in Sterlitamak (2, Oktyabrya pr., Sterlitamak, 453118, Russia). E-mail: musin_1995@list.ru. ResearcherID R-9142-2016, RSCI SPIN-code 9573-4624, https://orcid.org/0000-0002-8662-9680

Yulianna G. Borisova, Cand. Sci. (Chem.), Teacher, Department of General, Analytical and Applied Chemistry, Ufa State Petroleum Technological University (1, Kosmonavtov ul., Ufa, 450064, Russia). E-mail: yulianna_borisova@mail.ru. Scopus Author ID 56526865000, ResearcherID P-9744-2017, RSCI SPIN-code 3777-0375, https://orcid.org/0000-0001-6452-9454

Gul'nara Z. Raskil'dina, Dr. Sci. (Chem.), Professor, Department of General, Analytical and Applied Chemistry, Ufa State Petroleum Technological University (1, Kosmonavtov ul., Ufa, 450064, Russia). E-mail: graskildina444@mail.ru. Scopus Author ID 56069888400, ResearcherID F-1619-2017, RSCI SPIN-code 2183-3333, https://orcid.org/0000-0001-9770-5434

Artur R. Davletshin, Dr. Sci. (Eng.), Professor, Department of Oil and Gas Technology, Ufa State Petroleum Technological University (1, Kosmonavtov ul., Ufa, 450064, Russia). E-mail: davletshinar@list.ru. Scopus Author ID 39261319400, ResearcherID AGQ-4852-2022, RSCI SPIN-code 7531-4771, https://orcid.org/0000-0003-4284-5880

Rustem R. Daminev, Dr. Sci. (Eng.), Professor, Director, Institute of Oil & Gas Engineering and Digital Technology, Ufa State Petroleum Technological University (1, Kosmonavtov ul., Ufa, 450064, Russia). E-mail: daminew@mail.ru. Scopus Author ID 15026168000, RSCI SPIN-code 3431-0901, https://orcid.org/0000-0001-8673-5240

Simon S. Zlotskii, Dr. Sci. (Chem.), Professor, Head of the Department of General, Analytical and Applied Chemistry, Ufa State Petroleum Technological University (1, Kosmonavtov ul., Ufa, 450064, Russia). E-mail: nocturne@mail.ru. Scopus Author ID 6701508202, ResearcherID W-6564-2018, RSCI SPIN-code 6529-3323, https://orcid.org/0000-0001-6365-5010

Об авторах:

Мусин Айрат Ильдарович, аспирант кафедры общей, аналитической и прикладной химии, ФГБОУ ВО «Уфимский государственный нефтяной технический университет», филиал в г. Стерлитамак (453118, Россия, г. Стерлитамак, пр-т Октября, д. 2). E-mail: musin_1995@list.ru. ResearcherID R-9142-2016, SPIN-код РИНЦ 9573-4624, https://orcid.org/0000-0002-8662-9680

Борисова Юлианна Геннадьевна, к.х.н., преподаватель кафедры общей, аналитической и прикладной химии, ФГБОУ ВО «Уфимский государственный нефтяной технический университет» (450064, Россия, г. Уфа, ул. Космонавтов, д. 1). E-mail: yulianna_borisova@mail.ru. Scopus Author ID 56526865000, ResearcherID P-9744-2017, SPIN-код РИНЦ 3777-0375, https://orcid.org/0000-0001-6452-9454

Раскильдина Гульнара Зинуровна, д.х.н., профессор кафедры общей, аналитической и прикладной химии, ФГБОУ ВО «Уфимский государственный нефтяной технический университет» (450064, Россия, г. Уфа, ул. Космонавтов, д. 1). E-mail: graskildina444@mail.ru. Scopus Author ID 56069888400, ResearcherID F-1619-2017, SPIN-код РИНЦ 2183-3333, https://orcid.org/0000-0001-9770-5434

Давлетшин Артур Раисович, д.т.н., профессор кафедры технологии нефти и газа, ФГБОУ ВО «Уфимский государственный нефтяной технический университет» (450064, Россия, г. Уфа, ул. Космонавтов, д. 1). E-mail: davletshinar@list.ru. Scopus Author ID 39261319400, ResearcherID AGQ-4852-2022, SPIN-код РИНЦ 7531-4771, https://orcid.org/0000-0003-4284-5880

Даминев Рустем Рифович, д.т.н., профессор, директор Института нефтегазового инжиниринга и цифровых технологий ФГБОУ ВО «Уфимский государственный нефтяной технический университет» (450064, Россия, г. Уфа, ул. Космонавтов, д. 1). E-mail: daminew@mail.ru. Scopus Author ID 15026168000, SPIN-код РИНЦ 3431-0901, https://orcid.org/0000-0001-8673-5240

Злотский Семен Соломонович, д.х.н., заведующий кафедрой общей, аналитической и прикладной химии ФГБОУ ВО «Уфимский государственный нефтяной технический университет» (450064, Россия, г. Уфа, ул. Космонавтов, д. 1). E-mail: nocturne@mail.ru. Scopus Author ID 6701508202, ResearcherID W-6564-2018, SPIN-код РИНЦ 6529-3323, https://orcid.org/0000-0001-6365-5010

The article was submitted: April 05, 2022; approved after reviewing: April 29, 2022; accepted for publication: June 13, 2022.

Translated from Russian into English by H. Moshkov
Edited for English language and spelling by Thomas Beavitt

CHEMISTRY AND TECHNOLOGY OF MEDICINAL COMPOUNDS AND BIOLOGICALLY ACTIVE SUBSTANCES

ХИМИЯ И ТЕХНОЛОГИЯ ЛЕКАРСТВЕННЫХ ПРЕПАРАТОВ И БИОЛОГИЧЕСКИ АКТИВНЫХ СОЕДИНЕНИЙ

ISSN 2686-7575 (Online)

https://doi.org/10.32362/2410-6593-2022-17-3-210-230

UDC 547.78:54.057

RESEARCH ARTICLE

Obtaining substituted phenol derivatives with potential antimicrobial activity

Vera A. Sokhraneva, Dilyara A. Yusupova, Vladimir S. Boriskin, Nataliya V. Groza✉

MIREA – Russian Technological University (M.V. Lomonosov Institute of Fine Chemical Technologies), Moscow, 119454 Russia

✉*Corresponding author, e-mail: grozanv@gmail.com*

Abstract

Objectives. *With the growing resistance of pathogenic microorganisms to antibiotics, the development of new antimicrobial drugs offering specific mechanisms of action becomes an urgent task. Only few antimicrobials offer a broad spectrum of activity against gram-positive and gram-negative bacteria, molds, and yeasts. In this regard, the purpose of the work was to develop methods for synthesizing biologically active derivatives of alkyl-substituted phenols (reactions at the hydroxy group) to study their biological effect.*

Methods. *The synthesis of imidazole acetates of substituted phenols was carried out in two stages. At the first stage, the chloroacetyl derivative of the selected compounds was obtained, to which imidazole was then added. O-acylation reactions at the first stage of the synthesis were carried out under varying conditions. The first version of the synthesis was carried out using chloroacetyl chloride as an acylating agent together with a high-boiling solvent. In the second variant, chloroacetic anhydride was used, along with an attempt to replace the solvent with a low-boiling one. A thymol methoxy derivative was additionally synthesized by a known method using methyl iodide and varying the reaction parameters.*

Results. *The parameters of chloroacetylation and methoxylation of aromatic alcohols were optimized with rational selection of solvents and the ratio of reagents in the reactions. Synthesized thymol (2-isopropyl-5-methylphenol) and propofol (2,6-isopropylphenol) derivatives contained imidazole as an additional pharmacophore with affinity for microorganism cell membrane proteins. A thymol methoxy derivative comprising an aromatic ether exhibiting increased hydrophobicity was also obtained. The synthesized compounds were characterized by NMR spectroscopy.*

Conclusions. *Chloroacetyl derivatives of aromatic alcohols can be effectively synthesized by cooling the reaction mixture using an excess quantity of an acylating agent and increasing the reaction time (compared to literature data). The yield of thymol chloroacetate was 75%, while that of propofol chloroacetate was 30%. This can be explained by the sterically hindered reaction of the propofol alcohol group, which has isopropyl substituents at the second and sixth positions of the benzene ring.*

Keywords: *alkyl-substituted phenols, imidazole, thymol, propofol, chloroacetate*

For citation: Sokhraneva V.A., Yusupova D.A., Boriskin V.S., Groza N.V. Obtaining substituted phenol derivatives with potential antimicrobial activity. *Tonk. Khim. Tekhnol. = Fine Chem. Technol.* 2022;17(3):210–230 (Russ., Eng.). https://doi.org/10.32362/2410-6593-2022-17-3-210-230

НАУЧНАЯ СТАТЬЯ

Получение производных замещенных фенолов с потенциальной антимикробной активностью

В.А. Сохранева, Д.А. Юсупова, В.С. Борискин, Н.В. Гроза✉

МИРЭА – Российский технологический университет (Институт тонких химических технологий им. М.В. Ломоносова), Москва, 119454 Россия
✉*Corresponding author, e-mail: grozanv@gmail.com*

Аннотация

Цели. *В связи с растущей резистентностью патогенных микроорганизмов к антибиотикам актуальной задачей является разработка новых противомикробных препаратов с уникальным механизмом действия. Немногие антимикробные препараты обладают широким спектром действия на грамположительные и грамотрицательные бактерии, плесени и дрожжи. В связи с этим, цель нашей работы – разработать способы синтеза биологически активных производных алкил-замещенных фенолов (реакций по гидроксигруппе) для исследования их биологического действия.*

Методы. *Синтез имидазолацетатов замещенных фенолов проводился в две стадии. На первой стадии было получено хлорацетильное производное выбранных соединений, к которому далее присоединялся имидазол. Реакции О-ацилирования на первой стадии синтеза проводились в различных условиях. Первый вариант синтеза проводили с использованием хлорацетилхлорида в качестве ацилирующего агента и высококипящего растворителя. Во втором варианте использовали хлоруксусный ангидрид, и была предпринята попытка заменить растворитель на низкокипящий. Также было синтезировано метоксипроизводное тимола по известной методике, с применением метилйодида и варьирования параметров реакции.*

Результаты. *Проведена оптимизация параметров хлорацетилирования и метоксилирования ароматических спиртов. Осуществлен подбор растворителей и соотношения реагентов в реакциях. Были синтезированы производные тимола (2-изопропил-5-метилфенола) и пропофола (2,6-изопропилфенола), содержащие имидазол в*

качестве дополнительного фармакофора, имеющего сродство к белкам клеточных мембран микроорганизмов. Также было получено метоксипроизводное тимола – ароматический простой эфир с повышенной гидрофобностью. Синтезированные соединения были охарактеризованы методом ЯМР-спектроскопии.

Выводы. *Синтез хлорацетильных производных ароматических спиртов при охлаждении реакционной массы с использованием избытка ацилирующего агента и увеличением времени реакции (по сравнению с литературными данными) является более предпочтительным. Выход хлорацетета тимола составил 75%, хлорацетата пропофола – 30%, что можно объяснить стерически затрудненным реагированием спиртовой группы пропофола, имеющего изопропильные заместители по 2 и 6 положениям бензольного кольца.*

Ключевые слова: *алкил-замещенные фенолы, имидазол, тимол, пропофол, хлорацетат*

Для цитирования: Сохранева В.А., Юсупова Д.А., Борискин В.С., Гроза Н.В. Получение производных замещенных фенолов с потенциальной антимикробной активностью. *Тонкие химические технологии*. 2022;17(3):210–230. https://doi.org/10.32362/2410-6593-2022-17-3-210-230

INTRODUCTION

Infectious diseases remain highly prevalent, posing a continuing serious threat to human health. This risk is also associated with the growing resistance of pathogenic microorganisms to antibiotics. Despite significant advances in the understanding of antimicrobials, their use in the treatment of infections is impeded due to their high toxicity. It is also worth noting that few antimicrobials offer a wide spectrum of action on gram-positive and gram-negative bacteria, as well as fungi. Therefore, the development of new antimicrobial drugs that offer a unique mechanism of action is a relevant research direction [1].

Currently, there is increasing data indicating the positive effect on the human body of various diets rich in plant products. Products containing phenolic and polyphenolic compounds are considered to be one of the most valuable components of nutrition [2, 3]. Studies show that the consumption of natural substituted phenols can reduce the risk of developing many diseases, including cardiovascular and neurodegenerative pathologies, as well as some forms of cancer. Phenols have also been found to affect lipid metabolism [4]. In addition, it is known that natural phenols can suppress the negative effects of bacterial, viral and fungal infections, as well as interact with a wide number of proteins, such as enzymes, tissue proteins and membrane receptors, to modulate their activity [5].

Due to their antibacterial, antiviral, anti-inflammatory, antioxidant, and antitumor properties, phenolic compounds are among the most attractive potential antimicrobial agents [6].

On the other hand, imidazole compounds have been of interest to researchers for more than a century. As well as occupying a unique position in the chemistry of heterocycles, imidazole derivatives have recently been used more widely in chemistry and pharmacology. Imidazole is a nitrogen-containing five-membered heterocyclic ring of biological and pharmaceutical significance. The imidazole ring is part of several important natural molecules, including purine, histamine, histidine, and nucleic acid. Being a polar and ionizable aromatic compound, imidazole is used to optimize the parameters of solubility and bioavailability of poorly soluble drugs by improving the pharmacokinetic characteristics of synthesized complex molecules [7]. Moreover, the availability of several viable methods for synthesizing imidazole-containing compounds opens up wide opportunities in the field of medical chemistry. Imidazole derivatives, as well as substituted phenols, have a wide range of biological activity: antibacterial, anticancer, anti-tuberculosis, and antifungal.

In this regard, the aim of the present work was to develop methods for the synthesis of imidazole-containing derivatives of alkyl-substituted phenols in order to study their possible antimicrobial activity. In addition, there are suggestions that two types of bioactivity may occur during the hydrolysis of such conjugates. In this work, the initial phenolic compounds from which imidazolacetates were synthesized were thymol (2-isopropyl-5-methylphenol) and propofol (2,6-isopropylphenol).

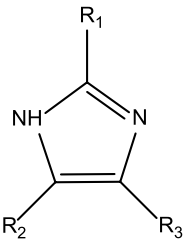

Fig. 1. General structure of imidazoles.

Examples of conjugation of phenols and polyphenols with imidazole and their biological activity

Imidazoles are well-known and widespread heterocyclic compounds (Fig. 1). As is known from many literary sources, imidazole derivatives exhibit various biological activities, including antitumor, antifungal [8] and antibacterial [9] ones.

Imidazole and nafimidone derivatives were obtained according to the schemes shown in Figs. 2 and 3 according to the methodology described in [10].

The compounds were evaluated *in vitro* in comparison with three *Candida* fungi, which are frequent pathogens of nosocomial infections and pathogenic to people with weakened immune systems: *Candida albicans* (ATCC 90028), *C. krusei* (ATCC 6258), and C. parapsilosis (ATCC 22019) [11], as well as against four conditionally pathogenic bacteria pathogens of nosocomial infections: *Staphylococcus aureus* (ATCC 25923), *Enterococcus faecalis* (ATCC 29212), *Escherichia coli* (ATCC 25922), and *Pseudomonas aeruginosa* (ATCC 27853) [12] (Table 1).

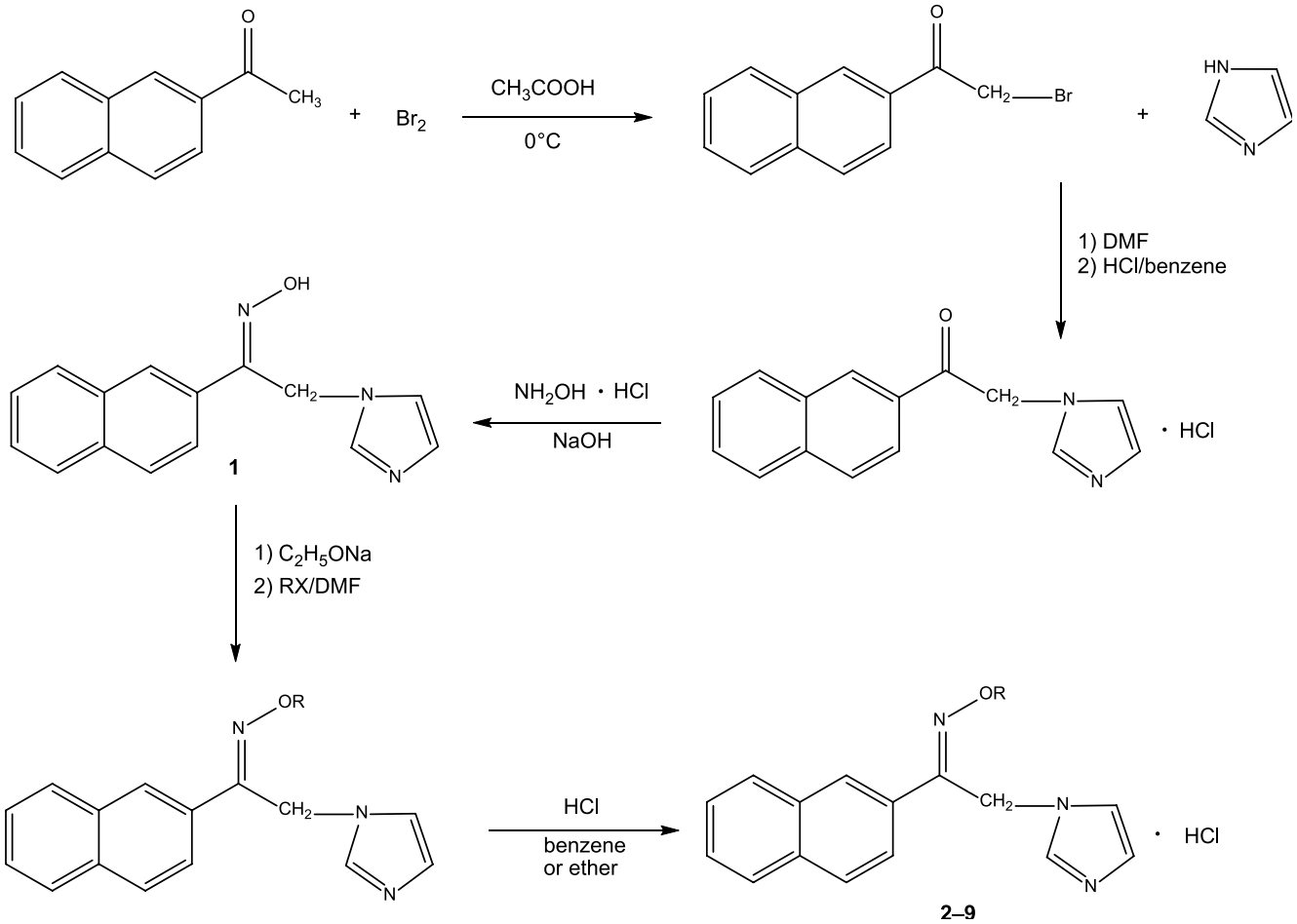

Fig. 2. Synthesis of nafimidone oxime and oxime ethers by *O*-alkylation of the oxime with an alkyl halide.

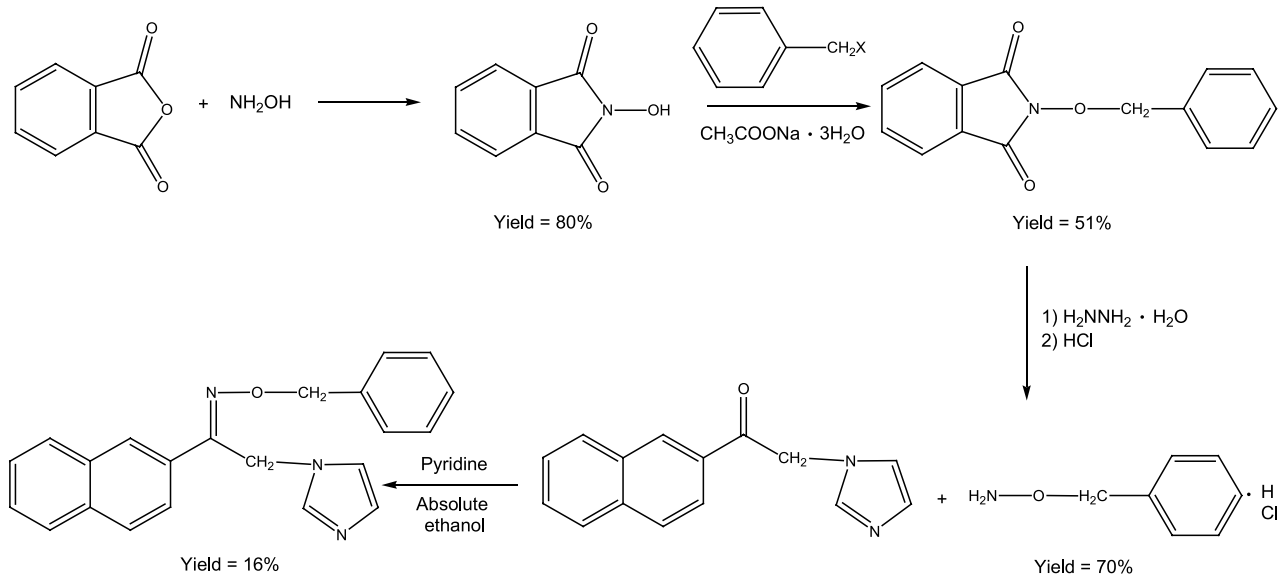

Fig. 3. Synthesis of nafimidone *O*-benzyloxime (**7**) by condensation of a ketone with an *O*-substituted hydroxylamine.

The results of the studies showed that only compound **1** was inactive against both bacteria and fungi. Most compounds (**2**, **3a**, **3b**, **4**, **6**, **7**, **8**, and **9**) were active against gram-positive bacteria, especially *S. aureus*, at low values of the minimum inhibitory concentration (MIC, Eng. minimum inhibitory concentration, MIC). Compounds **2**, **3a**, **3b**, **4**, and **9** demonstrated effective activity against *E. faecalis* at concentrations of 4–16 μg/mL, while the reference substance, amikacin, was active at a concentration

Table 1. Antibacterial and antifungal activity of compounds (MIC in μg/mL)

Compound	Bacteria (MIC μg/mL)				Fungi (MIC μg/mL)		
	S. aureus ATCC25923	*E. faecalis* ATCC 29212	*E. coli* ATCC 25922	*P. auruginosa* ATCC 27853	*C. albicans* ATCC 90028	*C. krusei* ATCC 6258	*C. parapsilosis* ATCC 22019
1	>64	>64	>64	>64	>64	>64	>64
2	32	16	>64	>64	64	32	64
3a	0.5	16	>64	>64	1	1	2
3b	8	16	>64	>64	2	4	4
4	8	4	>64	>64	16	32	32
5	>64	>64	>64	>64	8	16	8
6	1	>64	>64	>64	>64	>64	>64
7	0.5	>64	>64	>64	>64	>64	>64
8	0.5	>64	>64	>64	>64	>64	>64
9	2	4	32	>64	>64	>64	>64
Fluconazole	–	–	–	–	0.25	16	1
Amikacin	4	64	1	2	–	–	–

of 64 μg/mL. All derivatives (except compound **9** against *E. coli*) were inactive against gram-negative bacteria. Only five compounds (**2**, **3a**, **3b**, **4**, and **5**) demonstrated activity against fungi. In relation to *C. krusei* compounds, **3a** and **3b** showed even better activity than fluconazole. Compound **3a** showed the best activity against both bacteria and fungi [13].

The general structure of nafimidone oxime and oxime esters is shown in Fig. 4.

In order to study the effect of stilbenes conjugated with 2-aminoimidazole on biofilms *P. Aeruginosa* resistant to many known antibiotics, compounds **10**, **11**, and **13a-b** were synthesized (Fig. 5). Biofilms were grown in a modified M9 medium in 96-well microtiter plates. As a result, it was found that compounds **10** and **11** are able to inhibit the growth of *P. aeruginosa* film up to 24 h by 56% and 48%, respectively. Compounds **13a-b** did not demonstrate any antibacterial activity [14].

A series of new imidazole derivatives **17a-m** (Fig. 6) was synthesized to evaluate their antifungal activity *in vitro*. Five species of conditionally pathogenic *Candida* were selected for the tests, including *Candida glabrata* 80, *Candida glabrata* 67, *Candida albicans* 135, *Candida parapsilosis* 208, and *Candida pseudotropicalis* 801 [14].

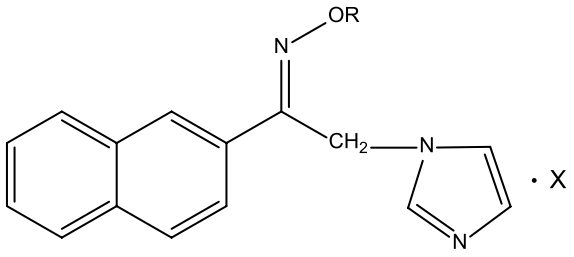

Fig. 4. General structure of nafimidone oxime and oxime ethers.

The synthesis was carried out in accordance with the scheme in Fig. 6. The synthesis of intermediates of (±)-2-bromo-1-(5-aryl-3-pyridine-2-yl-4,5-dihydro-pyrazole-1-yl)-ethanones (**16a-m**) was carried out by reacting bromoacetyl chloride with (±)-5-aryl-3-(pyridine-2-yl)-4,5-dihydro-1*H*-pyrazoles (**15a-m**), which were obtained from the corresponding 3-aryl-1-(pyridine-2-yl)-propenones (**14a-m**) treated with hydrazine hydrate. Further, the corresponding 4,5-dihydro-1*H*-pyrazoles (**15a-m**) were isolated, from which compounds **16a-m** were obtained. After that, treatment of compounds **16a-m**

Table 2. Structures, solvents used for recrystallization, yields (%) and melting points ($T_{m.p.}$) of compounds

Compound	R	X	Solvent used for recrystallisation	Yield, %	$T_{m.p.}$, °C
1	–H	HCl	Methanol	82	193–196
2	$–CH_3$	HCl	Methanol/Ethyl acetate	47	167–168
3a (E)	$–C_2H_5$	HCl	(1) Methanol/water, (2) Methanol/ Ethyl acetate	46	92–94
3b (Z)	$–C_2H_5$	HCl	Methanol/Ethyl acetate	33	82–84
4	$–C_3H_7$	HCl	(1) Methanol/water, (2) Methanol/Ethyl acetate	84	170–172
5	$–CH_2–CH=CH_2$	HCl	Methanol/Ethyl acetate	58	164–166
6	$–C_6H_{11}$ (cyclo)	HCl	(1) Ethyl acetate, (2) Benzene	34	179–181
7	$–CH_2C_6H_5$	HCl	(1) Methanol/water, (2) Benzene	97	158–160
8	$4–CH_2C_6H_4Cl$	HCl	(1) Methanol/water, (2) Dioxane	87	188–190
9	$2,4–CH_2C_6H_3Cl_2$	HCl	Dioxane/ether	56	186–187

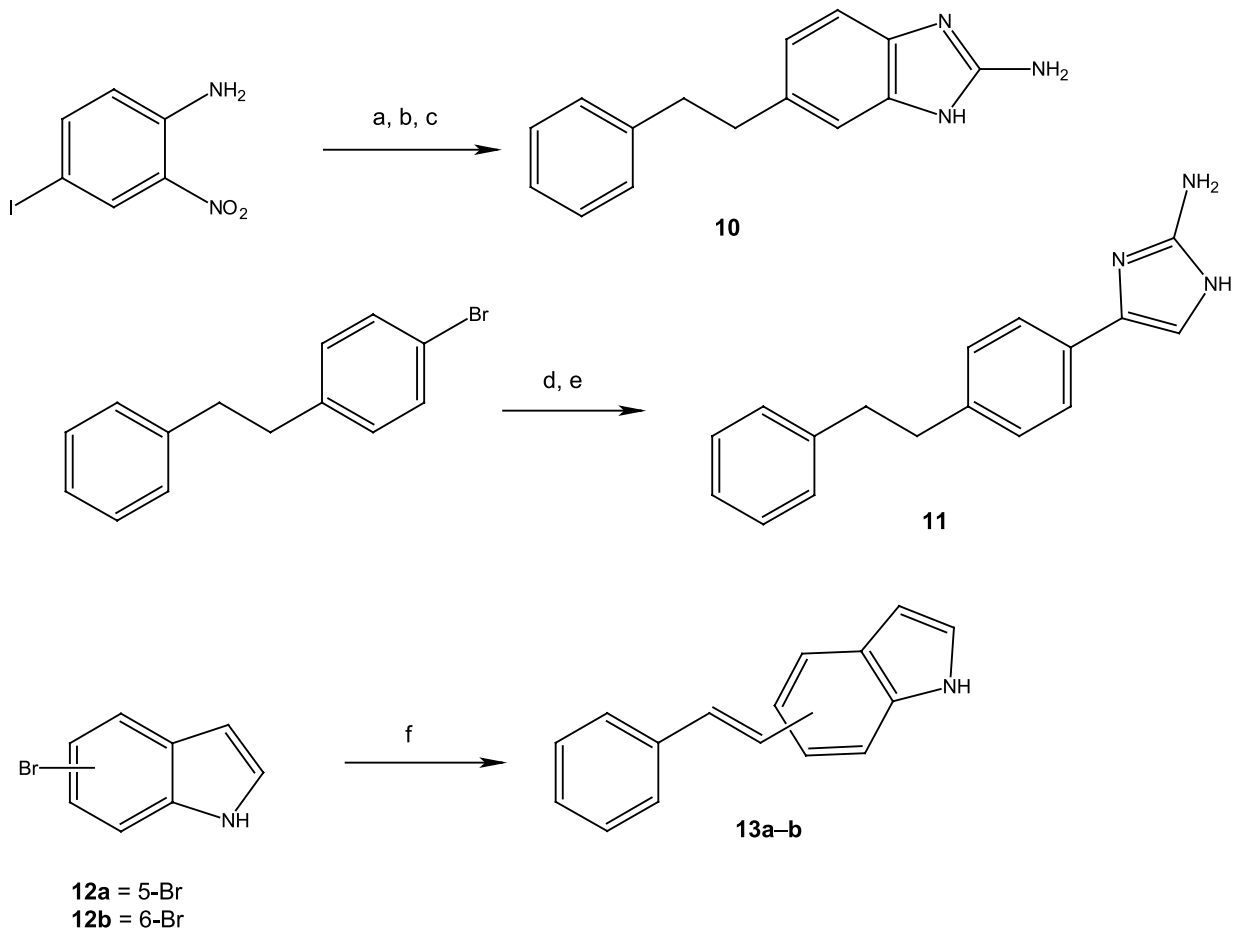

Fig. 5. Scheme for the synthesis of stilbene derivatives.
(a) Styrene, $Pd(OAc)_2$, CH_3CN, DIPEA, 80°C, 76%; (b) $SnCl_2 \cdot 2H_2O$, EtOAc, 80°C; (c) CNBr, MeOH/H_2O (1:1), 50°C, 91%; (d) imidazo [1,2-a]pyrimidine hydrobromide, $Pd(OAc)_2$, PPh_3, Cs_2CO_3, 1,4-dioxane, 100°C, 82%; (e) 20% N_2H_4/EtOH, 105°C, 84%; (f) styrene, $Pd(OAc)_2$, P(*o*-tolyl)$_3$, NEt_3, 100°C, 73–76%. DIPEA = *N*,*N*-diisopropylethylamine.

with imidazole in the presence of acetonitrile led to (±)-1-(5-aryl-3-pyridine-2-yl-4,5-dihydro-pyrazole-1-yl)-2-imidazole-1-yl-ethanones (**17a-m**) being obtained.

The synthesized compounds showed different antifungal activity *in vitro* against the tested *Candida* strains (Table 3). The following substances were used as reference substances: miconazole (Mic), 5-fluorouracil (5FC), and amphotericin B (AMB). Compounds **17a**, **17b**, **17e**, **17f**, and **17j** were equally active against *C. pseudotropicalis* 801 (CPs 801) and *C. glabrata* 80 (CG 80), MIC values were 62.5 μg/mL after 24 and 48 h. At the same time, with respect to the *C. glabrata* 67, MIC values from 62.5 μg/mL were increased to 125 μg/mL and 500 μg/mL after 24 and 48 h, respectively. With respect to *C. parapsilosis* 208 (CP 208), MIC values of 62.5 μg/mL showed only compounds **17h**, **17i**, and **17k**. None of the tested compounds demonstrated activity against *C. albicans* 135 [13].

Hydroxylated derivatives of thymol (**20a-e**) were synthesized to evaluate the inhibitory effect on fungal tyrosinase (Fig. 7). The intermediate chloroacetyl product **18** was obtained by esterification of the hydroxyl group of thymol with chloroacetyl chloride in the presence of triethylamine and methylene chloride as a solvent. The target synthesis product **20a-e** was obtained by nucleophilic substitution in the intermediate compound **18** with hydroxysubstituted benzoic acids **19a-e**.

The synthesis of mono- and dihydroxylated thymol derivatives with different positions of the hydroxyl group in the phenyl ring was carried out to study the role of multiple hydroxyl groups in tyrosinase inhibition. As a result, it was found out that the determining factor of inhibitory ability is not the number of hydroxyl groups, but their position [15]. Thus, the compound **20d** containing the 3,4-dihydroxy-substituted part of benzoic acid showed higher activity (IC_{50} = 45.0 μM) than **20c** and

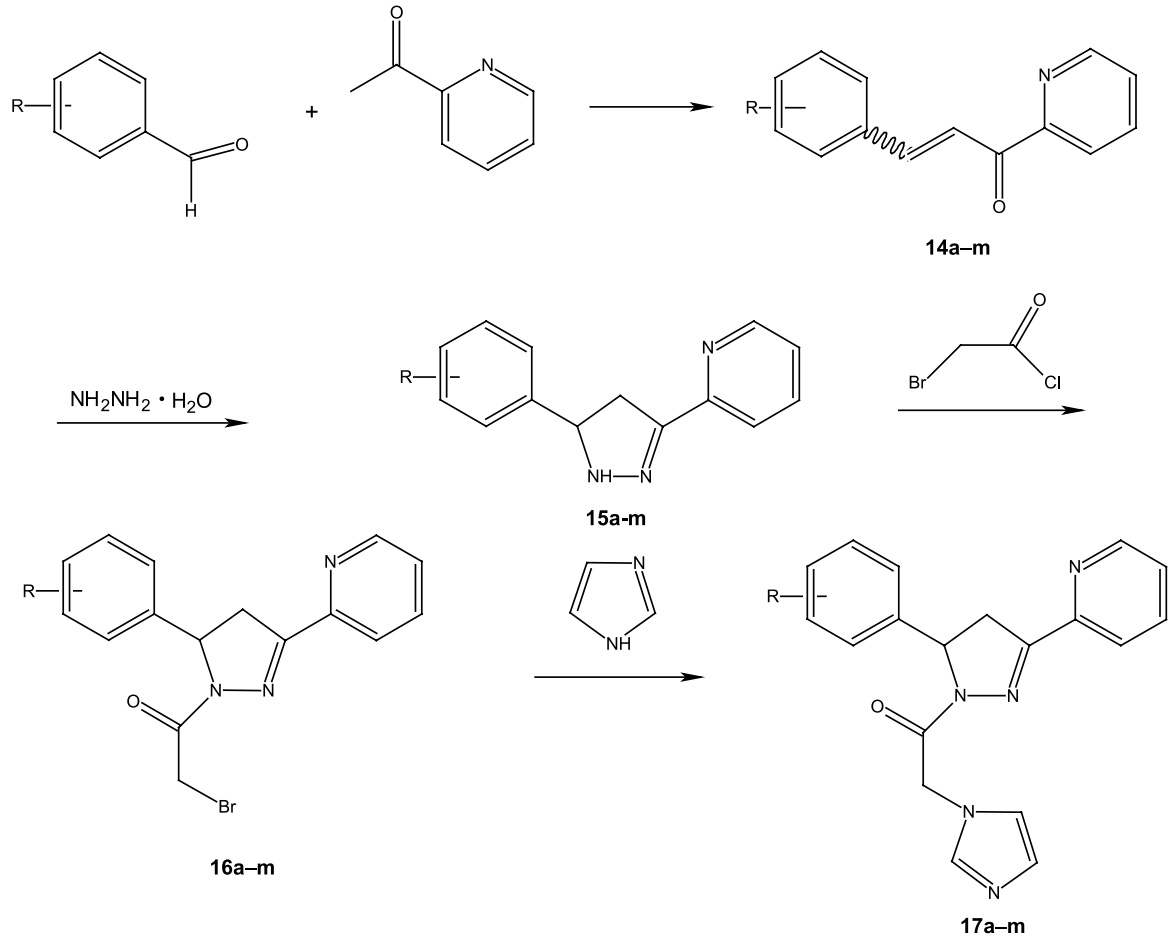

Fig. 6. Scheme for synthesis of (±)-1-(5-aryl-3-pyridin-2-yl-4,5-dihydro-pyrazol-1-yl)-2-imidazol-1-yl-ethanones (**17a-m**).

Table 3. Activity of derivatives of (±)-1-(5-aryl-3-pyridine-2-yl-4,5-dihydro-pyrazole-1-yl)-2-imidazole-1-yl-ethanones (**17**) against three strains of *Candida*

Compound	R	Yield, %	Range, μg/mL	CP 208		CPs 801		CG 80	
				24 h	48 h	24 h	48 h	24 h	48 h
AMB	–	–	0.5–8	1	2	2	<0.5	2	2
Mic	–	–	5–80	<5	<5	<5	<5	<5	<5
5FC	–	–	2–32	<2	4	<2	8	<2	<2
17a	H	53	1000–16	–	–	62.5	62.5	62.5	62.5
17b	2–Cl	45	1000–16	–	–	62.5	62.5	62.5	62.5
17e	2–Br	55	1000–16	–	–	62.5	62.5	62.5	62.5
17f	3–Br	56	1000–16	–	–	62.5	62.5	62.5	62.5
17h	2–F	48	1000–62.5	62.5	62.5	–	–	–	–
17i	3–F	46	1000–16	62.5	62.5	–	–	–	–
17j	4–F	49	1000–16	–	–	62.5	62.5	62.5	62.5
17k	2–CH_3	55	1000–16	62.5	62.5	–	–	–	–

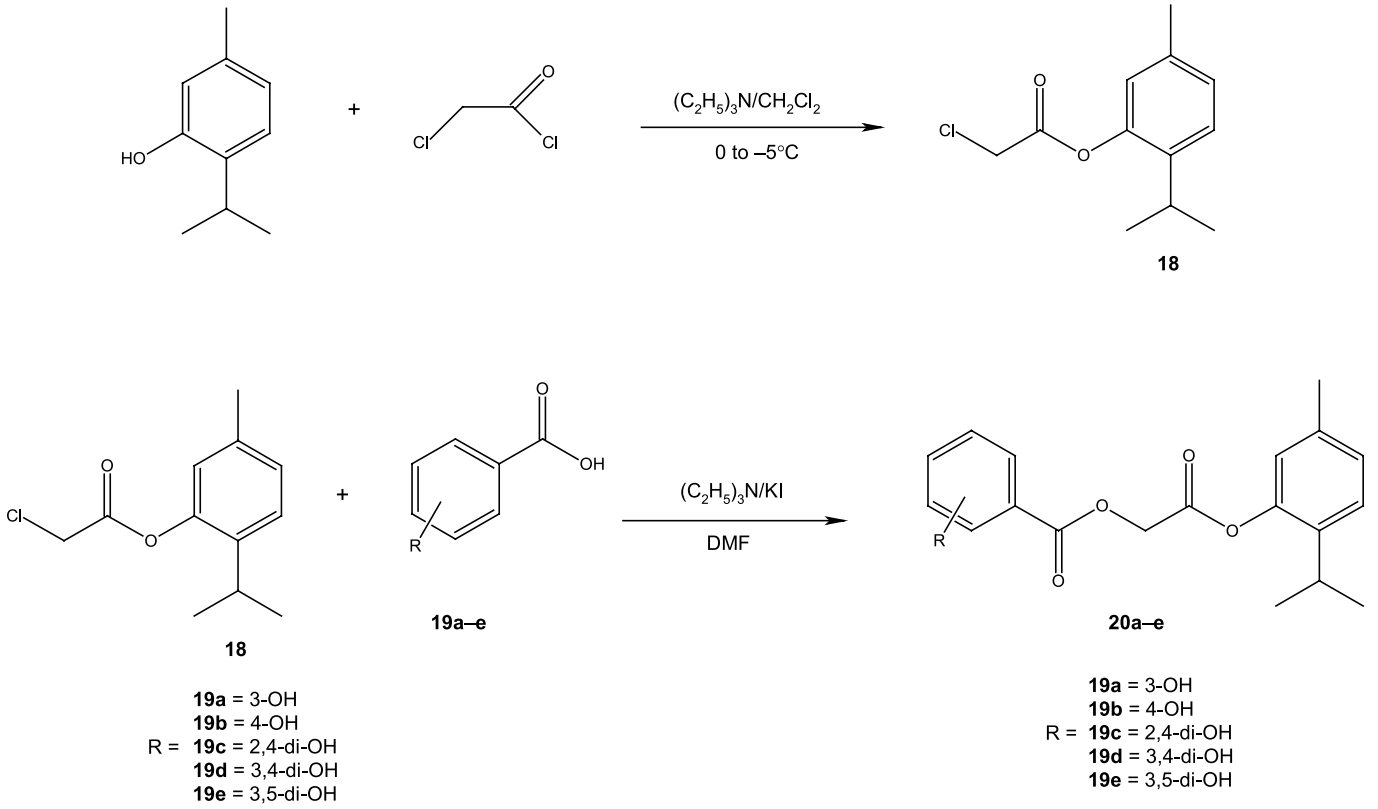

Fig. 7. Scheme for the synthesis of thymol derivatives (**20a-e**).

20e, for which the IC_{50} value was 56.1 and 220.9 μM, respectively. Derivatives **20c** and **20e** contain 2.4- and 3.5-dihydroxy-substituted benzoic acid residues, respectively. In the case of compound **20d**, two hydroxy groups are present in adjacent positions of the phenyl ring. This prevents the molecule from interacting well with the enzyme. This structural feature correlates well with L-3,4-dihydroxyphenylalanine (L-DOPA), which is used as a substrate for the enzyme tyrosinase during bioanalysis. Thus, the compound **20d** is the most active among the dihydroxylated thymol derivatives due to its close structural similarity to L-DOPA. Table 4 shows the IC_{50} values of synthesized thymol analogues. It can be seen that kojic acid exhibits better activity than all synthesized thymol derivatives [15].

In order to determine the optimal conditions for carrying out the acylation reaction of phenolic compounds, Uzbek scientists carried out syntheses under various conditions described in [16] (Fig. 8, Table 5). The chloroacetylation reaction of 4-hydroxyacetanilide was carried out in the presence of various catalysts and solvents. As a result of chloroacetylation of 4-hydroxyacetanilide in the presence of Lewis acids as a catalyst, two products are formed: 4-*N*-acetaminophenyl chloride and 5-*N*-acetamino-2-hydroxyphenacyl chloride. When the reaction is carried out in the absence of a catalyst, the *O*-acylation reaction predominates, resulting in a high observed yield of 4-*N*-acetaminophenyl chloroacetate. Table 5 shows that the best yield is observed when using chloroform as a solvent [16].

In this experimental work, we synthesized derivatives of thymol (2-isopropyl-5-methylphenol) and propofol (2,6-isopropylphenol) with imidazole via *O*-chloroacetates. A methoxy derivative of thymol was also obtained.[1]

EXPERIMENTAL

Devices and materials

^1H and ^{13}C NMR spectra was recorded on a pulsed Fourier spectrometer MSL-300 (*Bruker*, Germany) in $CDCl_3$ or DMSO-d_6 with tetramethylsilane as an internal standard. Chemical shifts are given in ppm; spin-spin interaction constants are in hertz. Column chromatography was performed using silica gel Kieselgel 60 (*Merck*,

[1] The numbering of connections in this and the following sections is autonomous.

Table 4. Activity of thymol derivatives **20a-e** against fungal tyrosinase

Compound	Tyrosinase inhibition activity	
	% Inhibition, 25 μg/mL	IC_{50} ± SEM μM
20a	48 ± 1	79.3 ± 5.3
20b	33 ± 2	91.5 ± 9.4
20c	68 ± 2	56.1 ± 5.9
20d	55 ± 3	45.0 ± 1.5
20e	5 ± 2	220.9 ± 11.6
Kojic acid	100	16.69 ± 2.8

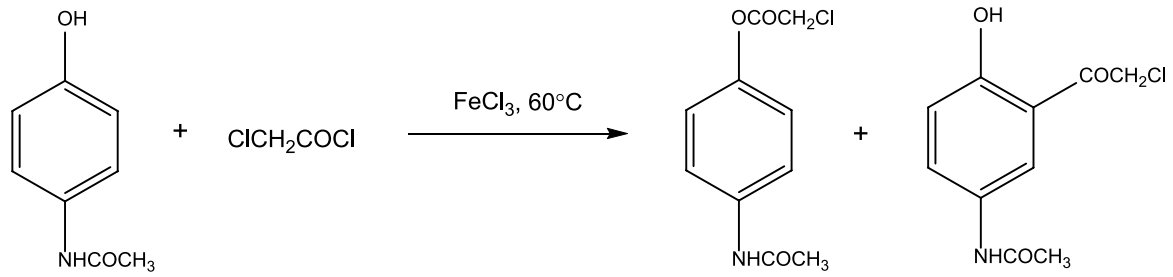

Fig. 8. Scheme for the synthesis of 4-*N*-acetaminophenylchloroacetate and 5-*N*-acetamino-2-hydroxyphenacyl chloride.

Table 5. Chloroacetylation of 4-hydroxyacetanilide in the presence of various solvents [16]

Reagents	Reagent ratio	Temperature, °C	Solvent	Yield, %
4-Hydroxyacetanilinide / chloroacetyl chloride	1:1	60–61	Chloroform	86
4-Hydroxyacetanilide / chloroacetyl chloride	1:1	98–100	Heptane	75
4-Hydroxyacetanilide / chloroacetyl chloride	1:1	83–84	Dichloroethane	79

Germany, particle size 40–63 μm). Silica Gel 60 F254 plates (*Merck*) were used for thin-layer chromatography (TLC) of the obtained compounds. The solvents were additionally dried or high purity reagents from *Merck* (Germany) and *Sigma-Aldrich* (USA) were used. The glassware was dried at 140°C before use.

Preparation of solvents for use in synthesis

The following solvents were used in the synthesis: methylene chloride (CH_2Cl_2), petroleum ether 40/70 (PE), ethyl acetate (EA), acetone, *N*,*N*-dimethylformamide (DMFA), tetrahydrofuran (THF),

and isopropyl alcohol (IPA). Drying and distillation of solvents was carried out according to standard methods.

Synthesis techniques of chloroacetyl derivatives of substituted phenols and polyphenols

The synthesis of 2-isopropyl-5-methylphenyl-2-chloroacetate (1) by heating is shown in Fig. 9.

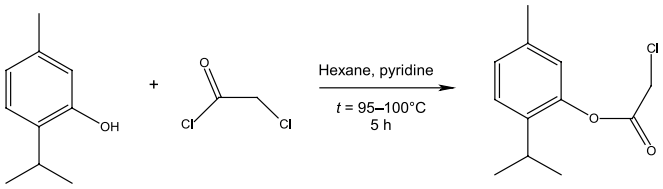

Fig. 9. Scheme for the synthesis of 2-isopropyl-5-methylphenyl-2-chloroacetate (**1**) by heating (method **I**).

Thymol (2.33 mmol, 350 mg) was dissolved in 15 mL of hexane and transferred to a flask fitted with a magnetic stirrer. After adding chloroacetyl chloride (3.26 mmol, 0.26 mL) dissolved in 5 mL of hexane to the thymol solution, the mixture was stirred and heated using a sand bath to a temperature of 95–100°C for 3 h. Then pyridine (0.36 mmol, 0.2 mL) was added to the reaction mass, which was continuously stirred for another 2 h under heating. The course of the reaction was controlled using TLC in a PE/EA solvent system in a ratio of 4:1. The reaction mass was washed from pyridine, dried over anhydrous sodium sulfate Na_2SO_4, and purified by column chromatography (PE/EA, 20:1→5:1). The yield was 254 mg (48%), R_f = 0.77 (PE/EA, 4:1).

^{1}H NMR spectrum (300 MHz, $CDCl_3$): δ=1.22–1.24(Ar–CH–$(CH_3)_2$, 6H), 2.35 (Ar–CH_3, 3H), 3.01 (Ar–CH, 1H), 4.34(–CH_2–Cl, 2H), 6.88(Ar–H4, 1H), 7.10 (Ar–H1, 1H), 7.23 (Ar–H2, 1H).

^{13}C NMR spectrum (75 MHz, $CDCl_3$): δ = 20.92 (C6), 23.14 (C7, C9), 27.19 (C8), 40.90 (C12), 122.36 (C4), 126.77 (C1), 127.81 (C2), 136.95 (C3, C5), 147.62 (C10), 166.27 (C14).

The synthesis of 2-isopropyl-5-methylphenyl-2-chloroacetate (2) by heating is shown in Fig. 10.

Thymol (0.67 mmol, 100 mg) was dissolved in 10 mL of methylene chloride and transferred to a flask with a magnetic stirrer. Chloroacetic anhydride (1.27 mmol, 216 mg) dissolved in 5 mL of pyridine was added to the thymol solution, and the mixture was stirred and heated using a sand bath to a temperature of 50–60°C for 5 h. The course of the reaction was controlled using TLC in a

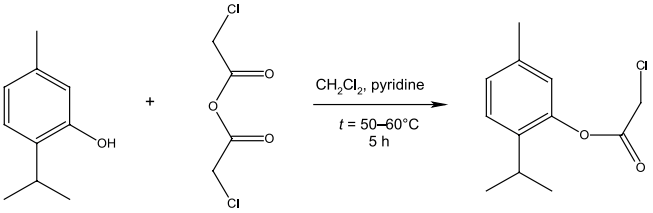

Fig. 10. Scheme for the synthesis of 2-isopropyl-5-methylphenyl-2-chloroacetate (**2**) by heating (method **II**).

PE/EA solvent system in a 10:1 ratio. The reaction mass was washed from pyridine, dried over Na_2SO_4 and purified by column chromatography (PE/EA, 25:1→10:1). The yield was 29 mg (19%), R_f = 0.67 (PE/EA, 10:1).

^{1}H NMR spectrum (300 MHz, DMSO-d_6): δ = 1.11–1.13 (Ar–CH–$(CH_3)_2$, 6H), 2.27 (Ar–CH_3, 3H), 2.96 (Ar–CH, 1H), 4.72 (–CH_2–Cl, 2H), 6.90 (Ar–H4, 1H), 7.09 (Ar–H1, 1H), 7.25 (Ar–H2, 1H).

The synthesis of 2-isopropyl-5-methylphenyl-2-chloroacetate (3) during cooling is shown in Fig. 11.

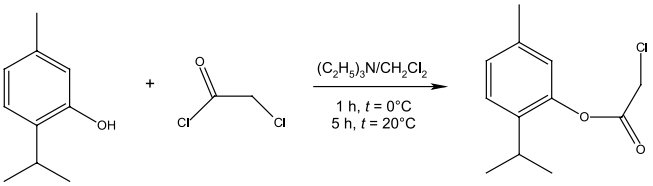

Fig. 11. Scheme for the synthesis of 2-isopropyl-5-methylphenyl-2-chloroacetate (**3**) during cooling (method **III**).

Thymol (1.26 mmol, 189 mg) and triethylamine (1.26 mmol, 0.18 mL) were dissolved in 20 mL of methylene chloride and transferred to a flask with a magnetic stirrer. The mixture was cooled in an ice bath to 0°C. Then chloroacetyl chloride (1.26 mmol, 0.1 mL) dissolved in 5 mL of methylene chloride was added to the reaction mixture drop by drop and cooled for 1 h. After that, the reaction continued at 20°C for another 5 h. The course of the reaction was controlled using TLC in a PE/EA solvent system in a 5:1 ratio. The reaction mass was extracted with 1% hydrochloric acid solution, 5% alkali solution, and with saturated salt solution and dried over Na_2SO_4. Further, the reaction mixture was purified by column chromatography (PE/EA, 30:1→10:1). The yield was 113 mg (40%), R_f = 0.63 (PE/EA, 5:1).

^{1}H NMR spectrum (300 MHz, DMSO-d_6): δ = 1.11–1.13 (Ar–CH–$(CH_3)_2$, 6H), 2.27 (Ar–CH_3, 3H),

2.96 (Ar–CH, 1H), 3.36 (Ar–OH, 4H), 4.72 (–CH_2–Cl, 2H), 6.90 (Ar–H4, 1H), 7.09 (Ar–H1, 1H), 7.25 (Ar–H2, 1H).

The synthesis of 2-isopropyl-5-methylphenyl-2-chloroacetate (4) during cooling is shown in Fig. 12.

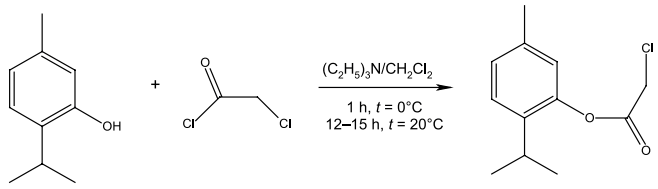

Fig. 12. Scheme for the synthesis of 2-isopropyl-5-methylphenyl-2-chloroacetate (**4**) during cooling (method **IV**).

Thymol (2.66 mmol, 400 mg) and triethylamine (5.32 mmol, 0.74 mL) were dissolved in 10 mL of methylene chloride and transferred to a flask with a magnetic stirrer. The mixture was cooled in an ice bath to 0°C. Then chloroacetyl chloride (13.32 mmol, 1.06 mL) dissolved in 7 mL of methylene chloride was added to the reaction mixture drop by drop and cooled for 1 h. After that, the reaction continued at 20°C for another 12–15 h. The course of the reaction was controlled using TLC in a PE/EA solvent system in a 10:1 ratio. The reaction mass was extracted with 1% hydrochloric acid solution, 5% alkali solution, and with saturated salt solution and dried over Na_2SO_4. Further, the reaction mixture was purified by column chromatography (PE/EA, 30:1→10:1). The yield was 450 mg (75%), R_f = 0.57 (PE/EA, 10:1).

^{1}H NMR spectrum (300 MHz, $CDCl_3$): δ = 1.22–1.24 (Ar–CH–$(CH_3)_2$, 6H), 2.35 (Ar–CH_3, 3H), 3.01 (Ar–CH, 1H), 4.34 (–CH_2–Cl, 2H), 6.88 (Ar–H4, 1H), 7.10 (Ar–H1, 1H), 7.23 (Ar–H2, 1H).

The synthesis of 2,6-diisopropylphenylchloroacetate (5) during cooling is shown in Fig. 13.

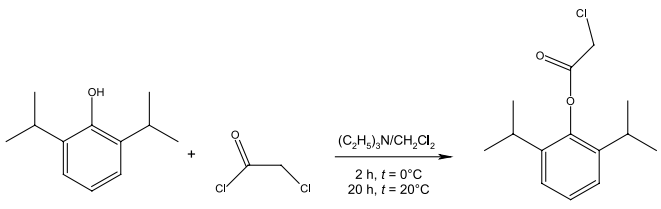

Fig. 13. Scheme for the synthesis of 2,6-diisopropylphenylchloroacetate (**5**) during cooling (method **IV**).

A mixture of propofol (1) (0.799 mmol), triethylamine (0.799 mmol) in anhydrous dichloromethane (25 mL) was cooled in a mixture of ice salt to 0–5°C. Chloroacetyl chloride (2) (0.799 mmol) was added to this reaction mixture in dry dichloromethane drop by drop with constant stirring for 2 h, maintaining a constant temperature. Then the reaction mixture was stirred at 20°C and left overnight, after that washed with 1% HCl and 5% sodium hydroxide solution. The organic layer was washed with saturated aqueous NaCl, dried over anhydrous sodium sulfate, and filtered and the solvent was removed at reduced pressure. The course of the reaction was controlled using TLC in a PE/EA solvent system in a 10:1 ratio. The mixture was purified by column chromatography (PE, PE/EA ratio was 15:1, 12:1, 10:1, 8:1, 6:1). The yield was 43 mg (30.3%). R_f = 0.72 (PE/EA, 10:1).

^{1}H NMR spectrum (300 MHz, DMSO-d_6): δ = 1.64–1.69 (Ar–CH–$(CH_3)_2$, 6H), 3.42–3.44 (Ar–CH, 1H), 5.33 (–CH_2–Cl), 7.73 (Ar–H3, 1H), 7.74 (Ar–H5, 1H), 7.76 (Ar–H4, 1H).

Methods of synthesis of imidazole derivatives of substituted phenols and polyphenols

The synthesis of 2-isopropyl-5-methylphenyl-2-(1*H*-imidazole-1-yl)acetate (6) at 20°C is shown in Fig. 14.

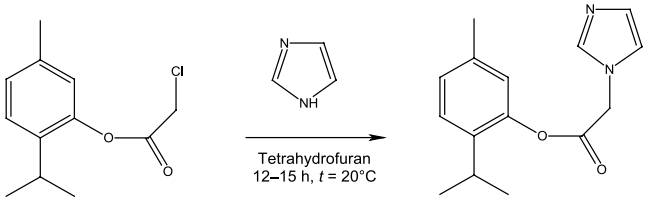

Fig. 14. Scheme for the synthesis of 2-isopropyl-5-methylphenyl-2-(1*H*-imidazol-1-yl) acetate (**6**) at 20°**C** (method **V**).

Imidazole (21.83 mmol, 1486 mg) and 2-isopropyl-5-methylphenyl 2-chloroacetate (1.98 mmol, 450 mg) were dissolved in 7 mL of THF and transferred to a flask with a magnetic stirrer. The mixture was continuously stirred at 20°C for 12–15 h. The course of the reaction was controlled using TLC in the IPS/CH_2Cl_2 solvent system in a 3:2 ratio. The reaction mass was washed with water and dried over Na_2SO_4. Further, the reaction mixture was purified by column chromatography (IPS/CH_2Cl_2, 2:3→3:1). The yield was 20 mg (4%), R_f = 0.85 (IPS/CH_2Cl_2, 3:2).

^{1}H NMR spectrum (300 MHz, DMSO-d_6): δ = 0.85–0.89 (Ar–CH–$(CH_3)_2$, 6H), 2.27 (Ar–CH_3, 3H),

2.91 (Ar–CH, 1H), 4.57–4.71 (–CH_2–N, 2H), 6.55 (Ar–H4, 1H), 6.70 (–N–CH=CH=, 1H), 6.72 (=CH–N–, 1H), 6.80 (Ar–H1, 1H), 6.95 (–N=CH–N–, 1H), 7.02 (Ar–H2, 1H).

The synthesis of 2-isopropyl-5-methylphenyl-2-(1*H*-imidazole-1-yl)acetate (7) at low temperature is shown in Fig. 15.

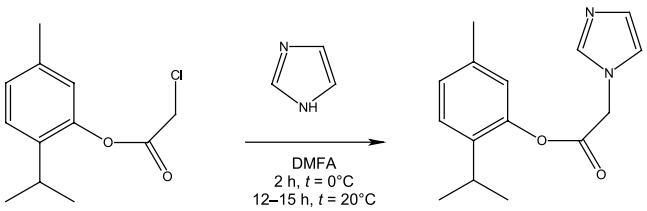

Fig. 15. Scheme for the synthesis of 2-isopropyl-5-methylphenyl-2-(1*H*-imidazol-1-yl) acetate (**7**) during cooling (method **VI**).

Imidazole (4.4 mmol, 300 mg) and 2-isopropyl-5-methylphenyl 2-chloroacetate (0.44 mmol, 100 mg) were dissolved in 3 mL of DMFA and transferred to a flask with a magnetic stirrer and cooled in an ice bath to 0°C for 2 h. After that, the reaction continued at a temperature of 20°C for 12–15 h. The course of the reaction was controlled using TLC in the IPS/CH_2Cl_2 solvent system in a 3:2 ratio. The reaction mass was diluted with water and extracted with CH_2Cl_2, then dried over Na_2SO_4 and evaporated using a rotary evaporator. After removing the solvent, the substance crystallized. The yield was 64 mg (57%), R_f = 0.85 (IPS/CH_2Cl_2, 3:2).

^{1}H NMR spectrum (300 MHz, DMSO-d_6): δ = 0.85–0.89 (Ar–CH–$(CH_3)_2$, 6H), 2.27 (Ar–CH_3, 3H), 2.91 (Ar–CH, 1H), 4.57–4.71 (–CH_2–N, 2H), 6.55 (Ar–H4, 1H), 6.70 (–N–CH=CH=, 1H), 6.72 (=CH–N–, 1H), 6.80 (Ar–H1, 1H), 6.95 (–N=CH–N–, 1H), 7.02 (Ar–H2, 1H).

The synthesis of 2,6-diisopropylphenylimidazol-acetate (8) at 20°C is shown in Fig. 16.

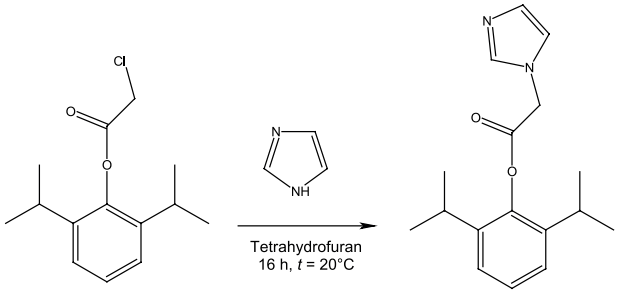

Fig. 16. Scheme for the synthesis of 2,6-diisopropyl-phenylimidazole acetate (**8**) at 20°C.

The ester of propofol and chloroacetyl chloride (130 mg, 0.51 mmol) and imidazole (521 mg, 7.65 mmol) were dissolved in 10 mL of THF and transferred to a round-bottomed flask with a magnetic stirrer. The reaction was placed in the shade because of the fact that under the influence of light, THF can form peroxides. The reaction was left overnight. Then the THF was evaporated on a rotary evaporator and the substance was re-dissolved into CH_2Cl_2. After that, the reaction mixture was washed twice with water and dried over Na_2SO_4. The course of the reaction was controlled using TLC in an isopropanol/CH_2Cl_2 solvent system in a 4:1 ratio. The mixture was purified by column chromatography (CH_2Cl_2, isopropanol/CH_2Cl_2 ratio was 2:3, 1:1, 3:2, 2:1, 3:1). The yield was 32 mg (23.3%). R_f = 0.80 (Isopropanol/CH_2Cl_2, 4:1).

^{1}H NMR spectrum (300 MHz, DMSO-d_6): δ = 1.31–1.35 (Ar–CH–$CH_3)_2$, 6H), 3.09–3.11 (Ar–CH, 1H), 5.62 (–CH_2–Im), 7.40 (Ar–H3, 1H), 7.41 (Ar–H5, 1H), 7.42 (Ar–H4, 1H), 7.15 (Im–H5, 1H), 7.17 (Im–H4, 1H), 7.45 (Im–2H, 1H).

Method of synthesis of methoxy derivatives of substituted phenols

The synthesis of methoxythymol (1-isopropyl-2-methoxy-4-methylbenzene) (9) is shown in Fig. 17.

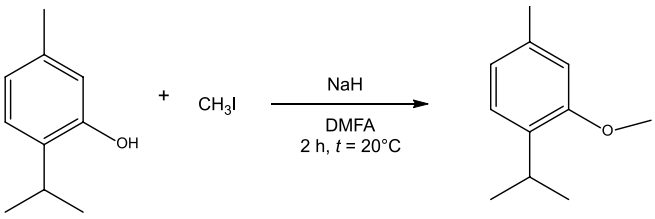

Fig. 17. Scheme for the synthesis of methoxythymol (1-isopropyl-2-methoxy-4-methylbenzene) (**9**).

A suspension of NaH (1.58 mmol, 38 mg) in DMFA was added to thymol (0.8 mmol, 120 mg) dissolved in 1 mL of DMFA and placed in a flask with a magnetic stirrer. The mixture was stirred for 45 min at 20°C. Then CH_3I (2.4 mmol, 0.15 mL) was added to the reaction mixture drop by drop and kept for 1 h at 20°C. The course of the reaction was controlled using TLC in a PE/EA solvent system in a 3:1 ratio. The reaction mass was decomposed with water, acidified with 1% hydrochloric acid solution to pH 4.0, extracted with methylene chloride, and dried over Na_2SO_4. Further, the reaction mixture was purified by column chromatography (PE/EA, 15:1→4:1). The yield was 60 mg (46%), R_f = 0.69 (PE/EA, 3:1).

^{1}H NMR spectrum (300 MHz, DMSO-d_6): δ = 1.11–1.13 (Ar–CH–$(CH_3)_2$, 6H), 2.26 (Ar–CH_3, 3H), 3.15–3.18 (Ar–CH–, 1H), 3.76 (–O–CH_3), 6.74 (Ar–H6, 1H), 6.77 (Ar–H4, 1H), 7.03 (Ar–H3, 1H).

RESULTS AND DISCUSSION

Preparation of chloroacetyl derivatives of substituted phenols and polyphenols

The synthesis of imidazole derivatives of alkyl-substituted phenols was carried out in two stages (Fig. 18). At the first stage of synthesis, *O*-chloroacetyl derivatives of selected alcohols, thymol, and propofol were obtained, to which imidazole was then added.

Chloroacetyl derivatives of aromatic alcohols were obtained using several techniques described in the literature. In particular, syntheses carried out during heating [16] and cooling [15] of the reaction mass were used.

In order to obtain a chloroacetyl derivative of thymol using heating, two syntheses were carried out under different conditions (Figs. 9 and 10). The first synthesis (method **I**) was carried out using chloroacetyl chloride as an acylating agent and *n*-hexane as a high-boiling solvent. In the second case (method **II**) involving the use of chloroacetic anhydride, an attempt was made to replace the solvent with low-boiling methylene chloride. As a result, the following product yields were obtained: for compound **1** (method **I**), the yield was 48%, whereas for compound **2** (method **II**), the yield was 19%, from which it follows that the change in the conditions of the synthesis did not lead to a better result.

We also investigated the possibilities of improving synthesis methods using reduced (0°C) and room temperature (20°C) using the example of two methods with chloroacetyl chloride as an *O*-acylating reagent, which differed in reaction time and reagent ratios (Figs. 11 and 12). Chloroacetyl derivatives of thymol were obtained with yields of 40% (method **III**) and 75% (method **IV**) for compounds **3** and **4**, respectively. Therefore, the synthesis by cooling the reaction mass using an excess of an acylating agent and increasing the reaction time is more preferable when obtaining chloroacetyl derivatives of aromatic alcohols. The results are presented in Table 6.

The *O*-acylation reaction of propofol proceeded similarly to the reaction with thymol, but the reaction time increased due to steric difficulties in attaching the chloroacetate fragment to propofol (Fig. 13). The product yield was 30%.

Preparation of imidazole chloroacetyl derivatives of alkyl-substituted phenols

We conducted a synthetic study to obtain imidazole derivatives of 2-isopropyl-5-methylphenyl--2-chloroacetate. In the course of the study, two syntheses were carried out according to the methods described in [15, 16], in which different temperatures and solvents were used (Figs. 14 and 15), and we also increased the reaction time in comparison with the literature sources used. When synthesizing at 20°C and using THF as a reaction medium (method **V**), the yield of product **6** was 4%, which is not a satisfactory result. In order to increase the yield of the product, synthesis was carried out using DMFA as a solvent, as well as at lower and room temperatures (method **VI**) the yield of product 7 was 57%.

The reaction of 2,6-isopropylphenylchloro-acetate with imidazole was carried out according to method **V**, similarly to the reaction with a thymol derivative, the yield was 23%. The results are presented in Table 7.

Preparation of methoxy derivatives of substituted phenols

The methoxy derivatives of thymol were synthesized according to the method [17]. Due to steric difficulties in attaching the methyl residue, the reaction time was increased (Fig. 17). In this case, methoxythymol (1-isopropyl-2-methoxy-4-methyl-benzene) (9) was obtained with a yield of 46%.

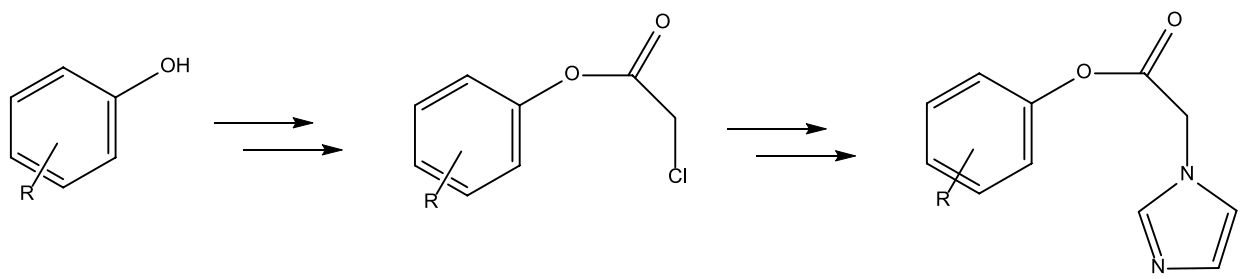

Fig. 18. General scheme for the synthesis of imidazole derivatives of substituted phenols and polyphenols.

Table 6. Chloroacetylation of thymol in the presence of various solvents

Reagents	Reagent ratio	Temperature, °C	Solvent	Yield, %
Thymol/Chloroacetyl chloride	1:1	95–100	Hexane	48
Thymol/Chloroacetic anhydride	1:1.9	50–60	Methylene chloride	19
Thymol/Chloroacetyl chloride	1:2	0–5	Methylene chloride	40
Thymol/Chloroacetyl chloride	1:4	0–5	Methylene chloride	75

Table 7. Preparation of imidazole chloroacetyl derivatives of alkyl-substituted phenols in the presence of various solvents

Reagents	Reagent ratio	Temperature, °C	Solvent	Yield, %
Thymol chloroacetyl chloride / imidazole	1:3	20	THF	4
Thymol chloroacetyl chloride / imidazole	1:10	0–5	DMFA	57
Propofol chloroacetyl chloride / imidazole	1:10	0–5	DMFA	23

Note: THF is tetrahydrofuran; DMFA is *N*,*N*-dimethylformamide.

Confirmation of the structure of the obtained compounds

The structures of the obtained compounds were confirmed by methods ^{1}H and ^{13}C NMR spectroscopy.

^{1}H NMR spectrum of 2-isopropyl-5-methylphenyl-2-chloroacetate (Fig. 19). Methyl protons of the isopropyl chain of the ring were observed at δ = 1.22–1.24 ppm. The signal belonging to Ar–CH_3 was recorded at δ = 2.35 ppm. The proton Ar–CH– gives a multiplet at 3.01 ppm. The spectrum also showed a signal at δ = 4.34 ppm, which indicates the presence of –CH_2–Cl. Aromatic protons appeared in the characteristic range from 6.88 to 7.23 ppm.

^{13}C NMR spectrum of 2-isopropyl-5-methylphenyl-2-chloroacetate (Fig. 20). The methyl carbon of the ring (Ar–CH_3) gave a signal at 20.92 ppm. The methyl carbons of the isopropyl chains of the ring were present at δ = 23.14 ppm. The carbon corresponding to Ar–CH resonated at δ = 27.19 ppm. The signal at δ = 40.90 ppm confirms the presence of chloroacetate (–CH_2–Cl). Signals in the range from 122.36 to 136.95 ppm confirm the presence of the aromatic ring. The signal at δ = 147.62 ppm corresponds to carbon, through which a complex ester bond is formed by oxygen. The spectrum also showed a signal at δ = 166.27 ppm, characteristic of the carboxyl group atom (C=O).

^{1}H NMR spectrum of 2,6-diisopropylphenyl-chloroacetate (Fig. 21). A multiplet corresponding to the methyl protons of the isopropyl chains of the ring was observed at δ = 1.64–1.69 ppm. The proton Ar–CH– gives a multiplet at δ = 3.42–3.44. The signal at δ = 5.33 ppm corresponded to protons –CH_2–Cl. The protons of the aromatic ring appeared in the range of 7.73–7.76 ppm.

^{1}H NMR spectrum of 2-isopropyl-5-methylphenyl-2-(1*H*-imidazole-1-yl)acetate (Fig. 22). Methyl protons of the isopropyl chain of the ring were observed at δ = 0.85–0.89 ppm. The signal belonging to Ar–CH_3 was recorded at δ = 2.27 ppm. The proton Ar–CH– gives a multiplet at 2.91 ppm. The spectrum

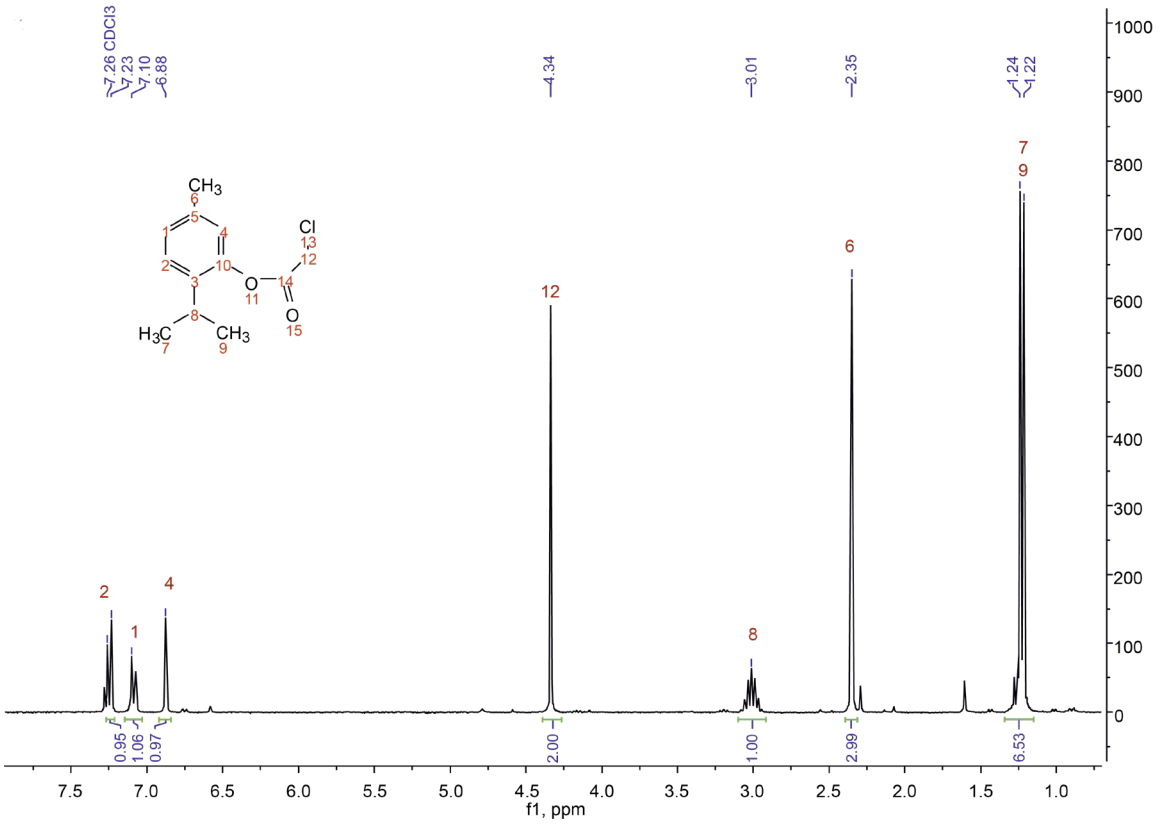

Fig. 19. [1]H NMR spectrum of 2-isopropyl-5-methylphenyl-2-chloroacetate.

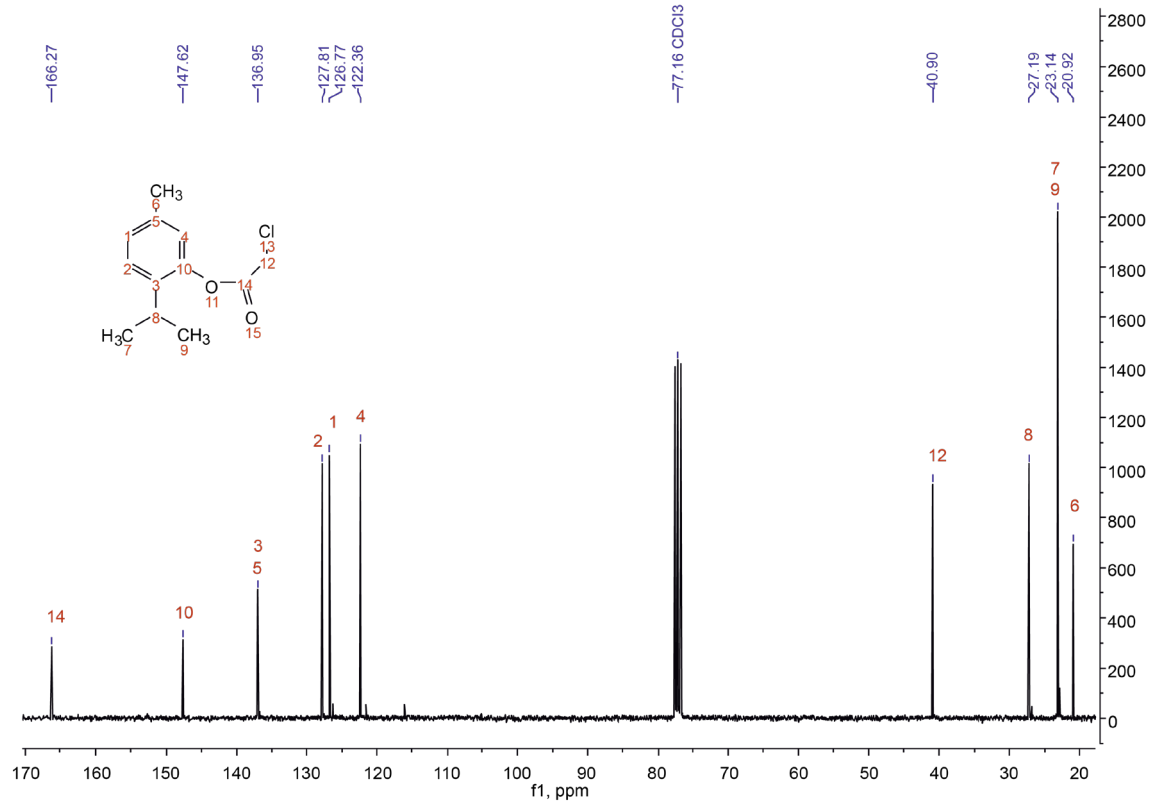

Fig. 20. [13]C NMR spectrum of 2-isopropyl-5-methylphenyl-2-chloroacetate.

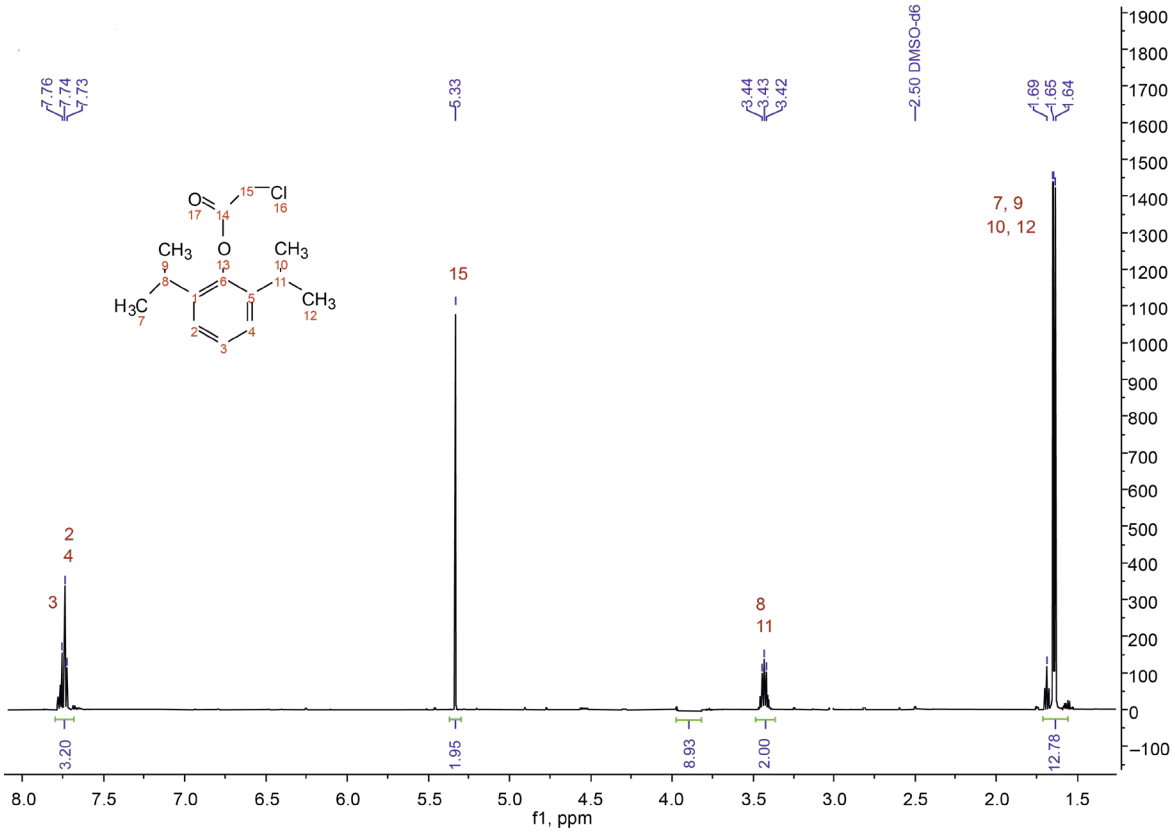

Fig. 21. [1]H NMR spectrum of 2,6-diisopropylphenylchloroacetate.

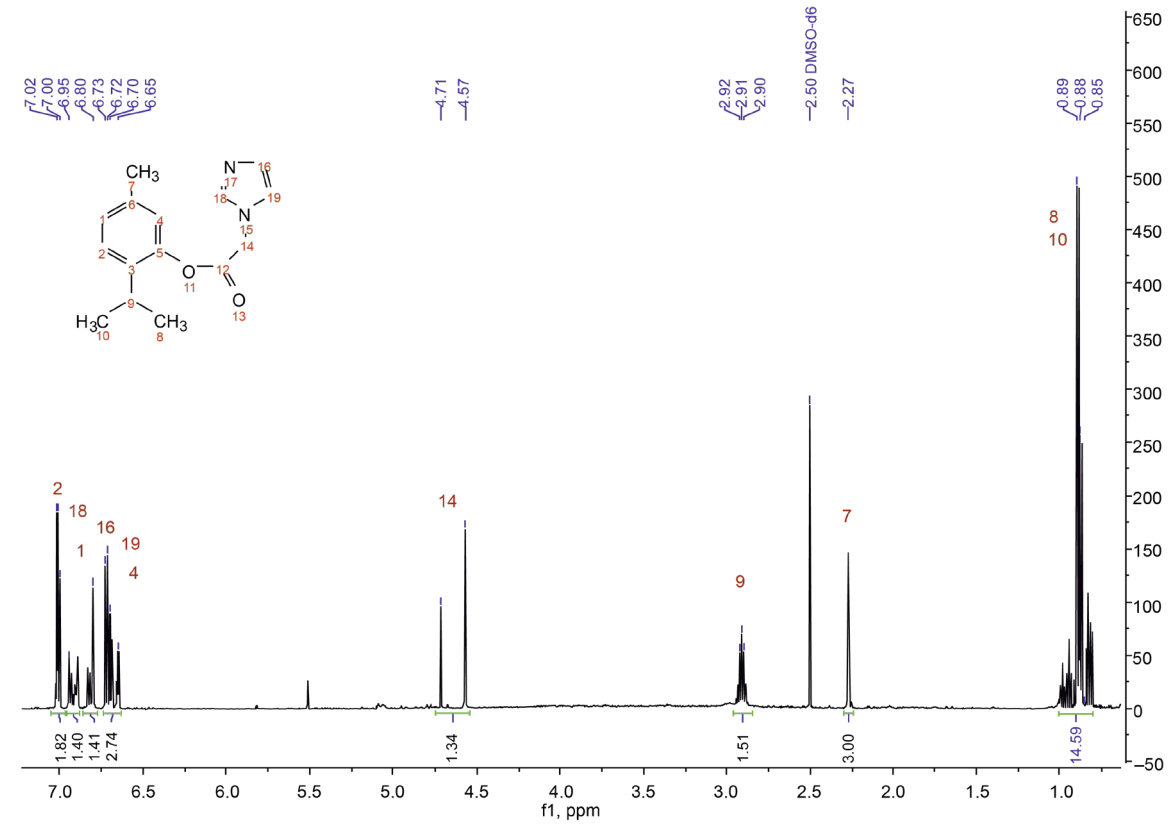

Fig. 22. [1]H NMR spectrum of 2-isopropyl-5-methylphenyl-2-(1*H*-imidazol-1-yl) acetate.

also showed signals at δ = 4.57–4.71 ppm, which indicates the splitting of protons –CH_2– groups located between –N– and –C=O groups.

It can be explained by the fleximeric structure of this molecule, which is confirmed by 3D modeling data (Fig. 23). Aromatic protons appeared in the characteristic range from 6.65 to 7.02 ppm. The protons of the imidazole fragment were observed in the range from 6.70 to 7.00 ppm. The split signal of the proton –CH– between two nitrogen atoms (δ = 7.00 ppm) also testifies in favor of the formation of a fleximer analog.

^{1}H NMR spectrum of 2,6-diisopropylphenyl-imidazolacetate (Fig. 24). A multiplet corresponding to the methyl protons of the isopropyl chains of the ring was observed at δ = 1.31–1.35 ppm. The proton Ar–CH– gives a multiplet at δ = 3.09–3.11. The signal at δ = 5.62 ppm corresponded to the protons –CH_2–Im. The protons of the aromatic ring appeared in the range of 7.40–7.42 ppm, and the protons of the imidazole ring in the range of 7.15–7.45 ppm.

^{1}H NMR spectrum of methoxythymol (Fig. 25). A doublet corresponding to the methyl protons of the isopropyl chain of the ring was observed at δ = 1.11–1.13 ppm. At δ = 2.26 ppm, a signal corresponding to Ar–CH_3 was recorded. The proton Ar–CH– gives a multiplet at δ = 3.15–3.18 ppm. The signal at δ = 3.76 ppm corresponded to the protons –O–CH_3. The protons of the aromatic ring appeared in the range of 6.74–7.03 ppm.

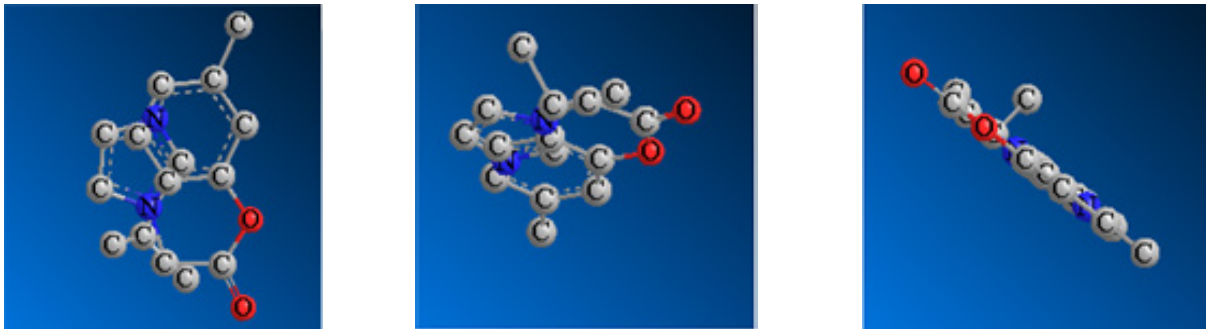

Fig. 23. 3D model of 2-isopropyl-5-methylphenyl-2-(1*H*-imidazol-1-yl) acetate.

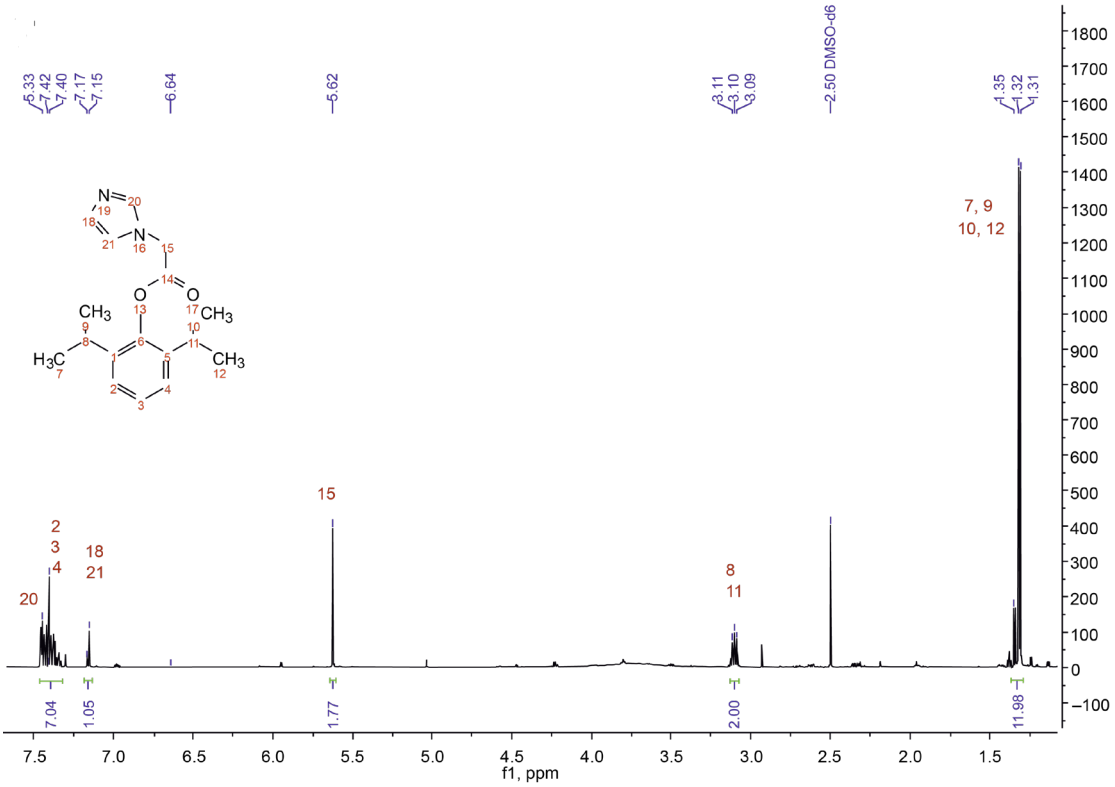

Fig. 24. ^{1}H NMR spectrum of 2,6-diisopropylphenylimidazole acetate.

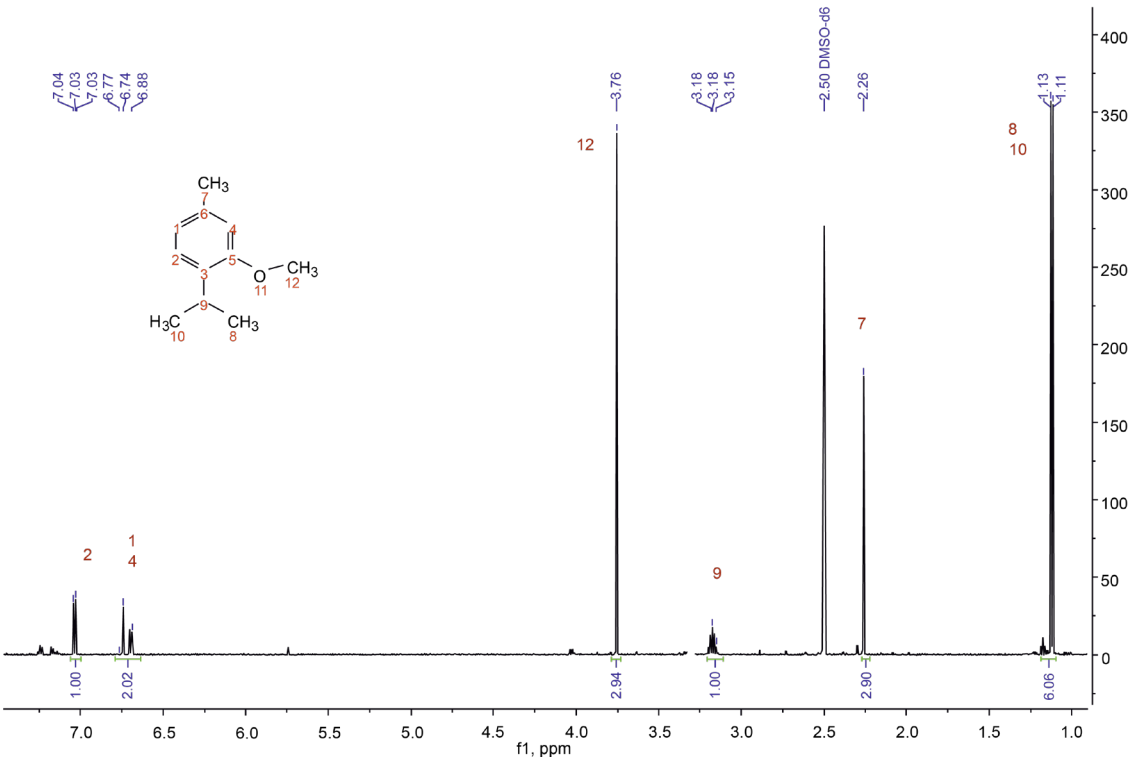

Fig. 25. ^{1}H NMR spectrum of methoxythymol.

CONCLUSIONS

When studying various approaches for the *O*-acylation of thymol and propofol, it was found that synthesis carried out during cooling of the reaction mass using an excess of chloroacetyl chloride in dichloromethane in the presence of triethylamine gives the highest yield, as well as allowing the conversion of the initial reagent to be controlled. For the stage of pharmacophore (heterocycle) administration, a reaction with imidazole in tetrahydrofuran at room temperature was worked out. The structure of the compounds was confirmed by NMR spectroscopy. Samples of the obtained compounds were transferred for biological studies on model yeast strains. Such methods are likely to be useful for obtaining a number of hydrophobic derivatives of aromatic alcohols.

Acknowledgments

The work was supported by a grant from the Ministry of Science and Higher Education of the Russian Federation (project No. 0706-2020-0019) using the equipment of the RTU MIREA Center for Collective Use.

Authors' contributions

V.A. Sokhraneva – conducting experiments on the synthesis of thymol–imidazole conjugates, processing the material, and writing the text of the article;

D.A. Yusupova – conducting experiments on the synthesis of thymol–imidazole conjugates, synthesis of thymol methoxy derivative;

V.S. Boriskin – conducting experiments on the synthesis of conjugates of propofol with imidazole;

N.V. Groza – development of the research concept, scientific guidance at all stages of the study.

The authors declare no conflicts of interest.

REFERENCES

1. Hoq M.I., Mitsuno K., Tsujino Y., Aoki T., Ibrahim, H.R. Triclosan–lysozyme complex as novel antimicrobial macromolecule: a new potential of lysozyme as phenolic drug-targeting molecule. *Int.l J. Biol. Macromol*. 2008;42(5):468–477. https://doi.org/10.1016/j.ijbiomac.2008.03.003

2. Kumar N., Goel N. Phenolic acids: natural versatile molecules with promising therapeutic applications. *Biotechnol. Rep.* 2019;24:e00370. https://doi.org/10.1016/j.btre.2019.e00370

3. Gligor O., Mocan A., Moldovan C., Locatelli M., Crișan G., Ferreira I.C. Enzyme-assisted extractions of polyphenols – a comprehensive review. *Trends in Food Science and Technology*. 2019;88:302–315. https://doi.org/10.1016/j.tifs.2019.03.029

4. Solovieva N.L., Sokurenko M.S. Technologies to improve the stability of polyphenolic compounds in drug discovery (review). *Razrabotka i registratsiya lekarstvennykh sredstv = Drug Development & Registration*. 2016;4(17):82–91 (in Russ.).

5. Lima M.C., Paiva de Sousa C., Fernandez-Prada C., Harel J., Dubreuil J.D., de Souza E.L. A review of the current evidence of fruit phenolic compounds as potential antimicrobials against pathogenic bacteria. *Microb. Pathog.* 2019;130:259–270. https://doi.org/10.1016/j.micpath.2019.03.025

6. Cai Y.-Z., Mei Sun, Jie Xing, Luo Q., Corke H. Structure–radical scavenging activity relationships of phenolic compounds from traditional Chinese medicinal plants. *Life Sciences.* 2006;78(25):2872–2888. https://doi.org/10.1016/j.lfs.2005.11.004

7. Rossi R., Ciofalo M. An Updated Review on the Synthesis and Antibacterial Activity of Molecular Hybrids and Conjugates Bearing Imidazole Moiety. *Molecules.* 2020;25(21):5133. https://doi.org/10.3390/molecules25215133

8. Verma A., Joshi S., Singh D. Imidazole: having versatile biological activities. *J. Chem.* 2013;2013:329412. https://doi.org/10.1155/2013/329412

9. Walker K.A.M., Wallach M.B., Hirschfeld D.R. 1-(Naphthylalkyl)-1H-imidazole derivatives, a new class of anticonvulsant agents. *J. Med. Chem.* 1981;24(1):67–74. https://doi.org/10.1021/jm00133a015

10. Karakurt A., Dalkara S., Özalp M., Özbey S., Kendi E., Stables J.P. Synthesis of some 1-(2-naphthyl)-2-(imidazole-1-yl)ethanone oxime and oxime ether derivatives and their anticonvulsant and antimicrobial activities. *Eur. J. Med. Chem.* 2001;36(5):421–433. https://doi.org/10.1016/s0223-5234(01)01223-5

11. Ksiezopolska E., Gabaldón T. Evolutionary Emergence of Drug Resistance in Candida Opportunistic Pathogens. *Genes.* 2018;9(9):461. https://doi.org/10.3390/genes9090461

12. Tosi M., Roat E., De Biasi S., Munari E., Venturelli S., Coloretti I., Biagioni E., Cossarizza A., Girardis M. Multidrug resistant bacteria in critically ill patients: a step further antibiotic therapy. *J. Emerg. Crit. Care Med.* 2018;2:103. https://doi.org/10.21037/JECCM.2018.11.08

13. Frei R., Breitbach A.S., Blackwell H.E. 2-Aminobenzimidazole derivatives strongly inhibit and disperse Pseudomonas aeruginosa biofilms. *Angew. Chem. Int. Ed.* 2012;51(21):5226–5229. https://doi.org/10.1002/anie.201109258

14. Mamolo M.G., Zampieri D., Falagiani V., Vio L., Banfi E. Synthesis and antifungal activity of (±)-1-(5-aryl-3-pyridin-2-yl-4,5-dihydro-pyrazol-1-yl)-2-imidazol-1-yl-ethanone derivatives. *Il Farmaco.* 2003;58(4):315–322. https://doi.org/10.1016/s0014-827x(02)00006-x

15. Ashraf Z., Rafiq M., Seo S.-Y., Kwon K.S., Babar M.M., Sadaf Zaidi N.-S. Kinetic and in silico studies of novel hydroxy-based thymol analogues as inhibitors of mushroom tyrosinase. *Eur. J. Med. Chem.* 2015;98:203–211. https://doi.org/10.1016/j.ejmech.2015.05.031

16. Abdushukurov A.K., Yusufov M.S., Khurramov E.N., Shakhriev H. Chlorocetylation of 4-hydroxyacetanilide. *Universum: Tekhnicheskie nauki = Universum: Eng. Sci.* 2018;5(50). URL: http://7universum.com/ru/tech/archive/item/5915

17. Horne G., Mills S.J., Potter B.V. First derivatives of myo-inositol 1,4,6-trisphosphate modified at positions 2 and 3: structural analogues of D-myo-inositol 1,4,5-trisphosphate. *Carbohydr. Res*. 2004;339(1):51–65. https://doi.org/10.1016/j.carres.2003.09.008

About the authors:

Vera A. Sokhraneva, Student, N.A. Preobrazhensky Department of Chemistry and Technology of Biologically Active Compounds, Medicinal and Organic Chemistry, M.V. Lomonosov Institute of Fine Chemical Technologies, MIREA – Russian Technological University (86, Vernadskogo pr., Moscow, 119571, Russia). E-mail: sokhraneva.v@mail.ru. https://orcid.org/0000-0003-0930-5604

Dilyara A. Yusupova, Master Student, N.A. Preobrazhensky Department of Chemistry and Technology of Biologically Active Compounds, Medicinal and Organic Chemistry, M.V. Lomonosov Institute of Fine Chemical Technologies, MIREA – Russian Technological University (86, Vernadskogo pr., Moscow, 119571, Russia). E-mail: dilyara.yus1997@mail.ru. https://orcid.org/0000-0002-6822-5383

Vladimir S. Boriskin, Student, N.A. Preobrazhensky Department of Chemistry and Technology of Biologically Active Compounds, Medicinal and Organic Chemistry, M.V. Lomonosov Institute of Fine Chemical Technologies, MIREA – Russian Technological University (86, Vernadskogo pr., Moscow, 119571, Russia). E-mail: vladimir.borisckin@gmail.com. https://orcid.org/0000-0001-6474-7005

Nataliya V. Groza, Cand. Sci. (Chem.), Associate Professor, N.A. Preobrazhensky Department of Chemistry and Technology of Biologically Active Compounds, Medical and Organic Chemistry, M.V. Lomonosov Institute of Fine Chemical Technologies, MIREA – Russian Technological University (86, Vernadskogo pr., Moscow, 119571, Russia). E-mail: grozanv@gmail.com. Scopus Author ID 6602326980, ResearcherID I-6156-2016, RSCI SPIN-code 7210-6410, https://orcid.org/0000-0002-6699-5907

Об авторах:

Сохранева Вера Александровна, студент кафедры химии и технологии биологически активных соединений, медицинской и органической химии им. Н.А. Преображенского Института тонких химических технологий им. М.В. Ломоносова ФГБОУ ВО «МИРЭА – Российский технологический университет» (119571, Россия, Москва, пр-т Вернадского, д. 86). E-mail: sokhraneva.v@mail.ru. https://orcid.org/0000-0003-0930-5604

Юсупова Диляра Ахметовна, магистрант кафедры химии и технологии биологически активных соединений, медицинской и органической химии им. Н.А. Преображенского Института тонких химических технологий им. М.В. Ломоносова ФГБОУ ВО «МИРЭА – Российский технологический университет» (119571, Россия, Москва, пр-т Вернадского, д. 86). E-mail: dilyara.yus1997@mail.ru. https://orcid.org/0000-0002-6822-5383

Борискин Владимир Сергеевич, студент кафедры химии и технологии биологически активных соединений, медицинской и органической химии им. Н.А. Преображенского Института тонких химических технологий им. М.В. Ломоносова ФГБОУ ВО «МИРЭА – Российский технологический университет» (119571, Россия, Москва, пр-т Вернадского, д. 86). E-mail: vladimir.borisckin@gmail.com. https://orcid.org/0000-0001-6474-7005

Гроза Наталья Викторовна, к.х.н., доцент кафедры химии и технологии биологически активных соединений, медицинской и органической химии им. Н.А. Преображенского Института тонких химических технологий им. М.В. Ломоносова ФГБОУ ВО «МИРЭА – Российский технологический университет» (119571, Россия, Москва, пр-т Вернадского, д. 86). E-mail: grozanv@gmail.com. Scopus Author ID 6602326980, ResearcherID I-6156-2016, SPIN-код РИНЦ 7210-6410, https://orcid.org/0000-0002-6699-5907

The article was submitted: December 21, 2021; approved after reviewing: March 10, 2022; accepted for publication: June 17, 2022.

Translated from Russian into English by N. Isaeva
Edited for English language and spelling by Thomas Beavitt

SYNTHESIS AND PROCESSING OF POLYMERS AND POLYMERIC COMPOSITES

СИНТЕЗ И ПЕРЕРАБОТКА ПОЛИМЕРОВ И КОМПОЗИТОВ НА ИХ ОСНОВЕ

ISSN 2686-7575 (Online)
https://doi.org/10.32362/2410-6593-2022-17-3-231-241
UDC 678

RESEARCH ARTICLE

Biodegradable packaging materials based on low density polyethylene, starch and monoglycerides

Ilya Yu. Vasilyev[1,✉], Vladimir V. Ananyev[1], Michel E. Chernov[2]

[1]Moscow Polytechnic University, Moscow, 127008, Russia
[2]K.G. Razumovsky Moscow State University of Technology, Moscow, 109004 Russia
[✉]Corresponding author, e-mail: iljanaras@yandex.ru

Abstract

Objectives. *To investigate the production and biological degradation of biodegradable hybrid compositions (BHCs), dispersed-filled with starch-containing products of various origins and distilled monoglycerides, along with the biodegradation of compositions based on low density polyethylene and thermoplastic starch (TPS) of various origins: corn, pea, and rice.*
Methods. *Thermoplastic starch was obtained based on native starches of several types, which were processed in Brabender and MashkPlast (Russia) laboratory extruders. BHCs in the form of strands, granules, and films were obtained by mixing thermoplastic starches with polyethylene in extruders. Structural BHC parameters were studied by optical and electron scanning microscopy. The biodegradability of the composite films was evaluated by placing them in biohumus for six months; during storage, the change in water absorption of the films was determined. Before and after the biodegradation process, tensile fracture stress and elongation at rupture were determined to evaluate BHC performance (physical and mechanical characteristics of films). Changes in the chemical structure during biodegradation were determined by Fourier infrared spectroscopy.*

Results. *The positive effect (acceleration of the biodegradation process) of using a novel type of starch plasticizer—monoglycerides distilled in TPS–polyethylene compositions—was confirmed. After six months, intensive sporulation of active microorganisms was observed on the surface of the samples. At the same time, water absorption by the samples reached 30%. The observed 60% decrease in strength and deformation properties indicates an intensive process of biodegradation.*
Conclusions. *The biodegradation rate was shown to depend on the concentration and even distribution of the natural biodegradable filler in the synthetic polymer composition.*

Keywords: *biodegradable compositions, polyolefins, thermoplastic starch, modifier, filler, biodegradation*

For citation: Vasilyev I.Yu., Ananyev V.V., Chernov M.E. Biodegradable packaging materials based on low density polyethylene, starch and monoglycerides. *Tonk. Khim. Tekhnol. = Fine Chem. Technol*. 2022;17(3):231–241 (Russ., Eng.). https://doi.org/10.32362/2410-6593-2022-17-3-231-241

НАУЧНАЯ СТАТЬЯ

Биоразлагаемые упаковочные материалы на основе полиэтилена низкой плотности, крахмала и моноглицеридов

И.Ю. Васильев[1,✉], В.В. Ананьев[1], М.Е. Чернов[2]

[1]*Московский политехнический университет, Москва, 127008 Россия*
[2]*Московский государственный университет технологий им. К.Г. Разумовского, Москва, 109004 Россия*
[✉]*Автор для переписки, e-mail: iljanaras@yandex.ru*

Аннотация

Цели. *Исследовать процесс производства биоразрушаемых гибридных композиций (БГК), дисперсно-наполненных крахмалсодержащими продуктами различного происхождения и дистиллированными моноглицеридами, и их биологическую деструкцию, а также процесс биоразложения композиций на основе полиэтилена низкой плотности и термопластичного крахмала (ТПК) различного происхождения: кукурузного, горохового и рисового.*
Методы. *Термопластичный крахмал получали на основе нативных крахмалов разных видов путем переработки их в лабораторных экструдерах фирм «Брабендер» и «МашПласт» (Россия). Смешивая в экструдерах термопластичные крахмалы с полиэтиленом, получали БГК в виде стренг, гранул и пленок. Структурные параметры БГК изучали методами оптической и электронной сканирующей микроскопии. Способность к биоразложению композитных пленок оценивали, помещая их на полгода в биогумус, и в процессе хранения определяли изменение водопоглощения пленок. Для оценки эксплуатационных свойств (физико-механических характеристик пленок) БГК определяли разрушающее напряжение при растяжении и относительное удлинение при разрыве до и после процесса биоразложения. Изменения химической структуры в процессе биоразложения определяли методом инфракрасной спектроскопии с преобразованием Фурье.*
Результаты. *Подтвержден положительный эффект (ускорение процесса биоразложения) от использования нового типа пластификатора крахмала – дистиллированных моноглицеридов в композициях ТПК–полиэтилен. По истечении полугода на поверхности*

образцов наблюдали интенсивное спороношение активных микроорганизмов. При этом водопоглощение образцов достигало 30%, прочностные и деформационные свойства снизились на 60%, что свидетельствует об интенсивном протекании процесса биоразложения.

Выводы. *Установлено, что скорость процесса биоразложения композиций зависит от концентрационного соотношения вводимого ТПК, а также от его равномерного распределения в синтетическим полимере.*

Ключевые слова: *биоразлагаемые композиции, полиолефины, термопластичный крахмал, моноглицериды, наполнитель, деструкция*

Для цитирования: Васильев И.Ю., Ананьев В.В., Чернов М.Е. Биоразлагаемые упаковочные материалы на основе полиэтилена низкой плотности, крахмала и моноглицеридов. *Тонкие химические технологии*. 2022;17(3):231–241. https://doi.org/10.32362/2410-6593-2022-17-3-231-241

INTRODUCTION

The global production of synthetic plastics is increasing every year. Polymeric materials are used in many branches of light industry and, especially, in the packaging industry [1]. In most cases, polymer films used for food packaging, plastic utensils, and rigid polymer containers are used once and then discarded [2]. Such “polymer waste” does not decompose for a long time, but instead accumulates in landfills or disposal sites to pollute the environment[1] [3]. In order to mitigate this problem, one of the most acceptable and already applied approaches involves the creation and use of biodegradable polymeric materials based on natural materials that do not harm the environment or human health [4].

A novel approach developed for the manufacture of biodegradable polymeric materials envisages the manufacture of products that retain their physical and mechanical characteristics only for the period of intended use. Afterwards, they are subjected to various destructive normal physicochemical, chemical, and biological processes under the influence of environmental factors to re-enter the metabolism of natural biosystems [5, 6].

Biodegradable polymers are macromolecular compounds capable of being degraded in the presence of active biological organisms in appropriate conditions. In an active medium, biodegradable polymers undergo significant changes in molecular weight and mechanical characteristics, themselves contributing to the formation of a nutrient medium for the growth of microorganisms [7–9]. In such media, hydrolysis and photochemical destruction of biodegradable polymers typically take place. Materials break down into components involved in the natural cycle: water, carbon dioxide, and biomass. In contrast to traditional polymers obtained from petrochemical raw materials, biodegradable polymers are characterized by their ability to decompose into components of biological life within a short period of time [10–12].

While a variety of natural polymers are used in the manufacture of biodegradable compositions, starch is one of the most important. This polysaccharide, which is present in many types of plants in the form of tubers, seeds, stems, and leaves, is typically produced from potato, rice, pea, wheat, or corn feedstocks [13, 14].

Conventionally, the processes for obtaining biodegradable polymeric materials can be divided into:

1) mixing native starch with synthetic polymers (polyethylene, polypropylene, etc.);

2) mixing native starch with natural polymers;

3) obtaining thermoplastic starch (TPS) [15–17].

In order to solve the problem of recycling packaging materials, one of the most promising directions involves the creation of biocomposites that combine the useful properties of TPS and synthetic polymers [18].

[1] Bio-based Building Blocks and Polymers – Global Capacities, Production and Trends 2019–2024. Hüerth, Germany; 2020. URL: http://bio-based.eu/downloads/bio-based-building-blocks-and-polymers-global-capacities-production-and-trends-2019-2024/

When manufacturing TPS, selection of the appropriate type of plasticizer is of great importance for ensuring the desired mechanical properties. In addition to starch and glycerin, sorbitol has long been used in the production of TPS. However, as follows from the results of studies [19–21], the use of sorbitol as a plasticizer for the manufacture of TPS subsequently used as a biodegradable hybrid composition (BHC) component is not suitable for all types of native starches.

The authors of the article [22] found a substitute for sorbitol. As plasticizers, they used monoesters of glycerol and higher fatty acids—distilled monoglycerides (DMG), [$CH_2OH–(CHOH)_4–CH_2–OCO–R$] [23]. As well as having higher physical and mechanical properties, biocomposite polymer films based on DMG also have a higher biodegradation index.

MATERIALS AND METHODS

Materials

The study used:

– low-density polyethylene (LDPE), 11503-070 brand (*Kazanorgsintez*, Russia), with an average molecular weight of 1.8·104 Da;

– glycerin, PK-94 grade, density 1240 kg/m^3 (*Vympel*, Russia), GOST 6824-96[2];

– distilled DMG produced according to TU 10-1197-95[3] specifications (*RusKhimtrade*, Russia);

– corn starch (*Krakhmalprodukt*, Russia), GOST 32159-2013[4];

– rice starch (*Vinh Thuan Trading Import-Export*, Vietnam);

– pea starch (*Roquette*, France);

– composite starch-containing materials based on polyethylene (PE) and TPS.

Research methods

BHC samples were obtained in an extruder (*MashPlast*, Russia) equipped with either a strand or a flat-slot extrusion head, at temperatures in the extruder zones from 115 (in the loading zone) to 140°C (in the head zone) [24].

The physical and mechanical properties of the samples under tension were determined using a testing machine RM-50 (*MashPlast*, Russia) equipped with a computer interface running the StretchTest software. The tensile stress at break (σ_b) and relative elongation at break (ε_b) of BHC were measured under normal conditions according to GOST 14236-81[5]. The limit of the permissible value of the load measurement error did not exceed ±1%. The limiting deviations in the diameter of strand samples and the cross-sectional areas of film samples were ±0.2 mm and 2–3%, respectively. The mean value was determined after 3–5 measurements. The tests were carried out at a strain rate of 100 mm/min. Film samples for testing were obtained using a special punching device. The samples shape was of type 1B (EN ISO 527-3[6]).

The water absorption of the studied BHC was determined according to GOST 4650-80[7].

In order to assess BHC biodegradation dynamics, the composting method was used. The samples were placed in special trays with biohumus at a temperature of 23 ± 2°C and a humidity of 70 ± 10% and kept from one month to six months. The degree of biodegradation of the polymer compositions was assessed in terms of changes in their physical and mechanical properties: breaking tensile stress (σ_t) and relative elongation at break (ε_b), according to GOST 54530-2011[8].

Optical studies of BHC appearance after composting were carried out using an Axio Imager.Z2m microscope (*Carl Zeiss*, Germany) in transmitted and reflected light at ×50 and ×200 magnifications.

The chemical structure of BHC was studied by Fourier-transform infrared spectroscopy (FTIR) on an FSM-1201 device (*EuroLab*, Russia) equipped by a multiple frustrated total internal reflection attachment with a resolution of 1.0 cm^{-1} (spectral range of wavenumbers 375–7900 cm^{-1}).

RESULTS AND DISCUSSION

When creating biodegradable composite polymer materials, it is necessary to take into account their technological, operational, and other properties, as well as data characterizing the rate of their biodegradation. One of the most important requirements for a created composite material is the preservation of the

[2] GOST 6824-96. Interstate Standard. Distilled glycerine. General specifications. Moscow: Izd. Standartov; 1997.

[3] TU 10-1197-95. Distilled monoglycerides. Technical conditions.

[4] GOST 32159-2013. Interstate Standard. Maize starch. General specifications. Moscow: Standartinform; 2019.

[5] GOST 14236-81. USSR State Standard. Polymer films. Tensile test method. Moscow: Izd. Standartov; 1992.

[6] ISO 527-3. International Standard. Plastics — Determination of tensile properties. Part 3: Test conditions for films and sheets. Second edition, 2018-11. URL: https://cdn.standards.iteh.ai/samples/70307/e804daa78e2747a6bbd08ac486d58225/ISO-527-3-2018.pdf

[7] GOST 4650-80. Interstate Standard. Plastics. Methods for the determination of water absorption. Moscow: Izd. Standartov; 2008.

[8] GOST 54530-2011. National Standard of the Russian Federation. Resources saving. Packaging. Requirements, criteria and test scheme through composting and biodegradation. Moscow: Standartinform; 2019.

technological characteristics inherent in the main polymer in order to ensure the possibility of its processing on standard equipment [25].

At the first stage of the work, BHC was prepared based on LDPE and TPS of various origins: corn, pea, and rice. The required range of concentration ratios of the components was chosen, in which the share of TPS is from 40 to 60 wt %, respectively [22].

The next stage of the study involved establishing the terms of biodegradation of the obtained compositions. To do this, a combination of several methods was used: composting in biohumus and assessing water absorption. Water is a necessary component for the vital activity of microorganisms. In addition, when water penetrates into the surface layers and diffuses deep into the material structure, it can have a plasticizing effect.

The results of the water absorption study are presented in Table 1. It can be seen that LDPE practically does not absorb water, while compositions modified with starch absorb it in significant amounts; moreover, as the TPS content in the compositions increases, water absorption also increases. It can be assumed that this is due to the structural processes occurring in the polymer–filler system. As the polymer matrix is loosened, the free volume between the macromolecules increases. This leads to an increase in the amount of absorbed water. The composition based on rice TPS has the highest water absorption among the studied BHS. It is logical to assume that this composition will be more rapidly biodegradable when it enters the soil.

The course of the biodegradation process was judged by the results of optical microscopy, as well as by observed changes in the physicochemical properties of the studied materials following their exposure in the soil.

The experiment was carried out at a temperature of 23°C and a soil moisture content corresponding to 70 ± 10% of its maximum moisture capacity. Composting times were one, three, and six months. BHC samples and a control PE sample were placed on a soil substrate and completely covered with a layer of soil, while providing constant air access to

Table 1. Results of BHC water absorption

Composition, wt %	Water absorption, %
Raw LDPE	0.2
BHC (TPS:PE corn starch 60:40)	7.6
BHC (TPS:PE corn starch 50:50)	4.1
BHC (TPS:PE corn starch 40:60)	2.3
BHC (TPS:PE pea starch 60:40)	7.9
BHC (TPS:PE pea starch 50:50)	3.8
BHC (TPS:PE pea starch 40:60)	2.1
BHC (TPS:PE rice starch 60:40)	8.1
BHC (TPS:PE rice starch 50:50)	5.6
BHC (TPS:PE rice starch 40:60)	2.5

Note: LDPE is low density polyethylene, BHCs are biodegradable hybrid compositions, TPS is thermoplastic starch, and PE is polyethylene.

the sample in order to avoid suppression of the vital activity of the microorganisms.

Figure 1 shows microphotographs of BHC samples of composition TPS:LDPE = 60:40 after six months of keeping in biohumus.

As can be seen from the presented microphotographs, local development of soil microorganisms occurs on the surface of the composite samples. While the amount of TPS introduced has little effect on the process during the initial period, the dynamics of microbial growth on different samples at the same content of TPS of different origin is not the same. The sample based on corn TPS (1) is characterized by surface development of microorganisms without intensive sporulation, while the samples based on pea TPS (2) and rice TPS (3) clearly show continuous growth of microorganisms, as well as intensive sporulation. The compositions have a loose structure and surface defects, and the destruction of the filler is observed throughout the entire volume of the samples.

The results of determining the tensile stress at break (σ_b) and relative elongation at break (ε_b) for BHC after half a year of composting are presented in Table 2.

As follows from the obtained data, following a six-month period of keeping the samples in biohumus with soil microorganisms, their physical and

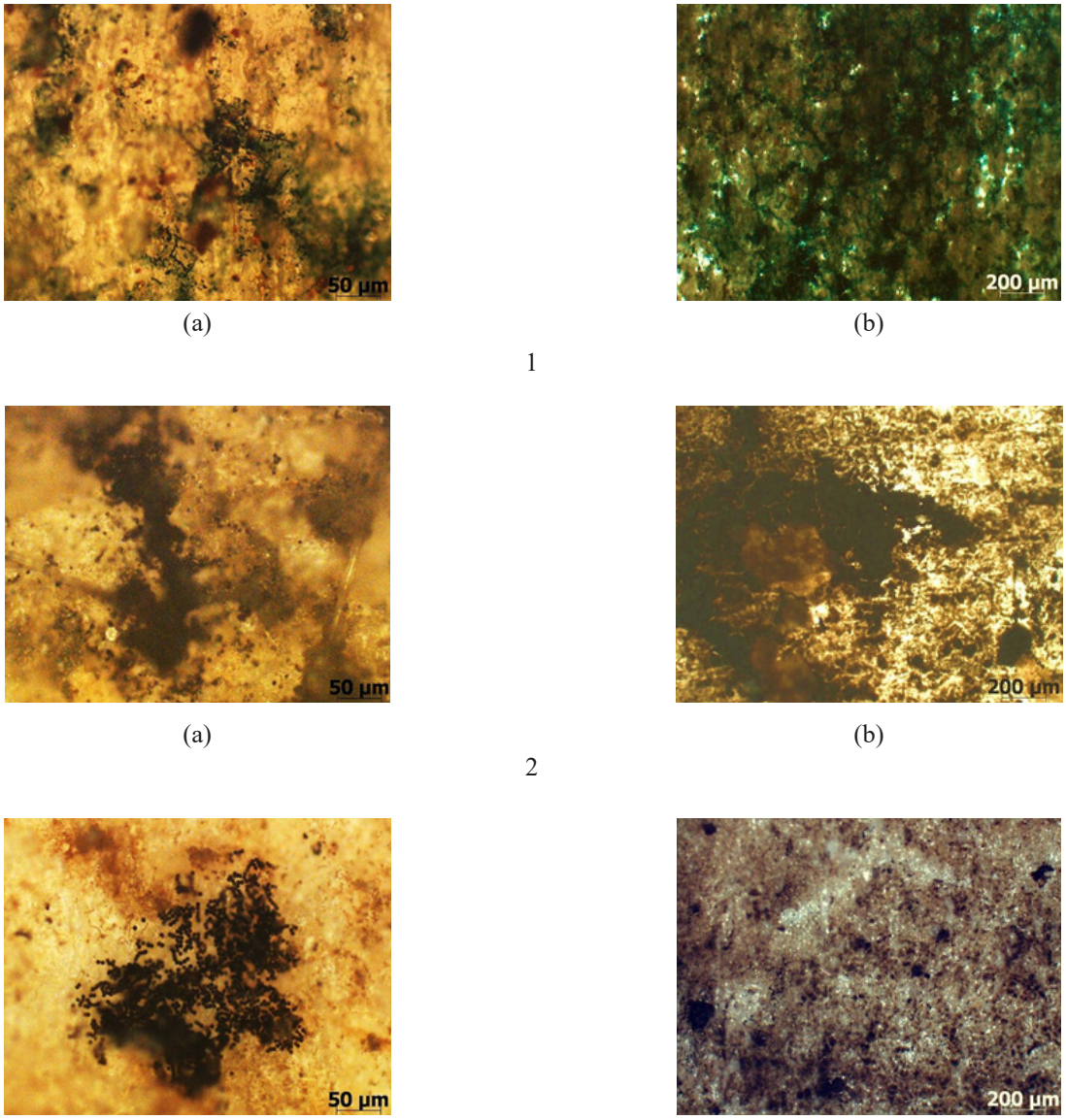

Fig. 1. Micrographs of film samples after removal from biohumus
(1) corn starch BHC, (2) pea starch BHC, (3) rice starch BHC
(a) increase ×50, (b) increase ×200.

mechanical characteristics deteriorate. In the process of biodegradation, water is absorbed by composite samples, resulting in a change in the material structure. It is likely that the intermolecular interactions that hold the polymer matrix and filler weaken together to produce visible defects: the formation of a loose surface structure due to the filler destruction over the entire surface of the samples. In the case of BHC based on corn starch, a 1.5-fold deterioration in physical and mechanical properties occurs; in BHC based on pea starch—a 1.3-fold change; in BHC based on rice starch—a 2.1-fold change. This supports the conclusion that the studied film compositions will biodegrade quickly under conditions of disposal.

In order to further assess the changes that occurred during biodegradation, spectral characteristics were determined using the FTIR method. As an example, Fig. 2 shows the spectrum of BHC based on rice TPS at a ratio of TPS:LDPE = 60:40 wt % before and after the biodegradation process.

First of all, it is of interest to estimate the intensity of the OH groups absorption bands located between 3000 and 3600 cm^{-1}, as well as that of the bands between 1000–1500 cm^{-1}, which are characteristic of CH_2, CH_3, and C–O groups. While the middle and far regions of the IR spectrum are less informative, they support the conclusion that the BHC–PE composition contains functional groups characteristic of fatty acids (forming part of DMG) in OH-groups of glycerol, as well as functional groups of starch.

Following six months of keeping BHC in biohumus, absorption peaks appear in the IR spectrum in the region of 1000–1200 cm^{-1}, indicating the

Table 2. Results of physical and mechanical tests of BHC before and after biodegradation process

TPS:PE ratio	σ_b, MPa (Δ ± 0.2)	ε_b, % (Δ ± 5)	σ_b, MPa (Δ ± 0.2)	ε_b, % (Δ ± 5)
1. 100% PE	16	195	–	–
–	With DMG before biodegradation		With DMG after biodegradation	
2. TPS based on corn				
60:40	10.9	78	7.2	45
50:50	11.6	84	8.3	67
40:60	12.8	93	10.3	84
3. TPS based on peas				
60:40	7.8	82	5.6	48
50:50	9.3	91	8.4	64
40:60	10.1	102	9.3	86
4. TPS based on rice				
60:40	11.2	96	5.2	41
50:50	11.9	104	7.3	56
40:60	12.8	115	8.9	87

Note: σ_b is a tensile stress at break, ε_b is a relative elongation at break, DMGs are distilled monoglycerides, TPS is thermoplastic starch, and PE is polyethylene.

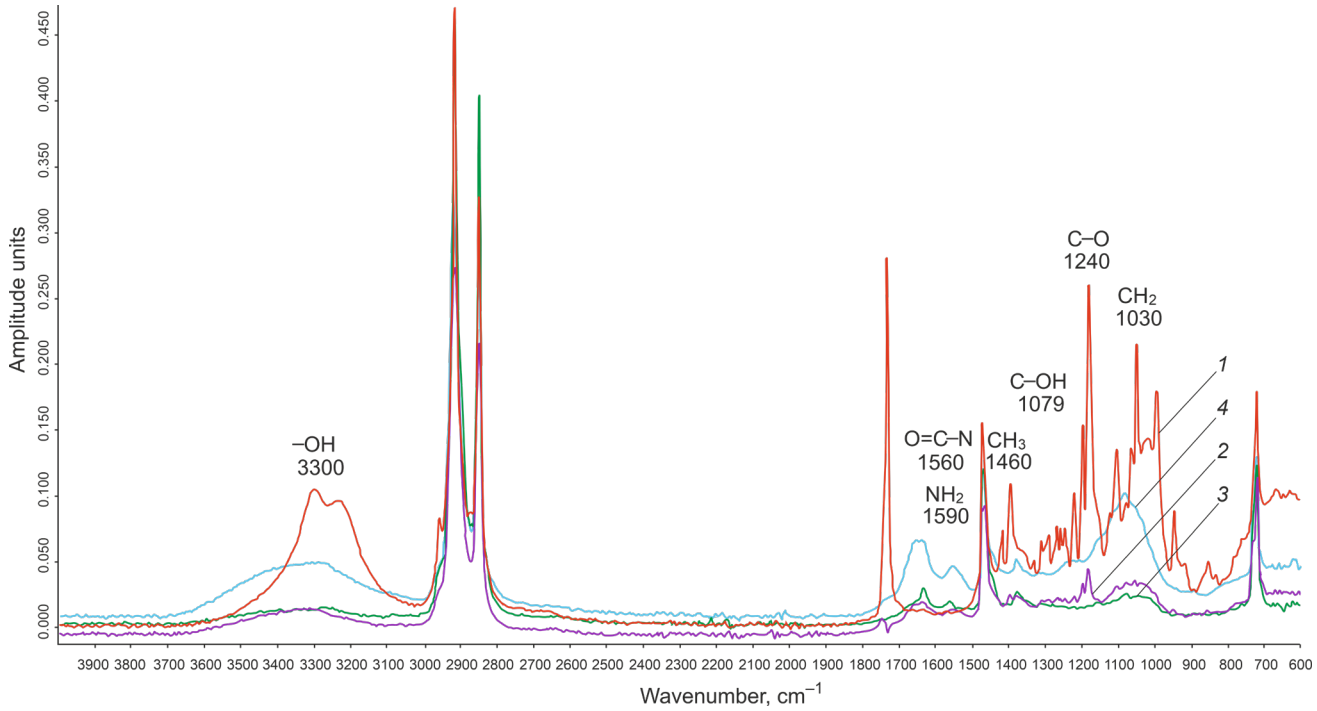

Fig. 2. Infrared spectrum of the BHC based on rice starch.
Red line (*1*) is the BHC absorption spectrum before biodegradation; violet line (*2*) is the BHC spectrum after one month of biodegradation; green line (*3*) is the BHC spectrum after three months of biodegradation; blue line (*4*) is the BHC spectrum after six months of biodegradation.

presence of the C–OH group, and 1500–1700 cm^{-1}, designating the presence of the acetamide groups O=C–N and amine groups NH_2. Thus, their appearance can be associated with the action of active microorganisms of the chitosan fungi group, which form the bacterial microflora. In the region of 3000–3600 cm^{-1}, changes in the intensity of the absorption peaks of the OH groups were observed. This is presumably due to the fact that TPS destroys the polymer matrix to some extent; most likely, TPS is partially washed out of the composition by water. This also supports the conclusion that the occurring biodegradation processes are intensive.

CONCLUSIONS

The process of the biodegradation of BHC compositions based on LDPE and TPS of various origins: corn, pea, and rice, with a TPS content in BHC from 40:60 wt % using the novel DMG plasticizer was studied. Biodegradation was carried out in biohumus for six months with periodic evaluation of the properties of control and working samples: following one month, three months, and six months.

It follows from the results of the experiment that the new modifier introduced into the samples composition increases the water absorption of the filled compositions in the case of BHC based on corn TPS by 20%; in the case of BHC based on pea TPS—by 26%; in the case of BHC based on rice TPS—by 31%.

The observed 60% degradation in the physical and mechanical characteristics of the samples as compared to the initial values is apparently due to a change in the material structure: weakening of energy bonds, destruction of the polymer matrix, partial washing out of the components from the system.

The results of optical microscopy and analysis carried out by FTIR confirmed the occurrence of sporulation of active microorganisms.

The obtained data support the conclusion that TPS can be used with the novel DMG plasticizer as a polyolefin modifier for the creation of biodegradable packaging materials.

Ackowledgments

This work was supported by the Russian Foundation for Basic Research, project No 19-33-90284.

Authors' contribution

All authors equally contributed to the research work.

The authors declare no conflicts of interest.

REFERENCES

1. Litvyak V.V. Prospects of manufacture of modern packaging materials with application of biodelessed polymer compositions. *Zhurnal Belorusskogo gosudarstvennogo universiteta. Ekologiya. = Journal of the Belarusian State University. Ecology*. 2019;(2):84–94 (in Russ.). URL: https://journals.bsu.by/index.php/ecology/article/view/2711/2295

2. Kalia S. *Biodegradable Green Composites*. John Wiley & Sons; 2016. 368 p.

3. Anan'ev V.V., Kulikov P.P., Vasil'ev I.Yu. Study of polyolefin compositions capable of degradation. *Packaging*. 2015;(3):46–48 (in Russ.).

4. Nishat N., Malik A. Synthesis, spectral characterization thermal stability, antimicrobial studies and biodegradation of starch–thiourea based biodegradable polymeric ligand and its coordination complexes with [Mn(II), Co(II), Ni(II), Cu(II), and Zn(II)] metals. *Journal of Saudi Chemical Society*. 2016;20(Suppl. 1):S7–S15. https://doi.org/10.1016/j.jscs.2012.07.017

5. Sudhakar Y.N., Selvakumar M. Lithium perchlorate doped plasticized chitosan and starch blend as biodegradable polymer electrolyte for supercapacitors. *Electrochimica Acta*. 2012;78:398–405. https://doi.org/10.1016/j.electacta.2012.06.032

6. Mendes J.F., Paschoalin R.T., Carmona V.B., Sena Neto A.R., Marques A.C.P., Marconcini J.M., Mattoso L.H.C., Medeiros E.S., Oliveira J.E. Biodegradable polymer blends based on corn starch and thermoplastic chitosan processed by extrusion. *Carbohydr. Polym*. 2016137:452–458. https://doi.org/10.1016/j.carbpol.2015.10.093

7. Nguyen D.M., Do T.V.V., Grillet A-C., Thuc H.H., Thuc C.N.H. Biodegradability of polymer film based on low density polyethylene and cassava starch. *Int. Biodeterior. Biodegradation*. 2016;115:257–265. https://doi.org/10.1016/j.ibiod.2016.09.004

8. Tang X., Alavi S. Recent advances in starch, polyvinyl alcohol based polymer blends, nanocomposites and their biodegradability. *Carbohydr. Polym*. 2011;85(1):7–16. https://doi.org/10.1016/j.carbpol.2011.01.030

9. Singh R., Sharma R., Shaqib M., Sarkar A., Dutt Chauhan K. In: *Biodegradable polymers as packaging materials. Biopolymers and their Industrial Applications. From Plant, Animal, and Marine Sources, to Functional Products.* 2021. Chapter 10. P. 245–259. https://doi.org/10.1016/B978-0-12-819240-5.00010-9

10. Ojogbo E., Ogunsona E.O., Mekonnen T.H. Chemical and physical modifications of starch for renewable polymeric materials. Materials Today Sustainability. 2020;7–8:100028. https://doi.org/10.1016/j.mtsust.2019.100028

11. Tudorachi N., Cascaval C.N., Rusu M., Pruteanu M. Testing of polyvinyl alcohol and starch mixtures as biodegradable polymeric materials. *Polym. Test*. 2000;19(7):785–799. https://doi.org/10.1016/S0142-9418(99)00049-5

12. Fonseca-García A., Jiménez-Regalado E., Aguirre-Loredo R-Y. Preparation of a novel biodegradable packaging film based on corn starch-chitosan and poloxamers. *Carbohydr. Polym*. 2021;251:117009. https://doi.org/10.1016/j.carbpol.2020.117009

13. Mittal A., Garg S., Bajpai S. Fabrication and characteristics of poly (vinyl alcohol)-starch-cellulosic material based biodegradable composite film for packaging application. *Materials Today: Proceedings*. 2020;21(3):1577–1582. https://doi.org/10.1016/j.matpr.2019.11.210

СПИСОК ЛИТЕРАТУРЫ

1. Литвяк В.В. Перспективы производства современных упаковочных материалов с применением биоразлагаемых полимерных композиций. *Журнал Белорусского государственного университета. Экология*. 2019;(2):84–94. URL: https://journals.bsu.by/index.php/ecology/article/view/2711/2295

2. Kalia S. *Biodegradable Green Composites*. John Wiley & Sons; 2016. 368 p.

3. Ананьев В.В., Куликов П.П., Васильев И.Ю. Исследование полиолефиновых композиций, способных к разложению. *Packaging*. 2015;(3):46–48.

4. Nishat N., Malik A. Synthesis, spectral characterization thermal stability, antimicrobial studies and biodegradation of starch–thiourea based biodegradable polymeric ligand and its coordination complexes with [Mn(II), Co(II), Ni(II), Cu(II), and Zn(II)] metals. *Journal of Saudi Chemical Society*. 2016;20(Suppl. 1):S7–S15. https://doi.org/10.1016/j.jscs.2012.07.017

5. Sudhakar Y.N., Selvakumar M. Lithium perchlorate doped plasticized chitosan and starch blend as biodegradable polymer electrolyte for supercapacitors. *Electrochimica Acta*. 2012;78:398–405. https://doi.org/10.1016/j.electacta.2012.06.032

6. Mendes J.F., Paschoalin R.T., Carmona V.B., Sena Neto A.R., Marques A.C.P., Marconcini J.M., Mattoso L.H.C., Medeiros E.S., Oliveira J.E. Biodegradable polymer blends based on corn starch and thermoplastic chitosan processed by extrusion. *Carbohydr. Polym*. 2016137:452–458. https://doi.org/10.1016/j.carbpol.2015.10.093

7. Nguyen D. M., Do T.V.V., Grillet A-C., Thuc H.H., Thuc C.N.H. Biodegradability of polymer film based on low density polyethylene and cassava starch. *Int. Biodeterior. Biodegradation*. 2016;115:257–265. https://doi.org/10.1016/j.ibiod.2016.09.004

8. Tang X., Alavi S. Recent advances in starch, polyvinyl alcohol based polymer blends, nanocomposites and their biodegradability. *Carbohydr. Polym*. 2011;85(1):7–16. https://doi.org/10.1016/j.carbpol.2011.01.030

9. Singh R., Sharma R., Shaqib M., Sarkar A., Dutt Chauhan K. In: *Biodegradable polymers as packaging materials. Biopolymers and their Industrial Applications. From Plant, Animal, and Marine Sources, to Functional Products.* 2021. Chapter 10. P. 245–259. https://doi.org/10.1016/B978-0-12-819240-5.00010-9

10. Ojogbo E., Ogunsona E.O., Mekonnen T.H. Chemical and physical modifications of starch for renewable polymeric materials. *Materials Today Sustainability*. 2020;7–8:100028. https://doi.org/10.1016/j.mtsust.2019.100028

11. Tudorachi N., Cascaval C.N., Rusu M., Pruteanu M. Testing of polyvinyl alcohol and starch mixtures as biodegradable polymeric materials. *Polym. Test*. 2000;19(7):785–799. https://doi.org/10.1016/S0142-9418(99)00049-5

12. Fonseca-García A., Jiménez-Regalado E., Aguirre-Loredo R-Y. Preparation of a novel biodegradable packaging film based on corn starch-chitosan and poloxamers. *Carbohydr. Polym*. 2021;251:117009. https://doi.org/10.1016/j.carbpol.2020.117009

13. Mittal A., Garg S., Bajpai S. Fabrication and characteristics of poly (vinyl alcohol)-starch-cellulosic material based biodegradable composite film for packaging application. *Materials Today: Proceedings*. 2020;21(3):1577–1582. https://doi.org/10.1016/j.matpr.2019.11.210

14. Tabasum S., Younas M., Zaeem M.A., Majeed I., Majeed M., Noreen A., NaeemIqbal M., Zia K.M. A review on blending of corn starch with natural and synthetic polymers, and inorganic nanoparticles with mathematical modeling. *Int. J. Biol. Macromol*. 2019;122:969–996. https://doi.org/10.1016/j.ijbiomac.2018.10.092

15. Wasserman L.A., Papakhin A.A., Borodina Z.M., *et al*. Some physico-chemical and thermodynamic characteristics of maize starches hydrolyzed by glucoamylase. *Carbohydr. Polym*. 2019;112:260–269. https://doi.org/10.1016/j.carbpol.2019.01.096

16. Kwon S.S., Kong B.J., Park S.N. Physicochemical properties of pH-sensitive hydrogels based on hydroxyethyl cellulose-hyaluronic acid and for applications as transdermal delivery systems for skin lesions. *Eur. J. Pharm. Biopharm.* 2015;92:146–154. https://doi.org/10.1016/j.ejpb.2015.02.025

17. Razavi S.M.A., Cui S.W., Ding H. Structural and physicochemical characteristics of a novel water-soluble gum from Lallemantia royleana seed. *Int. J. Biol. Macromol*. 2016;83:142–151. https://doi.org/10.1016/j.ijbiomac.2015.11.076

18. Lukin N.D., Kolpakova V.V., Usachev I.S., Sardzhvelazhdze A.S., Solomin D.A., Vasilyev I.Yu. Modification of polymer compositions with thermoplastic starch for bio-dependable packaging products. In: *Biotekhnologiya: sostoyanie i perspektivy razvitiya: Materialy mezhdunarodnogo kongressa* (*Biotechnology: State and Development Prospects: Proceedings of the International Congress*). 2019. P. 102–104 (in Russ.).

19. Kolpakova V.V., Usachev I.S., Sardzhveladze A.S., Solomin D.A., Ananiev V.V., Vasil'ev I.Yu. Perfection of technology of application of thermoplastic starch for biodegradable polymer film. *Pishchevaya promyshlennost' = Food Industry*. 2017;(8):34–38 (in Russ.).

20. Ananyev V.V., Nagornova I.V., Bablyuk E.B., Vasilyev I.Y., Varepo L.G. Polymer composites including natural additives degradation rate indication. In: AIP *Conference Proceedings*. 2017;1876(1):020091. https://doi.org/10.1063/1.4998911

21. Lukin N.D., Kolpakova V.V., Usachev I.S., Papakhin A.A., Sardzhveladze A.S., Borodina Z.M., Vasilev I.Yu., Ananev V.V. *Biologicheski razrushaemaya termoplastichnaya kompozitsiya* (*Biologically degradable thermoplastic composition*): Pat. RF 2691988. Publ. 19.06.2019. (in Russ.).

22. Vasilyev I.Yu., Ananyev V.V., Kolpakova V.V., Sardzhveladze A.S. Development of technology for producing biodegradable hybrid composites based on polyethylene, starch, and monoglycerides. *Fine Chem. Technol.* 2020;15(6):44–55 (in Russ.). https://doi.org/10.32362/2410-6593-2020-15-6-44-55

23. Vasilyev I., Ananiev V., Sultanova Yu., Kolpakova V. Effect of the biodegradable compounds composition with monoglycerides on mechanical properties. In: *Materials Science Forum*. 2021;1031:7–16. https://doi.org/10.4028/www.scientific.net/MSF.1031.7

24. Kolpakova V., Usachev I., Papakhin A., Sardzhveladze A., Ananiev V. Thermoplastic composition with modified porous corn starch of biodegradability properties. In: 2019 *Proceedings of the GEOLINS International Scientific Conference on Geosciences*. March 26–29, 2019. Athens, Greece. P. 33–41. https://doi.org/10.32008/geolinks2019/b2/v1/04

14. Tabasum S., Younas M., Zaeem M.A., Majeed I., Majeed M., Noreen A., NaeemIqbal M., Zia K.M. A review on blending of corn starch with natural and synthetic polymers, and inorganic nanoparticles with mathematical modeling. *Int. J. Biol. Macromol*. 2019;122:969–996. https://doi.org/10.1016/j.ijbiomac.2018.10.092

15. Wasserman L.A., Papakhin A.A., Borodina Z.M., *et al.* Some physico-chemical and thermodynamic characteristics of maize starches hydrolyzed by glucoamylase. *Carbohydr. Polym*. 2019;112:260–269. https://doi.org/10.1016/j.carbpol.2019.01.096

16. Kwon S.S., Kong B.J., Park S.N. Physicochemical properties of pH-sensitive hydrogels based on hydroxyethyl cellulose-hyaluronic acid and for applications as transdermal delivery systems for skin lesions. *Eur. J. Pharm. Biopharm*. 2015;92:146–154. https://doi.org/10.1016/j.ejpb.2015.02.025

17. Razavi S.M.A., Cui S.W., Ding H. Structural and physicochemical characteristics of a novel water-soluble gum from Lallemantia royleana seed. *Int. J. Biol. Macromol*. 2016;83:142–151. https://doi.org/10.1016/j.ijbiomac.2015.11.076

18. Лукин Н.Д., Колпакова В.В., Усачев И.С., Сарджвелаждзе А.С., Соломин Д.А., Васильев И.Ю. Модификация полимерных композиций с термопластичным крахмалом для биоразлагаемой упаковочной пленки. В: *Биотехнология: состояние и перспективы развития: Материалы международного конгресса*. 2019. С. 102–104.

19. Колпакова В.В., Усачев И.С., Сарджвеладзе А.С., Соломин Д.А., Ананьев В.В., Васильев И.Ю. Совершенствование технологии применения термопластичного крахмала для биоразлагаемой полимерной пленки. *Пищевая промышленность*. 2017;(8):34–38.

20. Ananyev V.V., Nagornova I.V., Bablyuk E.B., Vasilyev I.Y., Varepo L.G. Polymer composites including natural additives degradation rate indication. In: *AIP Conference Proceedings*. 2017;1876(1):020091. https://doi.org/10.1063/1.4998911

21. Лукин Н.Д., Колпакова В.В., Усачев И.С., Папахин А.А., Сарджвеладзе А.С., Бородина З.М., Васильев И.Ю., Ананьев В.В. *Биологически разрушаемая термопластичная композиция*: Пат. 2691988 РФ. Заявка № 2018146738; заявл. 26.12.2018. опубл. 19.06.2019.

22. Васильев И.Ю., Ананьев В.В., Колпакова В.В., Сарджвеладзе А.С. Разработка технологии получения биоразлагаемых композиций на основе полиэтилена, крахмала и моноглицеридов. *Тонкие химические технологии*. 2020;15(6):44–55. https://doi.org/10.32362/2410-6593-2020-15-6-44-55

23. Vasilyev I., Ananiev V., Sultanova Yu., Kolpakova V. Effect of the biodegradable compounds composition with monoglycerides on mechanical properties. In: *Materials Science Forum*. 2021;1031:7–16. https://doi.org/10.4028/www.scientific.net/MSF.1031.7

24. Kolpakova V., Usachev I., Papakhin A., Sardzhveladze A., Ananiev V. Thermoplastic composition with modified porous corn starch of biodegradability properties. In: *2019 Proceedings of the GEOLINS International Scientific Conference on Geosciences*. March 26–29, 2019. Athens, Greece. P. 33–41. https://doi.org/10.32008/geolinks2019/b2/v1/04

25. Васильев И.Ю., Ананьев В.В., Султанова Ю.М., Колпакова В.В. Влияние состава биоразлагаемых композиций на основе полиэтилена, крахмала и моноглицеридов на их физико-механические свойства и структуру. *Все материалы. Энциклопедический справочник*. 2021;(5):31–38. https://doi.org/10.31044/1994-6260-2021-0-5-31-38

25. Vasilyev I.Yu., Ananyev V.V., Sultanova Yu.M., Kolpakova V.V. Composition effect of biodegradable compounds based on polyethylene, starch and monoglycerides on their physical-mechanical properties and structure. *Vse materialy. Entsiklopedicheskii spravochnik* (*All Materials. Encyclopaedic Reference Manual*). 2021;(5):31–38 (in Russ.). https://doi.org/10.31044/1994-6260-2021-0-5-31-38

About the authors:

Ilya Yu. Vasilyev, Lecturer, Department of Innovative Materials for the Print Media Industry, Institute of Print Media and Information Technologies, Moscow Polytechnic University (38, Bolshaya Semenovskaya ul., Moscow, 127008, Russia). E-mail: iljanaras@yandex.ru. Scopus Author ID 57195569317, RSCI SPIN-code 2038-4156, https://orcid.org/0000-0001-8488-5907.

Vladimir V. Ananyev, Cand. Sci. (Eng.), Professor, Department of Innovative Materials for the Print Media Industry, Institute of Print Media and Information Technologies, Moscow Polytechnic University (38, Bolshaya Semenovskaya ul., Moscow, 127008, Russia). E-mail: vovan261147@yandex.ru. RSCI SPIN-code 3099-6905, https://orcid.org/0000-0002-2049-7929

Michel E. Chernov, Dr. Sci. (Eng.), Professor, Department Automated Control Systems, K.G. Razumovsky Moscow State University of Technologies and Management (73, Zemlyanoi Val ul., Moscow, 109004, Russia). E-mail: 1mishel@mail.ru. RSCI SPIN-code 3412-9777, https://orcid.org/0000-0001-9843-2183

Об авторах:

Васильев Илья Юрьевич, преподаватель кафедры Инновационные материалы принтмедиаиндустрии Института принтмедиа и информационных технологий ФГБОУ «Московский политехнический университет» (127008, Россия, Москва, ул. Большая Семеновская, 38). E-mail: iljanaras@yandex.ru. Scopus Author ID 57195569317, SPIN-код 2038-4156, https://orcid.org/0000-0001-8488-5907

Ананьев Владимир Владимирович, к.т.н., профессор кафедры Инновационные материалы принтмедиа-индустрии Института принтмедиа и информационных технологий ФГБОУ «Московский политехнический университет» (127008, Россия, Москва, ул. Большая Семеновская, 38). E-mail: vovan261147@yandex.ru. SPIN-код РИНЦ 3099-6905, https://orcid.org/0000-0002-2049-7929

Чернов Мишель Евгеньевич, д.т.н., профессор кафедры Систем автоматизированного управления ФГБОУ «Московский государственный университет технолгий и управления им. К.Г. Разумовского (ПКУ)» (109004, Россия, Москва, ул. Земляной Вал, д. 73). E-mail: 1mishel@mail.ru. SPIN-код РИНЦ 3412-9777, https://orcid.org/0000-0001-9843-2183

The article was submitted: March 30, 2022; approved after reviewing: April 04, 2022; accepted for publication: June 06, 2022.

Translated from Russian into English by M. Povorin
Edited for English language and spelling by Thomas Beavitt

SYNTHESIS AND PROCESSING OF POLYMERS AND POLYMERIC COMPOSITES

СИНТЕЗ И ПЕРЕРАБОТКА ПОЛИМЕРОВ И КОМПОЗИТОВ НА ИХ ОСНОВЕ

ISSN 2686-7575 (Online)

https://doi.org/10.32362/2410-6593-2022-17-3-242-252

UDC 541.64:544(72+77):547.1'128

RESEARCH ARTICLE

Polymerization of D,L-lactide in the presence of Boltorn™ polyester polyol

Vitaly I. Gomzyak[1,2,✉], Nikita V. Bychkov[2], Adu S. Aduev[2], Valeriia A. Ivanova[3], Anton D. Koshelev[4], Sergey N. Chvalun[1,2]

[1]MIREA – Russian Technological University (M.V. Lomonosov Institute of Fine Chemical Technologies), Moscow, 119571 Russia
[2]National Research Center "Kurchatov Institute," Moscow, 123182 Russia
[3]Moscow Institute of Physics and Technology, Dolgoprudny, 117303 Russia
[4]Technical University of Darmstadt, Darmstadt, 64277 Germany
[✉]Corresponding author, e-mail: vgomzyak@gmail.com

Abstract

Objects. *To synthesize monodisperse biodegradable hyperbranched polymers based on D,L-lactide in the presence of Boltorn™ H30 polyester polyol as a macroinitiator.*
Methods. *^{1}H and ^{13}C nuclear magnetic resonance (NMR) spectroscopy was used to study the chemical structure of the Boltorn™ H30 polyester polyol and (Boltorn™ H30)-PDLA hyperbranched copolymers. The molecular weight distribution of the polymers was studied by gel permeation chromatography (GPC). In order to study the thermal stability of Boltorn™ H30 polyester polyol, thermogravimetric analysis (TGA) was used. Polymerization of D,L-lactide was carried out in a block in the presence of Boltorn™ H30 polyester polyol.*
Results. *The degree of branching of Boltorn™ H30 polyester polyol was calculated from NMR data, while the TGA method was used to determine the upper operational temperature range. The polymerization of D,L-lactide in the presence of Boltorn™ H30 polyester polyol used as a macroinitiator was studied. The molecular weight characteristics of the obtained copolymers were studied by NMR and GPC.*

Conclusions. *Optimum conditions were determined for the polymerization of D,L-lactide when using Boltorn™ H30 polyester polyol as a macroinitiator. The possibility of synthesizing narrowly dispersed hyperbranched polymers (Boltorn™ H30)-PDLA under the described conditions was demonstrated.*

Keywords: *hyperbranched polymers, biodegradable polymers, polylactide, Boltorn™ polyester polyols*

For citation: Gomzyak V.I., Bychkov N.V., Aduev A.S., Ivanova V.A., Koshelev A.D., Chvalun S.N. Polymerization of D,L-lactide in the presence of Boltorn™ polyester polyol. *Tonk. Khim. Tekhnol. = Fine Chem. Technol*. 2022;17(3):242–252 (Russ., Eng.). https://doi.org/10.32362/2410-6593-2022-17-3-242-252

НАУЧНАЯ СТАТЬЯ

Полимеризация D,L-лактида в присутствии полиэфирполиола Boltorn™

В.И. Гомзяк[1,2,✉], Н.В. Бычков[2], А.Ш. Адуев[2], В.А. Иванова[3], А.Д. Кошелев[4], С.Н. Чвалун[1,2]

[1]МИРЭА – Российский технологический университет (Институт тонких химических технологий им. М.В. Ломоносова), Москва, 119571 Россия
[2]Национальный исследовательский центр «Курчатовский институт», Москва, 123182 Россия
[3]Московский физико-технический институт, Долгопрудный, 117303 Россия
[4]Технический университет Дармштадта, Дармштадт, 64277 Германия
[✉]Автор для переписки, e-mail: vgomzyak@gmail.com

Аннотация

Цели. *Синтез узкодисперсных биоразлагаемых сверхразветвленных полимеров на основе D,L-лактида в присутствии полиэфирполиола Boltorn™ H30 в качестве макроинициатора.*
Методы. *Для исследования химической структуры полиэфирполиола Boltorn™ H30 и сверхразветвленных сополимеров (Boltorn™ H30)-PDLA использовали ^{1}H и ^{13}C спектроскопию ядерного магнитного резонанса (ЯМР). Молекулярно-массовое распределение полимеров исследовали методом гель-проникающей хроматографии (ГПХ). Для исследования термической стабильности полиэфирполиола Boltorn™ H30 применяли метод термогравиметрического анализа (ТГА). Полимеризацию D,L-лактида в присутствии полиэфирполиола Boltorn™ H30 проводили в блоке.*
Результаты. *По данным ЯМР была рассчитана степень разветвленности полиэфирполиола Boltorn™ H30. Методом ТГА определен верхний температурный диапазон работы с полиэфирполиолом Boltorn™ H30. Исследована полимеризация D,L-лактида в присутствии полиэфирполиола Boltorn™ H30 в качестве макроинициатора. Молекулярно-массовые характеристики полученных сополимеров исследованы методами ЯМР и ГПХ.*
Выводы. *Подобраны оптимальные условия полимеризации D,L-лактида в присутствии полиэфирполиола Boltorn™ H30 в качестве макроинициатора. Показана возможность синтеза узкодисперсных сверхразветвленных полимеров (Boltorn™ H30)-PDLA в этих условиях.*

Ключевые слова: *сверхразветвленные полимеры, биоразлагаемые полимеры, полилактид, полиэфирполиолы Boltorn™*

Для цитирования: Гомзяк В.И., Бычков Н.В., Адуев А.Ш., Иванова В.А., Кошелев А.Д., Чвалун С.Н. Полимеризация D,L-лактида в присутствии полиэфирполиола Boltorn™. *Тонкие химические технологии*. 2022;17(3):242–252. https://doi.org/10.32362/2410-6593-2022-17-3-242-252

INTRODUCTION

Targeted drug delivery has become one of the leading directions of the medical research. While modern methods of treating diseases still employ a wide range of traditional drugs in the form of capsules, tablets, patches, injections, etc., polymer micro- and nanoparticles have been successfully used in the creation of new effective forms of drug delivery, allowing drugs to be delivered purposefully to the focus area of an inflammatory or pathological process [1]. One of the most promising directions in this field involves the use of nanoparticles based on lactide copolymers of varying topologies [2]. Due to the ability to decompose in a living organism without the formation of toxic products, polylactide (PLA) and its copolymers are widely used in surgery, orthopedics and dentistry, as well as in the capacity of carrier polymers for long-acting injectable dosage forms [3, 4].

Today, hyperbranched polymers, which differ significantly from linear, star-shaped and cross-linked analogues, have become increasingly important. As a rule, hyperbranched polymers have a spatially unloaded core, as well as a large number of free functional groups located in the surface layer. A special place among hyperbranched polymers is occupied by the polyester polyols based on 2,2-bis(hydroxymethyl)propionic acid. Such polyesters marketed under the Boltorn™ brand are widely used as auxiliary agents and modifiers in the production of synthetic resins, polyurethanes, organic glasses, etc. These polyesters are widely used in the production of biodegradable copolymers for targeted drug delivery due to the presence of a large number of hydroxyl groups [5, 6].

In recent decades, there has been increasing interest in the synthesis and study of the properties of highly branched polymers, whose main features in comparison with linear analogues are their smaller molecular sizes, higher density macromolecule structure, and lower viscosity values. Such high-molecular substances, which include polymer brushes, dendrimers, star-shaped and hyperbranched polymers, differ significantly in properties from their linear analogues. Their main distinguishing feature lies in the possibility of consistently regulating their structure and concomitant properties. From this point of view, star-shaped and hyperbranched polymers having free reactive functional groups, whose structure-dependent properties can be altered within broad limits, are of particular interest [7–10]. By carrying out additional modification of functionalized polymers, it becomes possible to obtain copolymers with regulated colloidal chemical properties [11–12].

Boltorn™ polyesters marketed under the H20, H30, and H40 product line comprise progressively branching dendrite-like macromolecules differing in molecular weight and average number of hydroxyl groups (16, 32, and 64, respectively) (Fig. 1). As biocompatible and biodegradable polymers, they offer bioavailability, bio-permeability, and low toxicity (LD_{50} = 2000 mg/kg). Although well soluble in some polar solvents, such as dimethylformamide (DMFA), dimethyl sulfoxide (DMSO), acetone, etc., polyester polyols of the Boltorn™ family do not dissolve in methylene

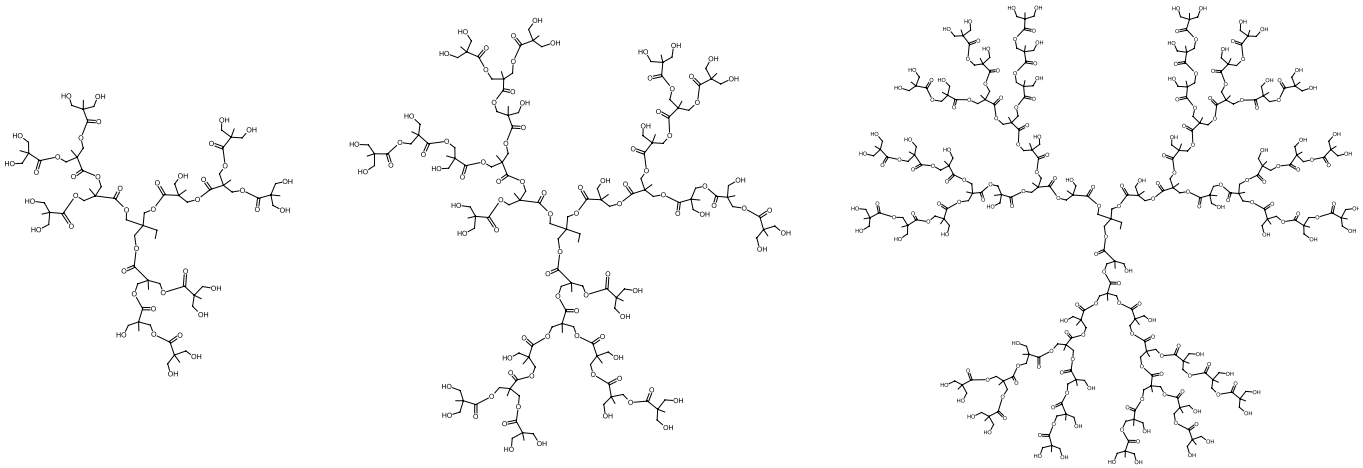

(1) (2) (3)

Fig. 1. Structure of Boltorn™ polyesters: (1) H20, (2) H30, and (3) H40.

chloride, tetrahydrofuran (THF), ethyl acetate, or acetonitrile. The pronounced intramolecular and intermolecular hydrogen bonds of polyester polyols, which persist even at elevated temperatures, is due to the presence of a large number of proton-donating and proton-acceptor groups in their structure [6].

A number of studies have shown that Boltorn™ polyester polyols can be used as a macroinitiator during copolymerization with L-lactide, ε-caprolactone, and glycolide [13–15], allowing macromolecules of high molecular weight to be obtained, along with the possibility of loading the hydrophobic core of the molecule with medicinal substances for targeted delivery. In this paper, studies of polymerization of D,L-lactide in the presence of Boltorn™ polyester have been carried out H30 as a macroinitiator.

EXPERIMENTAL

Boltorn™ H30 polyester polyol (M_w = 3608 g/mol; polydispersity index 1.78; ρ = 1.3 g/cm^3) and 2-ethylhexanoate of tin ($Sn(Oct)_2$) with 97% purity (*Acros Organics*, Belgium) were used without additional purification. D,L-lactide (*Purac*, Netherlands) was recrystallized twice from chemically pure butyl acetate (*Merck*, Germany).

Multiarm block copolymers Boltorn-$[(PDLA)_x]_y$ were synthesized in the block by polymerization with the opening of the cycle (ring-opening polymerization) of D,L-lactide, using Boltorn™ H30 (B32) polyester polyol as a polymerization macroinitiator, tin(II)2-ethylhexanoate ($Sn(Oct)_2$), and tin(II)2-ethylhexanoate ($Sn(Oct)_2$) as a catalyst. The synthesis was carried out as follows: an estimated quantity of macroinitiator (B32), D,L-lactide was loaded into a pre-calcined conical flat-bottomed reaction flask along with a catalyst solution in chemically pure hexane (*Merck*). After evaporating the hexane at reduced pressure, the flask was filled with an inert gas, hermetically sealed and placed in an oil bath. Polymerization was carried out with continuous stirring of the reaction mass for a given time. The obtained copolymers were isolated and purified from the catalyst and monomer residues by double precipitation in the tetrahydrofuran–hexane system, and then dried to a constant mass in a vacuum oven. The synthesis scheme is shown in Fig. 2.

Thermogravimetric studies were carried out on a Pyris 1 TGA device (*PerkinElmer*, USA) in dynamic mode in the temperature range 30–700°C in a nitrogen flow (99.999%) of 100 mL/min using a standard open platinum sample cup holder. The accuracy of temperature determination was 0.1°C, while the accuracy of the scales was up to 0.001 mg. The heating rate was 10°C/min. The experimental data were processed using the Pyris Software Thermal Analysis software package version 10.1.0.0412 (*PerkinElmer*).

Deuterated solvents were used for nuclear magnetic resonance (NMR) assays: 99.96% deuterated chloroform $CDCl_3$ (*Sigma-Aldrich*, Germany) and 99.8% DMSO-d_6 (*Sigma-Aldrich*). The NMR spectra were recorded on the AVANCE DPX high-resolution NMR spectrometer (*Bruker*, Germany).

The molecular mass characteristics of copolymers were determined by gel permeation chromatography (GPC) on the AZURA chromatographic system (*Knauer*, Germany) using a refractometric detector and a Phenogel™ column (*Phenomenex*, USA) with a size of 300 × 7.8 mm and a particle pore size of 10^4 Å and 10^5 Å. The columns were calibrated according to polystyrene standards. The studies were carried out at 40°C with an eluent flow rate of 1 mL/min. A polymer solution in 99.9% tetrahydrofuran for high performance liquid chromatography (*Sigma-Aldrich*) was prepared for the study with a concentration of 2–5 mg/mL. Prior to introduction into the chromatograph, the solution was filtered through a syringe filter with a hydrophobic membrane with a pore size of 0.45 μm.

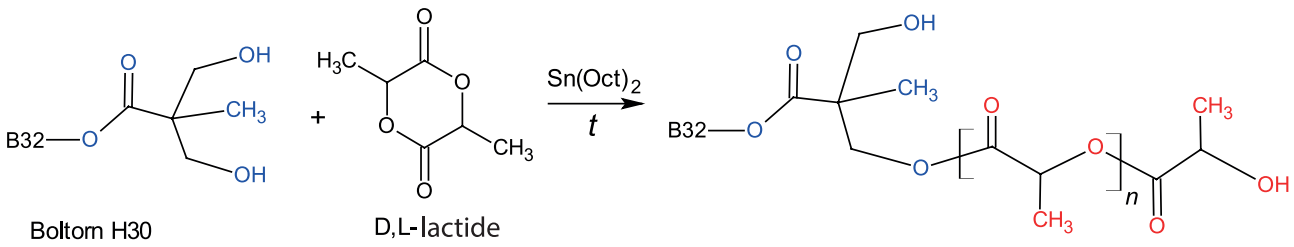

Fig. 2. Scheme for the synthesis of Boltorn™-$[(PDLA)_x]_y$ multiarm copolymers.

RESULTS AND DISCUSSION

The degree of branching of polymer macromolecules, which is closely related to their physicochemical properties, is an important parameter for their characterization. The structure of hyperbranched polyester polyols features not only dendritic (branching) and terminal (terminal) repeating structural units, but also linear links with unreacted functional groups (Fig. 3).

In order to assess the degree of branching of the investigated Boltorn™ H30 polyester polyol, proton and carbon NMR spectra were obtained in deuterated DMSO (Fig. 4). In order to detect weak interactions and improve the resolution of the signal, samples with a low concentration were used in the analysis.

In the ^{1}H NMR spectrum there are signals corresponding to methyl (three types: linear, dendritic, and terminal, a group of signals at 0.95–1.25 ppm), methylene (two types: $–CH_2–OH$ at 3.3–3.6 ppm and $–CH_2–OR$ at 3.9–4.2 ppm) and hydroxyl groups (4.3–5.0 ppm). Since the DMSO contains traces of water, there is a broadening of the signal in the region of 4.3–5.0 ppm.

To describe the structure of hyperbranched polymers, Fréchet [16] introduced the term "degree of branching" (DB) as a function of the ratio between dendritic (D), linear (L) and terminal (T) structural units calculated by the following ratio:

$$DB = \frac{D + T}{D + L + T}$$

Based on the data on the signal intensities of methyl groups of various types of links, we obtain the following ratio of terminal, linear, and dendritic types of links: 24%, 59%, and 17%, respectively. The degree of branching calculated by the formula is 0.4, which corresponds to the literature data for hyperbranched polymers [17].

Block copolymers based on D,L-lactide are usually synthesized in a melt at temperatures above 130°C. In order to study the thermal stability of Boltorn™ H30 polyester polyol, the thermogravimetric analysis (TGA) method was used to set the temperature of the beginning of thermal degradation of the polymer; this also determines the upper temperature range of operation with the polymer. Boltorn™ H30 polyester was studied both in dynamic (heating rate is 10°C/min) and in isothermal mode (160°C, 170°C, and 180°C). According to the obtained thermograms (Fig. 5), thermal oxidative degradation of Boltorn™ H30 polyester is observed at 200–220°C,

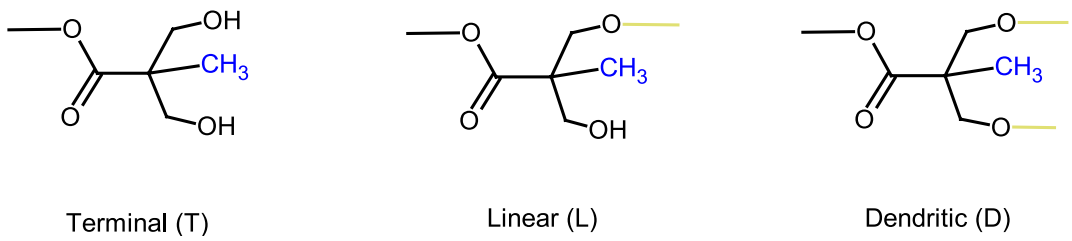

Fig 3. Basic repeating building blocks of Boltorn™ polyesters.

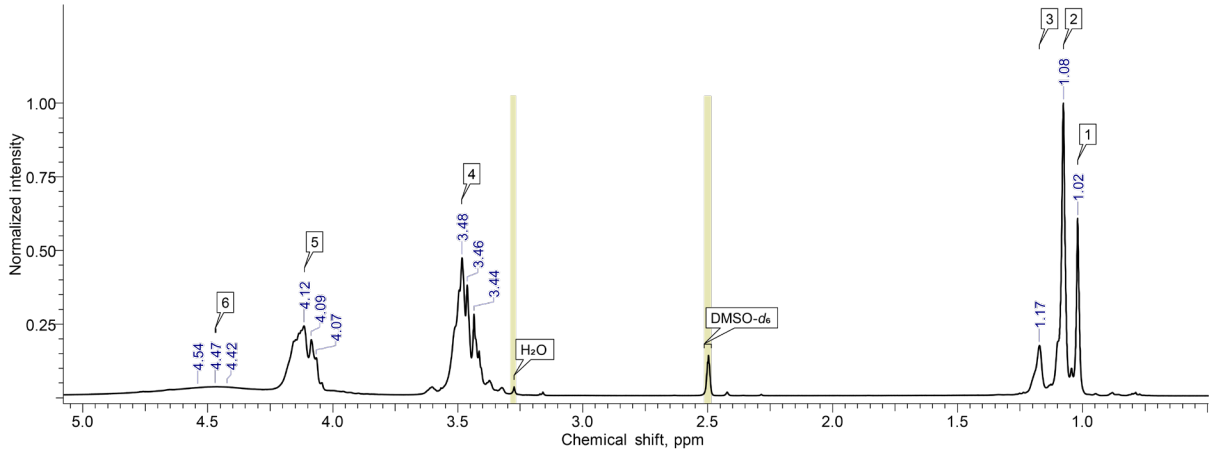

Fig. 4. ^{1}H NMR spectrum of Boltorn™ H30 in DMSO-d_6.

which allows the use of Boltorn™ H30 during copolymerization with lactide at reaction temperatures up to 180–190°C.

In order to select optimal conditions for copolymerization of D,L-lactide (monomer) with Boltorn™ H30 polyester (macroinitiator), the reaction was carried out in the temperature range of 160–180°C with a different molar ratio of monomer/macroinitiator, at a constant concentration of the tin(II) octanoate catalyst of 1400 ppm per monomer. Tin(II) octanoate is widely used as a catalyst in the polymerization of cyclic esters, including for the synthesis of biomedical polymers [18–20].

The reaction conditions, as well as the molecular weight characteristics and polydispersity coefficient of the synthesized copolymers determined by the GPC method, are given in Table.

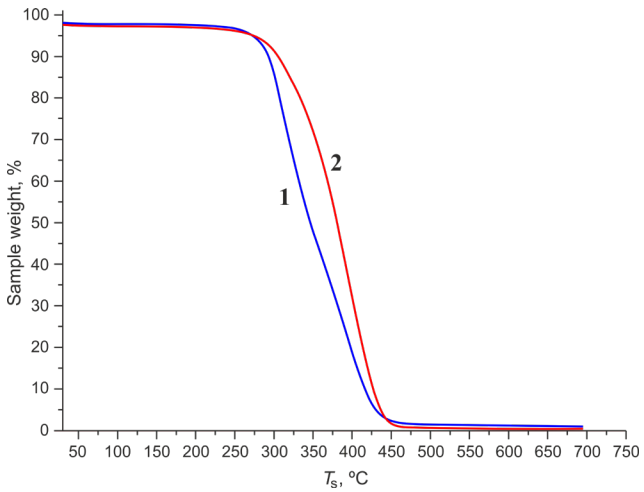

Fig. 5. TGA curves of Boltorn™ H30 polyester obtained in dynamic mode at a heating rate of 10 °C/min: (1) in an open crucible and (2) in a closed crucible.

Table. Molecular weight characteristics of copolymers

Sample	Reaction conditions				Molecular weights of copolymers (according to GPC)		
	T, °C	τ, h	*n*(B32), mol	*n*(D,L-lactide), mol	M_w	M_n	PDI
1	160	1	$2.77 \cdot 10^{-5}$	$1.04 \cdot 10^{-2}$	38 029	25 770	1.48
2	160	3	$2.77 \cdot 10^{-5}$	$1.04 \cdot 10^{-2}$	42 587	30 298	1.41
3	160	5	$2.77 \cdot 10^{-5}$	$1.04 \cdot 10^{-2}$	47 795	28 214	1.69
4	160	24	$2.77 \cdot 10^{-5}$	$1.04 \cdot 10^{-2}$	39 790	13 149	3.02
5	170	1	$2.77 \cdot 10^{-5}$	$1.04 \cdot 10^{-2}$	29 943	21 227	1.41
6 (DL32A)	170	3	$2.77 \cdot 10^{-5}$	$1.04 \cdot 10^{-2}$	52 219	35 534	1.47
7 (DL32B)	170	3	$2.77 \cdot 10^{-5}$	$2.08 \cdot 10^{-2}$	73 990	52 514	1.41
8 (DL32C)	170	3	$2.77 \cdot 10^{-5}$	$3.13 \cdot 10^{-2}$	121 054	91 812	1.32
9	170	5	$2.77 \cdot 10^{-5}$	$1.04 \cdot 10^{-2}$	38 936	28 639	1.36
10	170	24	$2.77 \cdot 10^{-5}$	$1.04 \cdot 10^{-2}$	51 143	9 700	5.27
11	180	24	$2.77 \cdot 10^{-5}$	$1.04 \cdot 10^{-2}$	41 663	27 407	1.52

Based on the obtained data, it was found that the optimal copolymerization time of D,L-lactide with Boltorn™ H30 polyester is 3 h at a temperature of 170°C and a catalyst concentration of 1400 ppm. Under these conditions, it is possible to obtain copolymers having a monomodal molecular mass distribution. With an increase in the content of D,L-lactide in the reaction mixture with respect to Boltorn™ H30 from $2.08 \cdot 10^{-2}$ to $3.13 \cdot 10^{-2}$ mol, a bimodal molecular mass distribution is observed on chromatograms (for the DL32C sample, Fig. 6).

The chemical structure of the synthesized copolymers was studied by NMR spectroscopy. Both the proton and carbon spectra have signals corresponding to the functional groups of Boltorn™ polyester and polylactide blocks. The proton NMR spectrum for the DL32B sample is given in Fig. 7. Here, the signals corresponding to the CH groups of the polylactide are in the range of 5.15–5.23 ppm, while the signal of protons of the same groups in the monomer is located in a stronger field: 5.02–5.03 ppm. In the region of 1.65–1.68 ppm, there is a signal of CH_3 group of the residual D,L-lactide monomer, while in the region of 1.55–1.59 ppm, the signal of CH3 groups of D,L-lactide links in the copolymer can be observed. In the range of 5.0–5.30 ppm chemical shifts, signals of CH groups appear, while in the range of 1.50–1.70 ppm, signals of methyl groups are visible. By integrating the peaks, it is possible to obtain the signal intensities of each group, thus forming a basis to calculate the degree of monomer conversion. For all the studied copolymers, the conversion rate was 91.0–96.0%.

From the carbon spectrum shown in Fig. 8, signals from carbon atoms of the following types can be seen in the structure of the DL32B copolymer: $–CH_3$ groups (16–19 ppm); –C=O groups (171–176 ppm); $–CH_2–OR$ groups (66–70 ppm).

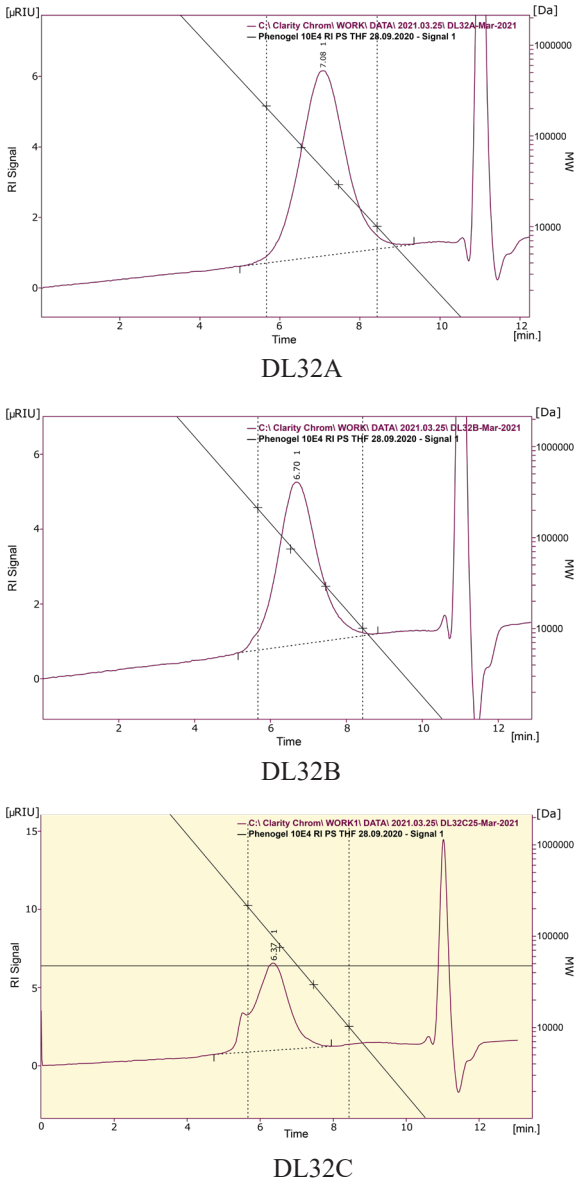

Fig. 6. Chromatograms of hyperbranched copolymers (Boltorn™ H30)-PDLA.

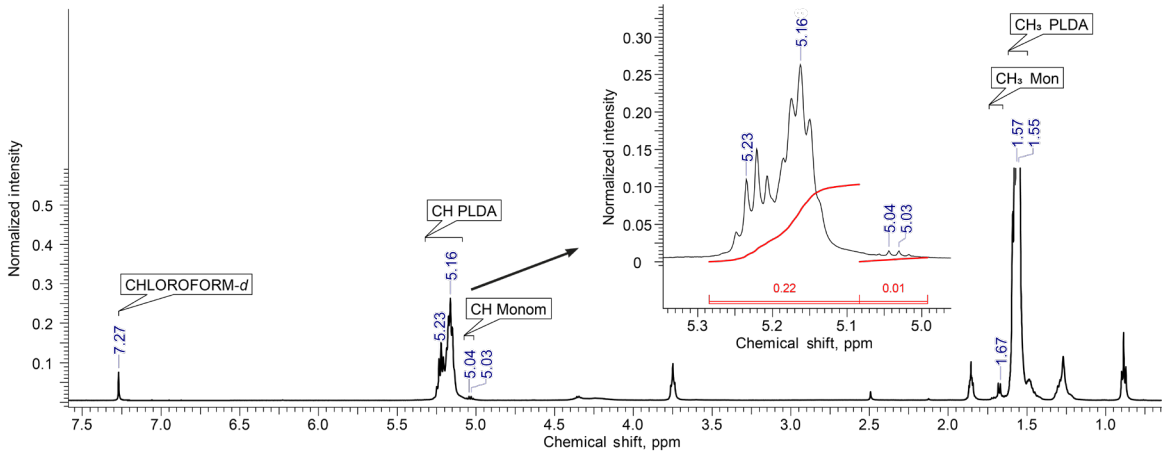

Fig. 7. ^{1}H NMR spectrum of (Boltorn™ H30)-PDLA (sample DL32B).

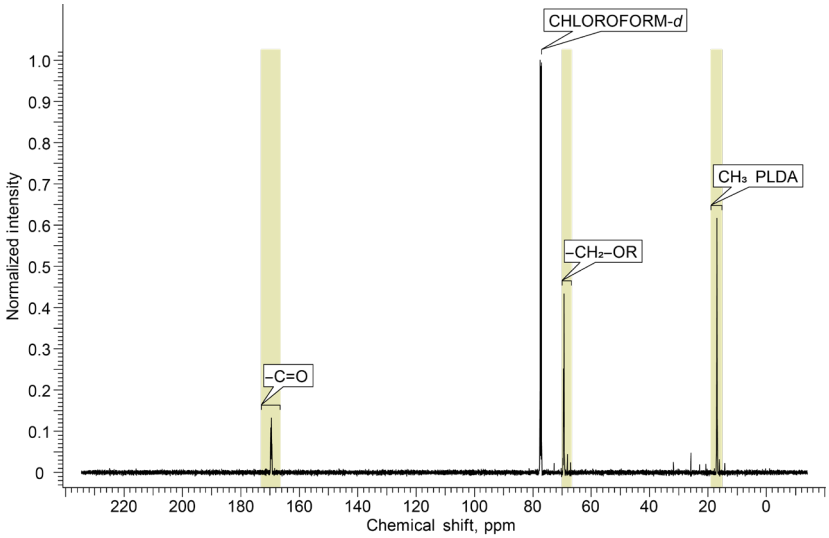

Fig. 8. ^{13}C NMR spectrum of (Boltorn™ H30)-PDLA (sample DL32B).

CONCLUSIONS

The obtained results demonstrate the possibility of synthesizing narrowly dispersed hyperbranched polymers using Boltorn™ H30 polyester polyol as a macroinitiator during polymerization of D,L-lactide. It was found that copolymers with a monomodal molecular mass distribution are formed in 3 h when the content of D,L-lactide and Boltorn™ H30 in the reaction system is $1.04 \cdot 10^{-2}$ and $2.77 \cdot 10^{-5}$ mol, respectively, using tin(II) octanoate taken at a concentration of 1400 ppm at a temperature of 170°C. A further increase in the content of D,L-lactide in the reaction mixture with respect to Boltorn™ H30 leads to the formation of copolymers having a bimodal molecular weight distribution. The synthesized copolymers contain a large number of peripheral hydroxyl groups, which can be further modified with polyethylene oxide to obtain amphiphilic block-copolymers having regulated colloidal chemical properties.

Acknowledgments

The structures of initial and synthesized compounds were studied using the Center for Collective Use equipment at the MIREA – Russian Technological University (assesment No. 075-15-2021-689, September 01, 2021, identification number 2296.61321X0010). The study was supported by the President of the Russian Federation, grant No. MK-70.2021.1.3.

Authors' contributions

V.I. Gomzyak – study idea, literature review, and writing the text of the article;

N.V. Bychkov – conducting experimental research, literature review;

A.S. Aduev – performing NMR spectroscopy of samples;

V.A. Ivanova – performing NMR spectroscopy of samples and analysis of experimental data;

A.D. Koshelev – literature review and writing the text of the article;

S.N. Chvalun – general supervision.

The authors declare no conflicts of interest.

REFERENCES

1. Gelperina S.E., Shvets V.I. Drug Delivery Systems based on Polymeric Nanoparticles. *Biotekhnologiya = Biotechnology in Russia*. 2009;(3):1–21 (in Russ.).

2. Gomzyak V.I., Sedush N.G., Puchkov A.A., *et al.* Linear and Branched Lactide Polymers for Targeted Drug Delivery Systems. *Polym. Sci. Ser. B*. 2021;63(3):257–271. https://doi.org/10.1134/S1560090421030064

[Original Russian Text: Gomzyak V.I., Sedush N.G., Puchkov A.A., Polyakov D.K., Chvalun S.N. Linear and Branched Lactide Polymers for Targeted Drug Delivery Systems. *Vysokomolekulyarnye soedineniya. Seriya B.* 2021;63(3):190–206 (in Russ.). https://doi.org/10.31857/S2308113921030062]

СПИСОК ЛИТЕРАТУРЫ

1. Гельперина С.Э., Швец В.И. Системы доставки лекарственных веществ на основе полимерных наночастиц. *Биотехнология*. 2009;(3):8–23.

2. Гомзяк В.И., Седуш Н.Г., Пучков А.А., Поляков Д.К., Чвалун С.Н. Линейные и разветвленные полимеры лактида для систем направленной доставки лекарственных средств. *Высокомолекулярные соединения. Серия Б.* 2021;63(3):190–206. https://doi.org/10.31857/S2308113921030062

3. Гомзяк В.И., Демина В.А., Разуваева Е.В., Седуш Н.Г., Чвалун С.Н. Биоразлагаемые полимерные материалы для медицины: от импланта к органу. *Тонкие химические технологии*. 2017;12(5):5–20. https://doi.org/10.32362/2410-6593-2017-12-5-5-20

3. Gomzyak V.I., Demina V.A., Razuvaeva E.V., Sedush N.G., Chvalun S.N. Biodegradable polymer materials for medical applications: from implants to organs. *Fine Chemical Technologies*. 2017;12(5):5–20 (in Russ.). https://doi.org/10.32362/2410-6593-2017-12-5-5-20

4. Agadzhanyan V.V., Pronskikh A.A., Demina V.A., Gomzyak V.I., Sedush N.G., Chvalun S.N. Biodegradable implants in orthopedics and traumatology. Our first experience. *Politravma = Polytrauma*. 2016;(4):85–93 (in Russ.)

5. Korake S., Shaikh A., Salve R., Gajbhiye K.R., Gajbhiye V., Pawar A. Biodegradable dendritic Boltorn™ nanoconstructs: A promising avenue for cancer theranostics. *Int. J. Pharm*. 2021;594:120177. https://doi.org/10.1016/j.ijpharm.2020.120177

6. Gomzyak V.I., Puchkov A.A., Artamonova N.E., *et al*. Physico-chemical properties of biodegradable hyperbranched polyester polyol based on 2,2-bis(methylol) propionic acid. *Fine Chemical Technologies*. 2018;13(4):67–73 (in Russ.). https://doi.org/10.32362/2410-6593-2018-13-4-67-73

7. Zhang X., Dai Y., Dai G. Advances in amphiphilic hyperbranched copolymers with an aliphatic hyperbranched 2,2-bis(methylol)propionic acid-based polyester core. *Polym. Chem*. 2020;11(5):964–973. https://doi.org/10.1039/c9py01608b

8. Prabaharan M., Grailer J.J., Pilla S., *et al*. Folate-conjugated amphiphilic hyperbranched block copolymers based on Boltorn H40, poly(l-lactide) and poly(ethylene glycol) for tumor-targeted drug delivery. *Biomaterials*. 2009;30(16):3009–3019. https://doi.org/10.1016/j.biomaterials.2009.02.011

9. Perše L.S., Huskić M. Rheological characterization of multiarm star copolymers. *Eur. Polym. J*. 2016;76:188–195. https://doi.org/10.1016/j.eurpolymj.2016.01.045

10. Hawker C.J., Lee R., Fréchet J.M.J. One-Step Synthesis of Hyperbranched Dendritic Polyesters. *J. Am. Chem. Soc*. 1991;113(12):4583–4588. https://doi.org/10.1021/ja00012a030

11. Žagar E., Žigon M. Characterization of a Commercial Hyperbranched Aliphatic Polyester Based on 2,2-Bis(methylol) propionic Acid. *Macromolecules*. 2002;35(27):9913–9925. https://doi.org/10.1021/ma021070o

12. Kricheldorf H.R., Kreiser-Saunders I., Boettcher C. Polylactones: 31. Sn(II)octoate-initiated polymerization of L-lactide: a mechanistic study. *Polymer*. 1995;36(6):1253–1259. https://doi.org/10.1016/0032-3861(95)93928-F

13. Kricheldorf H.R., Weidner S.M. High molar mass cyclic poly(L-lactide) obtained by means of neat tin(II) 2-ethylhexanoate. *Polym. Chem*. 2020;11(32):5249–5260. https://doi.org/10.1039/d0py00811g

14. Lecomte P., Jérôme C. Recent developments in ring-opening polymerization of lactones. In: Rieger B., Künkel A., Coates G., Reichardt R., Dinjus E., Zevaco T. (Eds.). Synthetic Biodegradable Polymers. *Advances in Polymer Science*. 2012;245:173–218. https://doi.org/10.1007/12_2011_144

15. Tikhonov P.A., Vasilenko N.G., Muzafarov A.M. Multiarm Star Polymers. Fundamental Aspects. *A Review. Doklady Chemistry*. 2021;496(1):3–20. https://doi.org/10.1134/S001250082101002X

16. Perevyazko I., Seiwert J., Schömer M., Frey H., Schubert U.S., Pavlov G.M. Hyperbranched Poly(ethylene glycol) Copolymers: Absolute Values of the Molar Mass, Properties in Dilute Solution, and Hydrodynamic Homology. *Macromolecules*. 2015;48(16):5887–5898. https://doi.org/10.1021/acs.macromol.5b01020

4. Агаджанян В.В., Пронских А.А., Демина В.А., Гомзяк В.И., Седуш Н.Г., Чвалун С.Н. Биодеградируемые импланты в ортопедии и травматологии. Наш первый опыт. *Политравма*. 2016;(4):85–93.

5. Korake S., Shaikh A., Salve R., Gajbhiye K.R., Gajbhiye V., Pawar A. Biodegradable dendritic Boltorn™ nanoconstructs: A promising avenue for cancer theranostics. *Int. J. Pharm*. 2021;594:120177. https://doi.org/10.1016/j.ijpharm.2020.120177

6. Гомзяк В.И., Пучков А.А., Артамонова Н.Е. и др. Физико-химические свойства биоразлагаемого сверхразветвленного полиэфирполиола на основе 2,2-бис(метилол) пропионовой кислоты. *Тонкие химические технологии*. 2018;13(4):67–73. https://doi.org/10.32362/2410-6593-2018-13-4-67-73

7. Zhang X., Dai Y., Dai G. Advances in amphiphilic hyperbranched copolymers with an aliphatic hyperbranched 2,2-bis(methylol)propionic acid-based polyester core. *Polym. Chem*. 2020;11(5):964–973. https://doi.org/10.1039/c9py01608b

8. Prabaharan M., Grailer J.J., Pilla S., *et al*. Folate-conjugated amphiphilic hyperbranched block copolymers based on Boltorn H40, poly(l-lactide) and poly(ethylene glycol) for tumor-targeted drug delivery. *Biomaterials*. 2009;30(16):3009–3019. https://doi.org/10.1016/j.biomaterials.2009.02.011

9. Perše L.S., Huskić M. Rheological characterization of multiarm star copolymers. *Eur. Polym. J*. 2016;76:188–195. https://doi.org/10.1016/j.eurpolymj.2016.01.045

10. Hawker C.J., Lee R., Fréchet J.M.J. One-Step Synthesis of Hyperbranched Dendritic Polyesters. *J. Am. Chem. Soc*. 1991;113(12):4583–4588. https://doi.org/10.1021/ja00012a030

11. Žagar E., Žigon M. Characterization of a Commercial Hyperbranched Aliphatic Polyester Based on 2,2-Bis(methylol) propionic Acid. *Macromolecules*. 2002;35(27):9913–9925. https://doi.org/10.1021/ma021070o

12. Kricheldorf H.R., Kreiser-Saunders I., Boettcher C. Polylactones: 31. Sn(II)octoate-initiated polymerization of L-lactide: a mechanistic study. Polymer. 1995;36(6):1253–1259. https://doi.org/10.1016/0032-3861(95)93928-F

13. Kricheldorf H.R., Weidner S.M. High molar mass cyclic poly(L-lactide) obtained by means of neat tin(II) 2-ethylhexanoate. *Polym. Chem.* 2020;11(32):5249–5260. https://doi.org/10.1039/d0py00811g

14. Lecomte P., Jérôme C. Recent developments in ring-opening polymerization of lactones. In: Rieger B., Künkel A., Coates G., Reichardt R., Dinjus E., Zevaco T. (Eds.). Synthetic Biodegradable Polymers. *Advances in Polymer Science*. 2012;245:173–218. https://doi.org/10.1007/12_2011_144

15. Tikhonov P.A., Vasilenko N.G., Muzafarov A.M. Multiarm Star Polymers. Fundamental Aspects. *A Review. Doklady Chemistry*. 2021;496(1):3–20. https://doi.org/10.1134/S001250082101002X

16. Perevyazko I., Seiwert J., Schömer M., Frey H., Schubert U.S., Pavlov G.M. Hyperbranched Poly(ethylene glycol) Copolymers: Absolute Values of the Molar Mass, Properties in Dilute Solution, and Hydrodynamic Homology. *Macromolecules*. 2015;48(16):5887–5898. https://doi.org/10.1021/acs.macromol.5b01020

17. Li H., Riva R., Kricheldorf H.R., Jérôme R., Lecomte P. Synthesis of eight- and star-shaped poly-(ε-caprolactone)s and their amphiphilic derivatives. *Chemistry–A European Journal*. 2008;14(1):358–368. https://doi.org/10.1002/chem.200700603

17. Li H., Riva R., Kricheldorf H.R., Jérôme R., Lecomte P. Synthesis of eight- and star-shaped poly-(ε-caprolactone)s and their amphiphilic derivatives. *Chemistry – A European Journal*. 2008;14(1):358–368. https://doi.org/10.1002/chem.200700603

18. Massoumi B., Sarvari R., Agbolaghi S. Biodegradable and conductive hyperbranched terpolymers based on aliphatic polyester, poly(D,L-lactide), and polyaniline used as scaffold in tissue engineering. *Int. J. Polym. Mater.* 2018;67(13):808–821. https://doi.org/10.1080/00914037.2017.1383248

19. Michalski A., Brzezinski M., Lapienis G., Biela T. Star-shaped and branched polylactides: Synthesis, characterization, and properties. *Prog. Polym. Sci*. 2019;89:159–212. https://doi.org/10.1016/j.progpolymsci.2018.10.004

20. Tabatabaei Rezaei S.J., Abandansari H.S., Nabid M.R., Niknejad H. PH-responsive unimolecular micelles self-assembled from amphiphilic hyperbranched block copolymer for efficient intracellular release of poorly water-soluble anticancer drugs. *J. Colloid Interface Sci*. 2014;425:27–35. https://doi.org/10.1016/j.jcis.2014.03.034

18. Massoumi B., Sarvari R., Agbolaghi S. Biodegradable and conductive hyperbranched terpolymers based on aliphatic polyester, poly(D,L-lactide), and polyaniline used as scaffold in tissue engineering. *Int. J. Polym. Mater*. 2018;67(13):808–821. https://doi.org/10.1080/00914037.2017.1383248

19. Michalski A., Brzezinski M., Lapienis G., Biela T. Star-shaped and branched polylactides: Synthesis, characterization, and properties. *Prog. Polym. Sci.* 2019;89:159–212. https://doi.org/10.1016/j.progpolymsci.2018.10.004

20. Tabatabaei Rezaei S.J., Abandansari H.S., Nabid M.R., Niknejad H. PH-responsive unimolecular micelles self-assembled from amphiphilic hyperbranched block copolymer for efficient intracellular release of poorly water-soluble anticancer drugs. *J. Colloid Interface Sci.* 2014;425:27–35. https://doi.org/10.1016/j.jcis.2014.03.034

About the authors:

Vitaly I. Gomzyak, Cand. Sci. (Chem.), Associate Professor, S.S. Medvedev Department of Chemistry and Technology of Macromolecular Compounds, M.V. Lomonosov Institute of Fine Chemical Technologies, MIREA – Russian Technological University (86, Vernadskogo pr., Moscow, 119571, Russia). E-mail: vgomzyak@gmail.com. Scopus Author ID 55841680300, ResearcherID E-4518-2017, RSCI SPIN-code 7314-4562, https://orcid.org/0000-0001-7468-1062

Nikita V. Bychkov, Student, Institute of Nano-, Bio-, Information, Cognitive and Socio-humanitarian Sciences and Technologies, Moscow Institute of Physics and Technology (4, Maksimova ul., Moscow, 123098, Russia). E-mail: nikita3262@yandex.ru. https://orcid.org/0000-0002-8590-9373

Adu Sh. Aduev, Student, Institute of Nano-, Bio-, Information, Cognitive and Socio-humanitarian Sciences and Technologies, Moscow Institute of Physics and Technology (4, Maksimova ul, Moscow, 123098, Russia). E-mail: adu_99@mail.ru. https://orcid.org/0000-0003-2327-1033

Valeriia A. Ivanova (Shpotya), Postgraduate Student, Moscow Institute of Physics and Technology (9, Institutskii per., Dolgoprudny, Moscow oblast, 141701, Russia). E-mail: valeriya.ivanova@phystech.edu. https://orcid.org/0000-0002-2644-2523

Anton D. Koshelev, Doctoral Candidate, Researcher, Volkswagen AG, Darmstadt University of Technology (TU Darmstadt) (64277 Darmstadt, Hessen, Germany). E-mail: anton.koshelev@volkswagen.de. https://orcid.org/0000-0003-4842-9482

Sergey N. Chvalun, Corresponding Member of the Russian Academy of Sciences, Dr. Sci. (Chem.), Professor, Head of the S.S. Medvedev Department of Chemistry and Technology of Macromolecular Compounds, M.V. Lomonosov Institute of Fine Chemical Technologies, MIREA – Russian Technological University (86, Vernadskogo pr., Moscow, 119571, Russia). E-mail: chvalun@mirea.ru. Scopus Author ID 7007011596, Researcher ID E-3924-2014, RSCI SPIN-code 8538-0603, https://orcid.org/0000-0001-9405-4509

Об авторах:

Гомзяк Виталий Иванович, к.х.н., доцент кафедры химии и технологии высокомолекулярных соединений им. С.С. Медведева Института тонких химических технологий им. М.В. Ломоносова ФГБОУ ВО «МИРЭА – Российский технологический университет» (Россия, 119571, Москва, пр-т Вернадского, д. 86). E-mail: vgomzyak@gmail.com. Scopus Author ID 55841680300, ResearcherID E-4518-2017, SPIN-код 7314-4562, https://orcid.org/0000-0001-7468-1062

Бычков Никита Васильевич, студент, Институт нано-, био-, информационных, когнитивных и социогуманитарных наук и технологий (ИНБИКСТ) ФГАОУ ВО «Московский физико-технический институт (национальный исследовательский университет) (Россия, 123098, г. Москва, ул. Максимова, д. 4). E-mail: nikita3262@yandex.ru. https://orcid.org/0000-0002-8590-9373

Адуев Аду Шарапудинович, студент, Институт нано-, био-, информационных, когнитивных и социогуманитарных наук и технологий (ИНБИКСТ) ФГАОУ ВО «Московский физико-технический институт (национальный исследовательский университет) (Россия, 123098, г. Москва, ул. Максимова, д. 4). E-mail: adu_99@mail.ru. https://orcid.org/0000-0003-2327-1033

Иванова (Шпотя) Валерия Антоновна, аспирант, ФГАОУ ВО «Московский физико-технический институт» (Национальный исследовательский университет) (Россия, 141701, Московская область, г. Долгопрудный, Институтский пер., д. 9). E-mail: valeriya.ivanova@phystech.edu. https://orcid.org/0000-0002-2644-2523

Кошелев Антон Дмитриевич, докторант (научный сотрудник), Концерн Фольксваген, Технический университет Дармштадта (Германия, 64277, Гессен, Дармштадт). E-mail: anton.koshelev@volkswagen.de. https://orcid.org/0000-0003-4842-9482

Чвалун Сергей Николаевич, член-корр. РАН, д.х.н., профессор, заведующий кафедрой химии и технологии высокомолекулярных соединений им. С.С. Медведева Института тонких химических технологий им. М.В. Ломоносова ФГБОУ ВО «МИРЭА – Российский технологический университет» (Россия, 119571, Москва, пр-т Вернадского, д. 86). E-mail: chvalun@mirea.ru. Scopus Author ID 7007011596, ResearcherID E-3924-2014, SPIN-код РИНЦ 8538-0603, https://orcid.org/0000-0001-9405-4509

The article was submitted: February 14, 2022; approved after reviewing: April 14, 2022; accepted for publication: June 06, 2022.

Translated from Russian into English by N. Isaeva
Edited for English language and spelling by Thomas Beavitt

ANALYTICAL METHODS IN CHEMISTRY AND CHEMICAL TECHNOLOGY

АНАЛИТИЧЕСКИЕ МЕТОДЫ В ХИМИИ И ХИМИЧЕСКОЙ ТЕХНОЛОГИИ

ISSN 2686-7575 (Online)

https://doi.org/10.32362/2410-6593-2022-17-3-253-267

UDC 543.544.5.068.7

RESEARCH ARTICLE

Validation of a method for the quantitative determination of narcotic and psychotropic substances in urine by UHPLC–MS/MS

Nadezhda B. Savelieva[1], Grigory V. Ishutenko[1], Andrey V. Polosin[1], Fedor V. Radus[2], Dmitry S. Polyansky[2], Sergey A. Kurbatkin[2], Yulia A. Efimova[2], Pavel V. Postnikov[1,✉]

[1]National Anti-Doping Laboratory (Institute), M.V. Lomonosov Moscow State University (NADL MSU), Moscow, 105005 Russia

[2]MIREA – Russian Technological University (M.V. Lomonosov Institute of Fine Chemical Technologies), Moscow, 119571 Russia

✉Corresponding author, e-mail: drpavelpostnikov@gmail.com

Abstract

Objectives. *To validate a new method for the quantitative determination of 31 potent and narcotic substances and their metabolites in urine that meets the requirements of ISO/IEC 17025 using a fast and highly sensitive method of chromato-mass spectrometry with a view to introducing such a method into the routine practice of the National Anti-Doping Laboratory of the Lomonosov Moscow State University (NADL MSU).*

Methods. *Urine samples soldered with standard solutions were analyzed using ultra high performance liquid chromatography-tandem mass spectrometry (UHPLC–MS/MS).*

Results. *Diagnostic precursor/ion-product pairs and collision energies were established to allow unambiguous identification of the analyzed substances. During sample preparation, hydrolysis conditions were optimized. Selectivity, linearity, limits of qualitative determination, limit of quantitative determination (established under the contract with the customer firm), matrix effect, and measurement uncertainty were defined. Systematized data grouped by classes of analytes are given in the final table.*

Conclusions. *The important advantages of the presented technique are the absence of complex and lengthy sample preparation, as well as the short time of the analysis method (about 10 min), which can significantly reduce duration along with labor and analysis costs. The addition of new analytes will ensure the versatility of the technique, as well as expanding its scope.*

Keywords: *UHPLC–MS/MS, GC–MS/MS, validation, quantitation, narcotic potent and psychotropic substances*

For citation: Savelieva N.B., Ishutenko G.V., Polosin A.V., Radus F.V., Polyansky D.S., Kurbatkin S.A., Efimova Yu.A., Postnikov P.V. Validation of a method for the quantitative determination of narcotic and psychotropic substances in urine by UHPLC–MS/MS. *Tonk. Khim. Tekhnol. = Fine Chem. Technol.* 2022;17(3):253–267 (Russ., Eng.). https://doi.org/10.32362/2410-6593-2022-17-3-253-267

НАУЧНАЯ СТАТЬЯ

Валидация методики количественного определения наркотических и психотропных веществ в моче методом СВЭЖХ-МС/МС

Н.Б. Савельева[1], Г.В. Ишутенко[1], А.В. Полосин[1], Ф.В. Радус[2], Д.С. Полянский[2], С.А. Курбаткин[2], Ю.А. Ефимова[2], П.В. Постников[1,✉]

[1]Национальная антидопинговая лаборатория (Институт) Московского государственного университета им. М.В. Ломоносова (НАДЛ МГУ), Москва, 105005 Россия
[2]МИРЭА – Российский технологический университет (Институт тонких химических технологий им. М.В. Ломоносова), Москва, 119571 Россия
[✉]Автор для переписки, e-mail: drpavelpostnikov@gmail.com

Аннотация

Цели. *Валидировать и ввести в рутинную практику НАДЛ МГУ новую, отвечающую требованиям ISO/IEC 17025, методику количественного определения 31 сильнодействующих и наркотических вещества и их метаболитов в моче с использованием быстрого и высокочувствительного метода хромато-масс-спектрометрии.*
Методы. *Анализ спайкованных с растворами стандартов образцов мочи проводили методом сверхэффективной жидкостной хроматографии–тандемной масс-спектрометрии (СВЭЖХ-МС/МС).*
Результаты. *В работе установлены диагностические пары прекурсор/ион-продукт и найдены энергии соударения, позволяющие однозначно идентифицировать анализируемые вещества; оптимизированы условия гидролиза при проведении пробоподготовки; определены селективность, линейность, предел качественного определения, предел количественного определения (установлен в рамках договора с фирмой-заказчиком), эффект матрицы и неопределенность измерения. Систематизированные данные приведены в итоговой таблице и сгруппированы по классам определяемых веществ.*

Выводы. *Представленная методика обладает важными преимуществами – отсутствием сложной и продолжительной пробоподготовки, а также коротким временем метода анализа – около 10 мин, что позволяет существенно снизить трудозатраты, продолжительность и себестоимость анализа. Дополнение новыми определяемыми веществами обеспечит ее универсальность и позволит расширить область применения.*

Ключевые слова: *СВЭЖХ-МС/МС, ГХ-МС/МС, валидация, количественное определение, наркотические сильнодействующие и психотропные вещества*

Для цитирования: Савельева Н.Б., Ишутенко Г.В., Полосин А.В., Радус Ф.В., Полянский Д.С., Курбаткин С.А., Ефимова Ю.А., Постников П.В. Валидация методики количественного определения наркотических и психотропных веществ в моче методом СВЭЖХ-МС/МС. *Тонкие химические технологии*. 2022;17(3):253–267. https://doi.org/10.32362/2410-6593-2022-17-3-253-267

INTRODUCTION

In recent decades, the emergence of new narcotic and psychotropic substances, which has been accompanied by a steady increase in their abuse, has become a global problem. According to information provided by the United Nations International Narcotics Control Board in 2020[1], despite the COVID-19 pandemic, which has created unprecedented challenges for the supply of controlled medicines and global health systems in general, the number of seizures of potent narcotic substances has remained at a stable high level. Meanwhile, the number of electronic marketplaces on the wider Internet—and in particular on the so-called "dark web"—has increased. Encrypted secure applications and social networks have begun to play a significant role in the search for such substances at the consumer level. In view of this, the relevance of chemical and toxicological analysis in order to control the intake of illegal substances has increased significantly. As a result of the active use of narcotic drugs and psychotropic substances, the number of people with drug addiction is steadily growing, while the number of severe intoxications leading to death is also increasing [1].

In this regard, one of the most urgent and significant tasks of modern toxicological analysis is the development of new, express, and accurate techniques, as well as improving already used methods for detecting controlled substances and their metabolites in objects of biological origin, as well as supporting their validation and implementation in the routine practice of laboratories.

To date, chromatographic methods of determination are widely used in combination with mass spectrometry in various chemical and toxicological studies, providing high rates of selectivity and sensitivity [2–4]. Although gas chromatography-mass spectrometry (GC–MS/MS) methods have long been used for routine analysis, the associated sample preparation, including the additional purification, extraction, and derivatization for low-volatile organic compounds, is time-consuming. For this reason, ultra high performance liquid chromatography in combination with tandem mass spectrometry (UHPLC–MS/MS) has become a popular method for screening analysis to determine the presence of narcotic, potent, and psychotropic substances [5].

Previously, the Anti-Doping Center—the predecessor of the National Anti-Doping Laboratory of M.V. Lomonosov Moscow State University (NADL MSU)—had introduced a method for toxicological monitoring of urine samples to identify classes of opiates, stimulants, cannabinoids, barbiturates, and benzodiazepines. The World Anti-Doping Agency (WADA) criteria for the analysis of urine samples

[1] Report of the International Narcotics Control Boards (INCB) for 2020. United Nations: International Narcotics Control Board). Vein; 2021. 167 p. URL: https://www.incb.org/documents/Publications/AnnualReports/AR2020/Annual_Report/E_INCB_2020_1_rus.pdf (Accessed February 10, 2022).

were taken as the basis for conducting method validation from the TD_IDCR and TD_DL technical documents associated with this period.[2,3] Although screening analysis and confirmation procedures for most compounds were performed by UHPLC–MS/MS, some substances and their metabolites were determined by GC–MS/MS.

In order to unify the analysis of substances using the UHPLC–MS/MS method and bring the methodology in line with the new regulatory documents[4], in 2020, the Laboratory revalidated the methodology for the quantitative determination of substances listed in Table 1. As a result, sample preparation was optimized, allowing the UHPLC–MS/MS parameters to be grouped according to the classes of analytes. Compliance of the method's validation with the requirements of the new version of ISO/IEC 17025 was confirmed by the Association of Analytical Centers "Analitika".[5]

The present study is aimed at developing an express and highly selective method for the quantitative determination of 31 substances and their metabolites included in the toxicological monitoring group.

The performance of chemico-toxicological analysis of employees of enterprises involved in work requiring increased attention, or in shift work around the clock, was carried out in accordance with the terms of the contract concluded with the customer company. The list of determined compounds is given in Table 1.

MATERIALS AND METHODS

Certified reference materials

For the experiments, certified standard samples with an initial concentration of 1.0 mg/mL were used: amphetamine, methylenedioxyamphetamine (MDA), methylenedioxymethamphetamine (MDEA), methylenedioxymethamphetamine (MDMA), methamphetamine, amobarbital, butabarbital, butalbital, pentabarbital, secobarbital, phenobarbital, alprazolam, clonazepam, lorazepam, midazolam, oxazepam, nordiazepam, temazepam, triazepam, flurazepam, benzoylecgonine, hydrocodone, hydromorphone, codeine, 6-monoacetylmorphine, morphine, oxycodone, oxymorphone, propoxyphene, methadone, and delta-9-tetrahydrocannabiol-9-acid (THC) purchased from *LGC* (United Kingdom).

Internal standards (ISTD) with an initial concentration of 0.01 mg/mL: demoxepam-d_5 (ISTD 1), morphine-d_3 (ISTD 2), and phenobarbital-d_5 (ISTD 3), purchased from *Cerilliant* (USA), bupranolol (ISTD 4) and mephruside (ISTD 5) purchased from *NMI* (Australia).

All manufacturers of certified reference materials meet the requirements of ISO 17034[6]. Manufacturers not accredited to ISO 17034 have documented the identity and purity of reference materials from competent laboratories that meet the requirements of ISO/IEC 17025 [9], which is confirmed by certificates of analysis.

Chemicals

Acetonitrile (*Merck*, Germany), methanol (*Merck*), and formic acid (*Acros Organics*, Belgium) were HPLC grade, deionized water for analysis (18.2 mΩ) was obtained using a Milli-Q system (*Millipore*, USA).

Sample preparation reagents: potassium carbonate (purity is 99% minimum), potassium bicarbonate (purity is 99% minimum), anhydrous sodium sulfate (purity is 99.5% minimum), and diethyl ether (purity is 95% minimum) manufactured by *Sigma-Aldrich* (USA); potassium dihydrogen phosphate (purity is not less than 99%), sodium phosphate dibasic dihydrate (purity is not less than 99%), and sodium azide (purity is not less than 99%) manufactured by *Merck*; *Escherichia Coli* K 12 β-glucuronidase (*Roche Diagnostics*, Switzerland); cartridges for solid phase extraction Oasis® MCX (*Waters*, USA).

Glass tubes with screw caps 16 × 125 mm (*Pyrex*, USA), 1.5 mL polypropylene tubes (*Eppendorf*, Germany), 2.0 mL glass vials (*Macherey-Nagel GmbH & Co*, Düren, Germany), 0.2 mL polypropylene vials (*Agilent Technologies*, USA), crimper, decapper, and gas tight caps for vials were used in the study.

Samples for analysis

Urine samples for chemico-toxicological analysis were taken from volunteers, each of whom provided a

[2] WADA Technical Document – TD2021IDCR. 2021. URL: https://www.wada-ama.org/en/resources/lab-documents/td2021idcr (Accessed February 11, 2022).

[3] WADA Technical Document – TD2021IDL. 2021. URL: https://www.wada-ama.org/en/resources/lab-documents/td2021dl (Accessed February 11, 2022).

[4] ISO/IEC 17025-2019. General requirements for the competence of testing and calibration laboratories. (In Russ.). URL: https://docs.cntd.ru/document/1200166732 (Accessed February 11, 2022).

[5] Association of Analytical Centers "Analytica." (In Russ.). URL: https://aac-analitica.ru/akkreditaciya.html (Accessed February 11, 2022).

[6] ISO 17034-2021 General requirements for the competence of reference material producers. (In Russ.). URL: https://docs.cntd.ru/document/1200181084 (Accessed February 11, 2022).

Table 1. Target compounds determined according to the program of chemico-toxicological analysis in accordance with the requirements of the customer company

Compounds/Metabolites	Thresholds, ng/mL
Amphetamine, Methylenedioxyamphetamine (MDA), Methylenedioxymethamphetamine (MDEA), Methylenedioxymethamphetamine (MDMA), Methamphetamine	250
Amobarbital, Butobarbital, Butalbital, Pentobarbital, Secobarbital, Phenobarbital	100
Alprazolam, Clonazepam, Lorazepam, Midazolam, Nordiazepam, Oxazepam, Temazepam, Triazolam, Flurazepam	100
Benzoylecgonine	100
Hydrocodone, Hydromorphone, Codeine, Morphine, Oxycodone, Oxymorphone	100
6-Monoacetylmorphine (6-MAM)	10
Methadone, Propoxyphene	200
Delta-9-tetrahydrocannabiol-9-acid (carboxy-THC)	10

written informed consent to the use of his biological material for scientific purposes, in accordance with the requirements of the laboratory code of ethics. The conducted studies do not contradict the Declaration of Helsinki of the World Medical Association.[7] These samples were previously examined for the absence of detectable components and used in the work as a certified negative urine control (blank urine, Blank).

Control samples were prepared for each group of compounds: a positive urine control containing the amounts of detectable compounds at the threshold level (positive control urine, PCU) and containing the amounts of detectable compounds with a given concentration different from the threshold value (LabQC). A certified negative urine control (Blank) was used as a matrix.

Equipment

In the study, the equipment was as follows: a triple quadrupole TSQ Vantage mass spectrometer (*Thermo Fisher Scientific*, San Jose, USA), in combination with a liquid UltiMate 3000 chromatograph (*Dionex*, Germany) (UHPLC–MS/MS), a thermostat-incubator with programmable temperature (*Binder*, Germany), low-temperature liquid thermostat (*Grant*, United Kingdom), solid-state incubator with programmable temperature (Grant), rotary stirrer, vortex V-1 plus (*BioSan*, Latvia), table centrifuge with Rotina horizontal rotor (*Hettich*, Germany), Discovery DV215CD (*OHaus*, USA) analytical balance (accuracy 5 digits), automatic batchers of variable volume (10–200 μL and 100–1000 μL) (*Eppendorf*, Germany), and 10-mL dispenser (*Brand*, Germany).

Sample preparation

Sample preparation included the following main steps: enzymatic hydrolysis, extraction, solvent removal, and resolubility for entry into the UHPLC–MS/MS system.

To perform sample preparation for the quantitative determination of target compounds, 12 tubes with screw caps (16 × 125 mm) were taken and labeled with Cal0 (Blank), Cal1, Cal2, Cal3, Cal4, Cal5, Cal6, and PCU markers in five repetitions. In the first 7 tubes, 1 mL of a certified negative urine control (Blank) was added, and in tubes 8–12, 1 mL of a urine sample containing the amount of analytes at the threshold level (PCU) was added.

The preparation of urine samples for validation was performed by two independent experts as follows: 20 μL of the mixture of ISTD 1–ISTD 3 internal standards were added to the tubes labeled

[7] Declaration of Helsinki. World Medical Association. URL: http://acto-russia.org/index.php?option=com_content&task=view&id=21 (Accessed February 11, 2022).

Cal0–Cal6 and PCU. Then, 1 mL of the hydrolysis buffer mixture (pH 7.4) was added to each tube and mixed on a Vortex contact mixer. Then the samples were placed in a thermostat-incubator with a programmed temperature of 57 ± 3°C for 60 ± 10 min. After that, the tubes were cooled to room temperature (25°C). Then 1 mL of carbonate buffer solution (pH 9–11) and 1–2 g of sodium sulfate were added to each tube and tubes were shaken for 5–10 s. Next, 5 mL of diethyl ether was added to each test tube, closed with a lid, and placed in a rotary mixer for 20 ± 5 min. Then, the tubes with the samples were centrifuged at 2700–3100 rpm for 3–4 min; were placed in a liquid thermostat with a programmable set temperature (−30°C) until the water layer was frozen (5–10 min). Next, the organic layer was transferred into test tubes 16 × 125 mm, evaporated to dryness in a solid-state heater at 70°C, 200 μL of a solution (Diluent) containing a 0.1% solution of formic acid in methanol/water = 5:95, *v*/*v*, was added to the dry residue with the internal standard solutions (ISTD 4, ISTD 5). Then, each tube was shaken on a Vortex mixer for 5–10 s, the obtained extracts were transferred into 0.2 mL polypropylene vials, closed with vial lids, and placed on the instrument.

Instrumental analysis

UHPLC–MS/MS analysis of the sample was performed under the following parameters: an Acquity BEH-C18 analytical column (100 mm, 2.1 mm, film thickness 1.7 μm, *Waters*, USA) was used. The flow rate of the mobile phase was 0.35 mL/min. The elution program started with a 0.5 min isocratic step at 95% of 0.1%-formic acid solution in water (A) and 5% of 0.1%-formic acid solution in methanol (B), followed by a linear increase to 95% solution B over 4.5 min, hold at 95% (B) for 2.5 min. The solution was then equilibrated to the end of the analysis for 10 min. The volume of the injected sample was 10 μL. Detection was performed in the mode of selective reaction monitoring (SRM) of positive and negative ions using a heated electrospray ion source (HESI II). The gas pressure in the impact chamber was 1.5 mTorr (argon 99.9995%). The evaporator temperature was 370°C, the capillary temperature was 350°C, and the spray voltage was 4000 V.

CHARACTERISTICS OF THE METHOD

The validation of the method was carried out in accordance with the requirements established in ISO/IEC 17025[8], GOST R 8.795-2012[9], the measurement uncertainty assessment guide ISO/IEC Guide 98-3:2008[10], as well as WADA technical documents TD2021IDCR and TD2021DL.

Selectivity

In order to investigate the potential interfering effect of the matrix, certified negative urine control (Blank) and control urine samples were prepared with the addition of a mixture of each group of compounds at the threshold level. There should be no interfering peaks of the matrix components with a signal-to-noise ratio exceeding 3:1 on the obtained mass chromatograms of the analytes in the corresponding intervals of scanning the retention time (RT) of the analytes within ± 0.1 min.

Linearity

In order to build a linear dependence of the quantitative determination of the components, a series of calibration solutions containing components in the range of 50–300% (Cal0–Cal6) of the threshold concentrations was conducted by sample preparation.

Based on the results of the analysis, we determined and built graphic dependences of the concentration on the received signal, the linearity of the calibration curves was evaluated using the correlation coefficients R^2, which should not be lower than 0.99.

Limits of quantitative and qualitative determinations

The limit of quantitation (LOQ) of a compound corresponds to the lowest concentration that falls within the linear range of the technique. In order

[8] ISO/IEC 17025-2019. General requirements for the competence of testing and calibration laboratories. (In Russ.). URL: https://docs.cntd.ru/document/1200166732 (Accessed February 11, 2022).

[9] GOST R 8.795-2012. National Standard of Russian Federation. State system for ensuring the uniformity of measurements. Identification of chemicals substance by a chromato-mass spectrometry method. The general requirements. (In Russ.). URL: https://docs.cntd.ru/document/1200102300 (Accessed February 11, 2022).

[10] ISO/IEC Guide 98-3:2008. Uncertainty of measurement. Part 3. Guide to the expression of uncertainty in measurement. 2008. URL: https://docs.cntd.ru/document/1200146871 (Accessed February 11, 2022).

to obtain this validation parameter, a certified negative urine control (Blank) was prepared with the addition of the least significant concentration of the calibration solution.

The limit of detection (LOD) of the method was set earlier during the development and validation of the primary analysis procedure by preparing a series of sequential dilutions of solutions in urine with a final concentration of analytes at a level of 10% (or less) of the threshold value.

Matrix effect

In order to assess the effect of urine components on the analyte determination (matrix effect, ME), control urine samples were studied with the addition of a mixture of each group of compounds at the threshold level and the corresponding solutions of the same analytes in a solvent with the same concentration. The influence of the urine matrix was evaluated by the formula (1):

$$\text{ME} = \frac{\text{Control peak area (PCU)}}{\text{Control solution peak area}} \times 100\% . \quad (1)$$

An ME value greater than 100% indicated an increase in ionization, and a value below 100% indicated suppression of ionization by the sample matrix.

Measurement uncertainty

The determination was carried out in accordance with the Guidelines for the Expression of Uncertainty of Measurement (GUM)[11], which establishes general rules for assessing and expressing measurement uncertainty in laboratories accredited to ISO/IEC 17025. When assessing uncertainty, an intralaboratory approach based on the determination of intermediate precision (intralaboratory reproducibility) was used. This approach consists of a three-component measurement model: the sum of measurements of the average value of the measurement method (m), estimates of the systematic error of the method (B), and the contribution of random error (e) (2):

$$y = m + B + e . \quad (2)$$

The combined standard uncertainty (u_c) was calculated as the root sum of the squares of the intermediate PCU precision (u_{prec}), the intermediate precision of the calibrators (u_{cal}), the bias uncertainty about the PCU setpoint in the presence of a systematic error (u_{bias}), and the uncertainty considering the analyte sample preparation process (u_{other}) according to the formula (3):

$$u_c = \sqrt{u_{prec}^2 + u_{cal}^2 + u_{bias}^2 + u_{other}^2} . \quad (3)$$

In order to assess the measurement uncertainty, a series of calibration solutions for each group of compounds and the corresponding positive urine controls containing the amounts of analytes at the threshold level were used.

RESULTS AND DISCUSSION

The main aim of this work was to develop and validate a rapid and reliable method for the quantitative determination of target compounds in urine samples. Precursor/product ion diagnostic pairs and collision energies were established to unambiguously identify the analyzed compounds. During the development of the method, optimal ionization conditions were obtained for each compound. The final data for the entire list of analytes are presented in Table 2.

Prior to validating the method, the conditions for the main stages of sample preparation, hydrolysis, and extraction were selected. Possibilities for using acid and enzymatic hydrolysis to determine compounds forming conjugates during metabolism were evaluated. The majority of the metabolites form derivatives of glucuronic acid, with only a small amount being excreted in the form of sulfates, acetates, and some other salts [6]. Although both types of hydrolysis are used to determine most of the substances during sample preparation, rather aggressive conditions are required when selecting an acid hydrolysis method: hydrochloric acid in high concentration (10N) and prolonged thermostating (at least 30 min) at high temperature (above 90°C), which may have a negative effect on the structures of some polar metabolites of the analyzed compounds (benzodiazepines, THC) [7]. By contrast, enzymatic hydrolysis does not require such conditions; instead,

[11] ISO/IEC Guide 98-3:2008. Uncertainty of measurement. Part 3. Guide to the expression of uncertainty in measurement. 2008. URL: https://docs.cntd.ru/document/1200146871 (Accessed February 11, 2022).

Table 2. Chromato-mass-spectrometric characteristics of analytes

Compound	RT, min	Type of ionization	Precursor ion, *m*/*z* (a.u.m.)	Product ion (collision energy), *m*/*z* (V)
Demoxepan-d_5 (ISTD 1)	3.60	+	292.1	180.1 (22)
				124.1 (37)
Morphine-d_3 (ISTD 2)	1.27	+	302.1	199.1 (25)
				128.1 (34)
Phenobarbital-d_5 (ISTD 3)	1.77	–	236.1	193.1 (13), 42.0 (20)
Bupranolol (ISTD 4)	4.10	+	272.1	216.1 (15)
				218.1 (15)
Mephruside (ISTD 5)	4.28	+	380.9	189.0 (30)
Amphetamine	2.78	+	136.1	119.1 (7)
				91.1 (16)
MDA	2.80	+	180.1	163.1 (10)
				135.1 (20)
MDMA	2.83	+	194.0	163.1 (12)
				135.1 (21)
MDEA	3.00	+	208.1	135.1 (21)
				163.1 (12)
Methamphetamine	2.85	+	150.1	91.1 (23)
				119.1 (10)
Amobarbital	3.66	–	225.1	42.1 (25)
				182.1 (10)
Butabarbital	4.35	–	201.1	168.1 (13)
				42.1 (20)
Butalbital	2.45	–	223.1	180.2 (10)
				42.1 (25)
Pentabarbital	3.52	–	225.1	42.1 (25)
				182.1 (10)
Secobarbital	4.60	–	237.1	42.1 (25)
				194.1 (10)
Phenobarbital	4.04	–	231.1	188.1 (12)
				42.1 (19)
Alprazolam	4.15	+	309.1	205.1 (41)
			311.1	205.1 (40)
Clonazepam	3.75	+	316.1	270.1 (24)
				214.1 (37)

Table 2. Continued

Compound	RT, min	Type of ionization	Precursor ion, *m*/*z* (a.u.m.)	Product ion (collision energy), *m*/*z* (V)
Lorazepam	4.10	+	323.1	277.1 (21)
			321.1	275.1 (21)
Midazolam	2.95	+	326.1	291.1 (26)
			328.1	291.1 (26)
Nordiazepam	4.37	+	271.1	140.1 (27)
				208.1 (27)
Oxazepam	4.10	+	287.1	241.1 (22)
			289.1	243.1 (21)
Temazepam	4.25	+	301.1	255.1 (29)
			303.1	257.1 (22)
Triazolam	4.14	+	343.1	308.1 (25)
			345.1	308.1 (25)
Flurazepam	2.90	+	388.1	315.1 (25)
			390.1	317.1 (22)
Benzoylecgonine	3.30	+	290.1	168.1 (19)
				105.1 (30)
Hydrocodone	2.73	+	300.1	128.1 (10)
				199.1 (11)
Hydromoron	1.87	+	286.1	157.1 (11)
				185.1 (20)
Codeine	2.58	+	300.1	152.1 (17)
				165.1 (14)
Morphine	1.36	+	386.1	152.1 (15)
				165.1 (8)
Oxycodone	2.67	+	316.1	241.1 (5)
				256.1 (20)
Oxymorphone	1.54	+	302.1	227.1 (11)
				284.1 (12)
6-MAM	2.76	+	328.1	165.1 (13)
				211.1 (12)
Propoxyphene	3.40	+	266.1	143.1 (19)
				128.1 (33)
Methadone	4.40	+	310.1	265.1 (14)
				219.1 (24)
Carboxy-THC	5.82	–	343.1	245.2 (31)
				191.2 (39)

E-coli beta-glucuronidase enzymes can be added to a phosphate buffer solution (pH 6.5–7.0) and incubation carried out at a temperature of 57°C for 60 min [8, 9]. Another important advantage of enzymatic hydrolysis is its high specificity due to the reduction in the urine matrix of interfering peaks associated with the cleavage of polysaccharide fragments of molecules, as well as the prevention of the breakdown of labile compounds and the exclusion of the use of aggressive media (reduction of hazard class). After taking the above factors into account, as well as the possible unification of sample preparation for all compounds, the choice was made in favor of enzymatic hydrolysis.

Some literature sources provide evidence that solid phase extraction (SPE) offers significant advantages as compared with liquid–liquid extraction (LLE) due to allowing purer eluates to be obtained [10]; this is especially important when determining substances at low concentrations. In the process of choosing the conditions for sample preparation, we compared the results after LLE of samples with diethyl ether and a carbonate buffer solution (pH 9.5–11) with added sodium sulfate with the results of SPE using Oasis® cartridges. Due to the threshold values for the quantitative determination of the validated compounds significantly exceeding the LOD (see Table 3), no significant difference was found in the analysis of the obtained extracts. Therefore, the choice was made in favor of LLE, which ultimately significantly reduced the cost and time of sample preparation for analysis.

Selectivity

An analysis of the mass chromatogram sections showed that the obtained mass chromatograms of the analytes in the corresponding intervals of scanning the RT of the analytes within ±0.1 min did not contain interfering peaks of the matrix components with a signal-to-noise ratio exceeding 3:1.

Linearity

For each analyte, a linear dependence of the concentration of a series of calibration solutions [11, 12], containing components in the range of 50–300% (Cal0–Cal6) of the threshold concentration value on the ratio of the signal of the analyte component to the signal of the corresponding internal standard was plotted. As an example, Figure shows a graph of a linear calibration curve for hydromorphone.

The results obtained indicate that the R^2 correlation coefficients for each compound were higher than the established value of 0.99 (the minimum value was 0.9918 for 6-MAM and the maximum value was 0.9992 for clonazepam and triazolam). The results obtained indicate a linear dependence in the selected concentration range (see Table 3).

Limit of quantitation

The obtained data on LOQ and LOD for each substance are presented in Table 3. LOQ and LOD values met the requirements of the customer's company (see Table 1).

Matrix effect

Most of the analyzed compounds showed ME values in the range of 85–115%, which indicates that the resulting matrix effect is negligible [13]. The minimum ME value was obtained for butalbital, 59.2 ± 7%, and the maximum for benzoylecgonine, 130.0 ± 2.0%. The data are given in Table 3.

Measurement uncertainty

The determination of intermediate precision was performed based on a data set of 5 PCU samples performed by two specialists within 5 days (n = 50). Each PCU result, in turn, was the average of three replicate measurements. The obtained data array was evaluated for outliers: the median of the sample, the lower and upper quartiles, and the inner and outer limits of the range were determined according to the method proposed in ISO/IEC Guide 98-3:2008. In a homogeneous sample of corrected (if necessary) values of the PCU samples, the mean, standard deviation, and relative standard deviation were determined under reproducibility conditions (intermediate precision, u_{prec}). The intermediate precision of the calibration solutions (u_{cal}) for each analyte was calculated as the root sum of the squares of the relative standard deviation of the levels of the calibration curve and the accuracy between the given and obtained concentration value for each level. The bias uncertainties about the PCU setpoint were evaluated in the presence of a systematic error (u_{bias}). The systematic error was determined using the Student's test. The uncertainty, which takes into account the process of sample preparation of u_{other} analytes, was calculated as the root sum of the squares of the uncertainties of the standard sample (according to the quality certificate),

Table 3. Validation characteristics of the methodology

Compound	LOD, ng/mL	LOQ*, ng/mL	Linearity, ng/mL	R^2 (n = 10)	ME, %	u_c, %
Amphetamine	0.5	125	125–750	0.9986 ± 0.0008	95.9 ± 5.1	6.5
MDA	2.0	125	125–750	0.9990 ± 0.0004	99.2 ± 4.6	6.2
MDEA	0.5	125	125–750	0.9983 ± 0.0012	101.5 ± 2.8	7.3
MDMA	0.5	125	125–750	0.9986 ± 0.0007	99.8 ± 3.3	7.6
Methamphetamine	0.5	125	125–750	0.9986 ± 0.0008	101.5 ± 3.9	6.7
Amobarbital	10	100	100–1000	0.9956 ± 0.0024	86.1 ± 5	8.8
Butabarbital	10	100	100–1000	0.9943 ± 0.0020	98.0 ± 5	8.7
Butalbital	10	100	100–1000	0.9950 ± 0.0020	59.2 ± 7	7.3
Pentabarbital	10	100	100–1000	0.9952 ± 0.0025	79.4 ± 6	8.6
Secobarbital	10	100	100–1000	0.9958 ± 0.0021	85.6 ± 8	8.3
Phenobarbital	10	50	50–2000	0.9979 ± 0.0014	86.1 ± 5	10.6
Alprazolam	0.5	50	50–300	0.9987 ± 007.00	94.7 ± 2.4	8.7
Clonazepam	0.5	50	50–300	0.9992 ± 0.0004	95.2 ± 4.6	7.1
Lorazepam	0.5	50	50–300	0.9987 ± 0.0006	106.0 ± 3.7	8.3
Midazolam	0.5	50	50–300	0.9987 ± 0.0005	92.1 ± 3.0	8.1
Oxazepam	0.5	50	50–300	0.9972 ± 0.0025	102.7 ± 4.3	9.8
Nordiazepam	0.5	50	50–300	0.9990 ± 0.0030	90.8 ± 3.7	7.2
Temazepam	0.5	50	50–300	0.9971 ± 0.0016	99.1 ± 4.3	8.2
Triazolam	0.5	50	50–300	0.9992 ± 0.0003	90.5 ± 2.1	6.8
Flurazepam	0.5	50	50–300	0.9980 ± 0.0013	100.8 ± 1.9	8.5
Benzoylecgonine	1.0	50	50–300	0.9989 ± 0.0006	130.0 ± 2.0	5.6
Hydrocodone	1.0	50	50–300	0.9971 ± 0.0030	105.1 ± 3.0	11.9
Hydromorphone	2.0	50	50–300	0.9989 ± 0.0003	109.6 ± 3.1	6.9

Table 3. Continued

Compound	LOD, ng/mL	LOQ*, ng/mL	Linearity, ng/mL	R^2 (n = 10)	ME, %	u_c, %
Codeine	1.0	50	50–300	0.9968 ± 0.0034	106.9 ± 2.6	12.7
Morphine	1.0	50	50–300	0.9987 ± 0.0006	100.3 ± 1.0	11. 6
Oxycodone	1.0	50	50–300	0.9959 ± 0.0038	100.9 ± 3.0	13.2
Oxymorphone	2.0	50	50–300	0.9965 ± 0.0024	95.6 ± 2.7	12.1
6-MAM	0.2	5	5–30	0.9918 ± 0.0025	97.5 ± 1.5	16.2
Propoxyphen	10	100	100–600	0.9985 ± 0.0010	112.2 ± 5.7	7.5
Methadone	0.5	100	100–600	0.9982 ± 0.0009	99.0 ± 4.5	6.9
Carboxy-THC	2.0	5	5–200	0.9983 ± 0.0012	95.2 ± 6	19.0

***** In accordance with the terms of the contract with the customer.

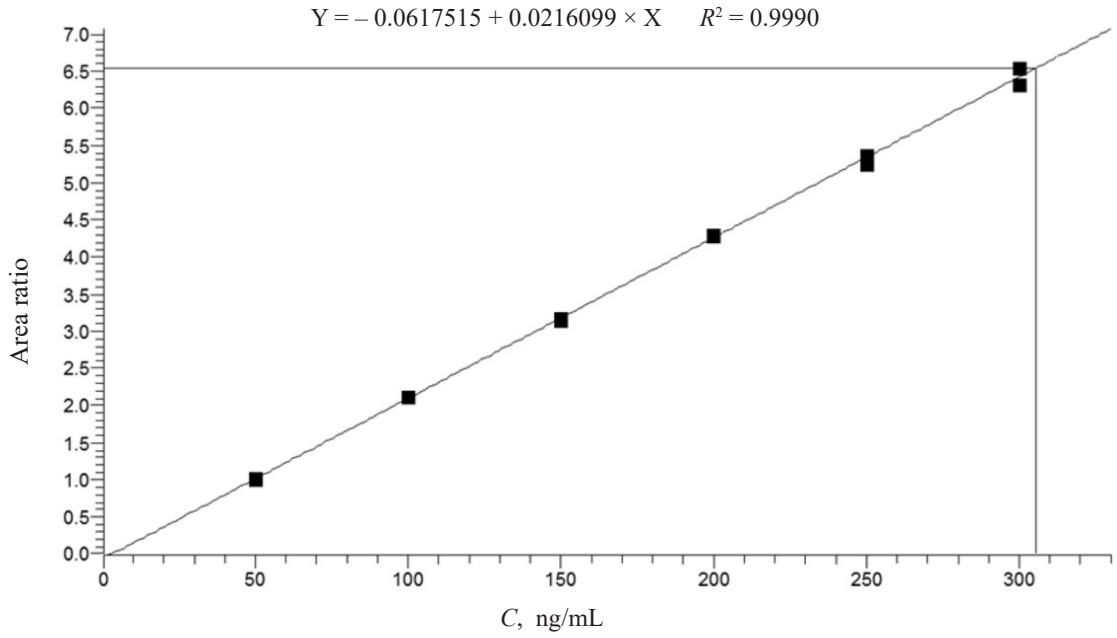

Figure. Linear calibration curve plot of hydromorphone.

aliquoting the urine sample with automatic dispensers, and diluting the urine sample (during the preparation of solutions).

The combined uncertainty value was calculated by formula (3). The maximum uncertainty value was 19%, the data are presented in Table 3. This method can be used to quantify the presented list of substances (see Table 1).

CONCLUSIONS

A new approach for the quantitative determination of 31 potent and narcotic substances and their metabolites in urine intended for introduction into the routine practice of NADL MSU was significantly revised and validated using a fast and highly sensitive UHPLC–MS/MS method.

The important advantages of the technique are the absence of complex and lengthy sample preparation (e.g., SPE and the formation of TMS derivatives), as well as a short analysis time of about 10 min. This allows the duration of the determination to be significantly reduced, along with labor and analysis costs. The addition of new detectable compounds will ensure the adopted method's versatility and allow its scope to be expanded without loss of sensitivity and selectivity when performing chemico-toxicological analysis or doping control.

The improved methodology has been revalidated in accordance with the requirements of ISO/IEC 17025-2019 and included in the scope of NADL MSU accreditation. Since the introduction of the validated methodology, more than 750 urine samples have been analyzed and more than 30 confirmed positive samples have been identified, which confirms the high level of detectability and sensitivity.

Authors' contributions

N.B. Savelieva – development of a plan for conducting experiments, analysis of the results obtained, primary processing of experimental data, and writing the text of the article;

G.V. Ishutenko – conducting experimental research, scientific and technical support, analysis of the obtained results, primary processing of experimental data, and editing the final version of the article;

A.V. Polosin – conducting experimental studies, scientific and technical support, analysis of the results obtained, and editing the final version of the article;

F.V. Radus – primary processing of experimental data;

D.S. Polyansky – verification and systematization of data validation parameters;

S.A. Kurbatkin – primary processing of experimental data;

Yu.A. Efimova – systematization and processing of the obtained results, editing the manuscript, and preparation of materials for publication;

P.V. Postnikov – formulation of aims and objectives, discussion of experiments and results, general management of the validation process, writing the text of the article, editing the manuscript, editing the final version of the article, and preparing materials for publication.

The authors declare no conflicts of interest.

REFERENCES

1. Buser G.L., Gerona R.R., Horowitz B.Z., Vian K.P., Troxell M.L., Hendrickson R.G., Houghton D.C., Rozansky D., Su S.W., Leman R.F. Acute kidney injury associated with smoking synthetic cannabinoid. *Clin. Toxicol*. (Phila). 2014 52(7):664–673. https://doi.org/10.3109/15563650.2014.932365

2. Negishi S., Nakazono Y., Iwata Y.T., Kanamori T., Tsujikawa K., Kuwayama K., Inoue H. Differentiation of regioisomeric chloroamphetamine analogs using gas chromatography–chemical ionization-tandem mass spectrometry. *Forensic Toxicol.* 2015;33(2):338–347. https://doi.org/10.1007/s11419-015-0280-y

3. Maresová V., Chadt J., Prikryl L. Simultaneous determination of amphetamines and amphetamine-derived designer drugs in human urine by GC-MS. *Neuro Endocrinol. Lett*. 2006;27(Suppl. 2):121–124.

4. Choi H., Heo S., Choe S., Yang W., Park Y., Kim E., Lee J. Simultaneous analysis of synthetic cannabinoids in the materials seized during drug trafficking using GC-MS. *Anal. Bioanal. Chem*. 2012;405(12):3937–3944. https://doi.org/10.1007/s00216-012-6560-z

5. Aszyk J., Kot-Wasik A. The use of HPLC-Q-TOF-MS for comprehensive screening of drugs and psychoactive substances in hair samples and several "legal highs" products. *Monatsh. Chem*. 2016;147:1407–1414. https://doi.org/10.1007/s00706-016-1773-z

6. Illarionova E.A., Syrovatskii I.P. *Khimiko-toksikologicheskii analiz psikhotropnykh lekarstvennykh preparatov:* uchebnoe posobie (*Chemico-toxicological analysis of psychotropic drugs.* Textbook). Irkutsk: ISMU; 2021. 81 p. (in Russ.).

СПИСОК ЛИТЕРАТУРЫ

1. Buser G.L., Gerona R.R., Horowitz B.Z., Vian K.P., Troxell M.L., Hendrickson R.G., Houghton D.C., Rozansky D., Su S.W., Leman R.F. Acute kidney injury associated with smoking synthetic cannabinoid. *Clin. Toxicol.* (Phila). 2014 52(7):664–673. https://doi.org/10.3109/15563650.2014.932365

2. Negishi S., Nakazono Y., Iwata Y.T., Kanamori T., Tsujikawa K., Kuwayama K., Inoue H. Differentiation of regioisomeric chloroamphetamine analogs using gas chromatography–chemical ionization-tandem mass spectrometry. *Forensic Toxicol.* 2015;33(2):338–347. https://doi.org/10.1007/s11419-015-0280-y

3. Maresová V., Chadt J., Prikryl L. Simultaneous determination of amphetamines and amphetamine-derived designer drugs in human urine by GC-MS. *Neuro Endocrinol. Lett*. 2006;27(Suppl. 2):121–124.

4. Choi H., Heo S., Choe S., Yang W., Park Y., Kim E., Lee J. Simultaneous analysis of synthetic cannabinoids in the materials seized during drug trafficking using GC-MS. *Anal. Bioanal. Chem*. 2012;405(12):3937–3944. https://doi.org/10.1007/s00216-012-6560-z

5. Aszyk J., Kot-Wasik A. The use of HPLC-Q-TOF-MS for comprehensive screening of drugs and psychoactive substances in hair samples and several "legal highs" products. *Monatsh. Chem.* 2016;147:1407–1414. https://doi.org/10.1007/s00706-016-1773-z

6. Илларионова Е.А., Сыроватский И.П. *Химико-токсикологический анализ психотропных лекарственных препаратов*: учебное пособие. Иркутск: Издательство ИГМУ; 2021. 81 с.

7. Starovoitova M.K., Minachenkova A.S., Krys'ko M.V., Slustovskaya Yu.V., Strelova O.Yu., Kuklin V.N. Comparative characteristics of enzymatic hydrolysis methods for isolating toxic substances from whole blood and hair. *Sudebno-Meditsinskaya Ekspertiza*. 2020;63(3):23–29 (in Russ.). https://doi.org/10.17116/sudmed20206303123

8. Mazzarino M., de la Torre X., Botrè F. A screening method for the simultaneous detection of glucocorticoids, diuretics, stimulants, anti-oestrogens, beta-adrenergic drugs and anabolic steroids in human urine by LC-ESI-MS/MS. *Anal. Bioanal. Chem*. 2008;392(4):681–698. https://doi.org/10.1007/s00216-008-2292-5

9. Thevis M., Thomas A., Schänzer W. Current role of LC-MS(/MS) in doping control. *Anal. Bioanal. Chem*. 2011;401(2):405–420. https://doi.org/10.1007/s00216-011-4859-9

10. Kim Y., Jeon M., Min H., Son J., Lee J., Kwon O.-S., Kim K.H. Development of a multi-functional concurrent assay using weak cation-exchange solid-phase extraction (WCX-SPE) and reconstitution with a diluted sample aliquot for anti-doping analysis. *Rapid Commun. Mass Spectrom*. 2018;32(11):897–905. https://doi.org/10.1002/rcm.8119

11. Zybin D.I., Seregin A.S., Askretkov A.D., Orlova N.V., Seregin Y.A., Prostyakova A.I., Kapustin D.V. Development and validation of a method for the determination of the specific activity of recombinant monoclonal antibody eculizumab. *Fine Chem. Tech*. 2020;15(2):77–85. https://doi.org/10.32362/2410-6593-2020-15-2-77-85

12. Du L., Li G., Gong W., Zhu J., Liu L., Zhu L., Liu Z. Establishment and validation of the LC-MS/MS method for the determination of lincomycin in human blood: Application to an allergy case in forensic science. *J. Forensic Leg. Med*. 2021;77:102094. https://doi.org/10.1016/j.jflm.2020.102094

13. Márta Z., Bobály B., Fekete J., Magda B., Imre T., Szabó P.T. Simultaneous determination of ten nonsteroidal anti-inflammatory drugs from drinking water, surface water and wastewater using micro UHPLC-MS/MS with on-line SPE system. *J. Pharm. Biomed. Anal.* 2018;160:99–108. https://doi.org/10.1016/j.jpba.2018.07.016

7. Старовойтова М.К., Миначенкова А.С., Крысько М.В., Слустовская Ю.В., Стрелова О.Ю., Куклин В.Н. Сравнительная характеристика методик ферментативного гидролиза для изолирования токсичных веществ из цельной крови и волос. *Судебно-медицинская экспертиза*. 2020;63(3):23–29. https://doi.org/10.17116/sudmed20206303123

8. Mazzarino M., de la Torre X., Botrè F. A screening method for the simultaneous detection of glucocorticoids, diuretics, stimulants, anti-oestrogens, beta-adrenergic drugs and anabolic steroids in human urine by LC-ESI-MS/MS. *Anal. Bioanal. Chem.* 2008;392(4):681–698. https://doi.org/10.1007/s00216-008-2292-5

9. Thevis M., Thomas A., Schänzer W. Current role of LC-MS(/MS) in doping control. *Anal. Bioanal. Chem.* 2011;401(2):405–420. https://doi.org/10.1007/s00216-011-4859-9

10. Kim Y., Jeon M., Min H., Son J., Lee J., Kwon O.-S., Kim K.H. Development of a multi-functional concurrent assay using weak cation-exchange solid-phase extraction (WCX-SPE) and reconstitution with a diluted sample aliquot for anti-doping analysis. *Rapid Commun. Mass Spectrom*. 2018;32(11):897–905. https://doi.org/10.1002/rcm.8119

11. Zybin D.I., Seregin A.S., Askretkov A.D., Orlova N.V., Seregin Y.A., Prostyakova A.I., Kapustin D.V. Development and validation of a method for the determination of the specific activity of recombinant monoclonal antibody eculizumab. *Fine Chem. Tech.* 2020;15(2):77–85. https://doi.org/10.32362/2410-6593-2020-15-2-77-85

12. Du L., Li G., Gong W., Zhu J., Liu L., Zhu L., Liu Z. Establishment and validation of the LC–MS/MS method for the determination of lincomycin in human blood: Application to an allergy case in forensic science. *J. Forensic Leg. Med*. 2021;77:102094. https://doi.org/10.1016/j.jflm.2020.102094

13. Márta Z., Bobály B., Fekete J., Magda B., Imre T., Szabó P.T. Simultaneous determination of ten nonsteroidal anti-inflammatory drugs from drinking water, surface water and wastewater using micro UHPLC-MS/MS with on-line SPE system. *J. Pharm. Biomed. Anal*. 2018;160:99–108. https://doi.org/10.1016/j.jpba.2018.07.016

About the authors:

Nadezhda B. Savelieva, Chief Specialist of the Doping Control Department, National Anti-Doping Laboratory (Institute), Lomonosov Moscow State University (10-1, Elizavetinskii per., Moscow, 105005, Russia). E-mail: nsavelieva@hotmail.com. https://orcid.org/0000-0002-3988-6043

Grigory V. Ishutenko, Deputy Head of the Doping Control Department, National Anti-Doping Laboratory (Institute), Lomonosov Moscow State University (10-1, Elizavetinskii per., Moscow, 105005, Russia). E-mail: pathfinder111@yandex.ru. https://orcid.org/0000-0001-5406-2571

Andrey V. Polosin, Chief Specialist of the Doping Control Department, National Anti-Doping Laboratory (Institute), Lomonosov Moscow State University (10-1, Elizavetinskii per., Moscow, 105005, Russia). E-mail: streanger72@yandex.ru. https://orcid.org/0000-0002-0009-7362

Fedor V. Radus, Assistant, I.P. Alimarin Department of Analitical Chemistry, M.V. Lomonosov Institute of Fine Chemical Technologies, MIREA – Russian Technological University (86, Vernadskogo pr., Moscow, 119571, Russia). E-mail: radus20@mail.ru. https://orcid.org/0000-0003-0938-9609

Dmitry S. Polyansky, Assistant, I.P. Alimarin Department of Analitical Chemistry, M.V. Lomonosov Institute of Fine Chemical Technologies, MIREA – Russian Technological University (86, Vernadskogo pr., Moscow, 119571, Russia). E-mail: polyansky@medgamal.ru. https://orcid.org/0000-0003-0792-7063

Sergey A. Kurbatkin, Assistant, I.P. Alimarin Department of Analitical Chemistry, M.V. Lomonosov Institute of Fine Chemical Technologies, MIREA – Russian Technological University (86, Vernadskogo pr., Moscow, 119571, Russia). E-mail: kurbatkins@mail.ru. https://orcid.org/0000-0002-2984-2178

Yuliya A. Efimova, Cand. Sci. (Chem.), Assistant Professor, I.P. Alimarin Department of Analitical Chemistry, M.V. Lomonosov Institute of Fine Chemical Technologies, MIREA – Russian Technological University (86, Vernadskogo pr., Moscow, 119571, Russia). E-mail: efimova_yulia@bk.ru. https://orcid.org/0000-0002-3582-0012

Pavel V. Postnikov, Cand. Sci. (Chem.), Head of the Doping Control Department, National Anti-Doping Laboratory (Institute), Lomonosov Moscow State University (10-1, Elizavetinskii per., Moscow, 105005, Russia). E-mail: drpavelpostnikov@gmail.com. RSCI SPIN-code 7251-9937, https://orcid.org/0000-0003-3424-0582

Об авторах:

Савельева Надежда Борисовна, главный специалист отдела допингового контроля Национальной антидопинговой лаборатории (Института) Московского государственного университета им. М.В. Ломоносова (105005, Россия, Москва, Елизаветинский пер., д. 10, стр. 1). E-mail: nsavelieva@hotmail.com. https://orcid.org/0000-0002-3988-6043

Ишутенко Григорий Владимирович, зам. начальника отдела допингового контроля Национальной антидопинговой лаборатории (Института) Московского государственного университета им. М.В. Ломоносова (105005, Россия, Москва, Елизаветинский пер., д. 10, стр. 1). E-mail: ishutenko@dopingtest.ru. https://orcid.org/0000-0001-5406-2571

Полосин Андрей Вячеславович, главный специалист отдела допингового контроля Национальной антидопинговой лаборатории (Института) Московского государственного университета им. М.В. Ломоносова (105005, Россия, Москва, Елизаветинский пер., д. 10, стр. 1). E-mail: polosin@dopingtest.ru. https://orcid.org/0000-0002-0009-7362

Радус Федор Валерьевич, ассистент кафедры аналитической химии им. И.П. Алимарина Института тонких химических технологий им. М.В. Ломоносова ФГБОУ ВО «МИРЭА –Российский технологический университет» (119571, Россия, Москва, пр-т Вернадского, д. 86). E-mail: radus20@mail.ru. https://orcid.org/0000-0003-0938-9609

Полянский Дмитрий Сергеевич, ассистент кафедры аналитической химии им. И.П. Алимарина Института тонких химических технологий им. М.В. Ломоносова ФГБОУ ВО «МИРЭА – Российский технологический университет» (119571, Россия, Москва, пр-т Вернадского, д. 86). E-mail: polyansky@medgamal.ru. https://orcid.org/0000-0003-0792-7063

Курбаткин Сергей Александрович, ассистент кафедры аналитической химии им. И.П. Алимарина Института тонких химических технологий им. М.В. Ломоносова ФГБОУ ВО «МИРЭА – Российский технологический университет» (119571, Россия, Москва, пр-т Вернадского, д. 86). E-mail: kurbatkins@mail.ru. https://orcid.org/0000-0002-2984-2178

Ефимова Юлия Александровна, к.х.н., доцент кафедры аналитической химии им. И.П. Алимарина Института тонких химических технологий им. М.В. Ломоносова ФГБОУ ВО «МИРЭА – Российский технологический университет» (119571, Россия, Москва, пр-т Вернадского, д. 86). E-mail: efimova_yulia@bk.ru. https://orcid.org/0000-0002-3582-0012

Постников Павел Викторович, к.х.н., начальник отдела допингового контроля Национальной антидопинговой лаборатории (Института) Московского государственного университета им. М.В. Ломоносова (105005, Россия, Москва, Елизаветинский пер., д. 10, стр. 1). E-mail: drpavelpostnikov@gmail.com. SPIN-код РИНЦ 7251-9937, https://orcid.org/0000-0003-3424-0582

The article was submitted: March 09, 2022; approved after reviewing: April 11, 2022; accepted for publication: June 16, 2022.

Translated from Russian into English by H. Moshkov
Edited for English language and spelling by Thomas Beavitt

MIREA – Russian Technological University
78, Vernadskogo pr., Moscow, 119454, Russian Federation.
Signed to print on *June 30, 2022.*
Not for sale

МИРЭА – Российском технологическом университет
119454, РФ, Москва, пр-кт Вернадского, д. 78.
Дата опубликования *30.06.2022.*
Не для продажи

www.finechem-mirea.ru